Republic of Iraq
Ministry of Higher Education
And Scientific Research
University of Baghdad
College of Education For
Pure Science Ibn-Al-Haitham
Department of Physics

Theoretical Study for Neodymium-Doped Optical Fiber Laser

A thesis

Submitted to the Counsil of College of Education for Pure Science / Ibn Al-Haitham - Baghdad University in Partial Fulfillment of The Requirements for the Degree of Master of Science in Physics

By

Amjed Abdul hameed Salman

BSc. in Physics / 2013

Supervised by

Dr. Mudhir Shihab Ahmed

1437 A.H **2016 A.D**

بسم الله الرحمن الرحيم

(فَمَنْ يَعْمَلْ مِثْقَالَ ذَرَّةٍ خَيْرًا يَرَهُ)

صدق الله العظيم

Dedication

To my family and my fiancee..

Whom they always urge me to continue my studies and continuously pray Allah for enlighting my way towards success and happiness, God bless them.

Amjed

Acknowledgments

I would like to express my thanks to "Allah" for all help in the production of this work.

With the blessing of Allah the project leading to this thesis has been completed.

It is great pleasure to express my deep appreciation and sincere gratitude to my supervisors**, *Dr. Mudhir Shihab Ahmed*** for suggesting the project of research, and for helpful comments and stimulating discussion through the work.

All my thanks to ***Dr. Ahlaam Husain ja'afar*** for help and advise in my study.

Deep thanks are extended to the Department of Physics in ***College of Education for Pure Science / Ibn Al-Haitham***

Finally, I am very grateful to my family for their help and support to continue my study .

Amjed

Supervisors Certification

We certify that this thesis was prepared by (**Amjed Abdul hameed Salman)** Under our supervision at Physics Department, College of Education for pure Science Ibn-Al-Haitham University of Baghdad as partial requirement for the degree of Master of Science in Physics.

Signature:

Name: **Dr. Mudhir Shihab Ahmed**

Title: Instructor
Date: / / 2016

In view of the available recommendation, I forward this thesis for debate by the examination committee.

Signature:

Name: **Dr. Kareem Ali Jasim**

Title: Professor
Date: / / 2016

Committee Certification

We certify that we have read this thesis titled "***Theoretical Study for Neodymium-Doped Optical Fiber Laser***

submitted by **Amjed Abdul hameed Salman** and as examining committee examined the student in its content and that in our opinion it is adequate with standard as thesis for degree of Master of Science in Physics.

Chairman

Signature:
Name: Dr. Ahmed Farhan Atwan
Title: Prof.
Address: Dep. of Physics – College of Education- University of Al Mustansiriyah
Date: /10/2016

Member

Signature:
Name: Dr. Hussain S.Hasan
Title: Assistant Prof.
Address: Dep. of Physiology and Medical Physics – College of Medicine – University of Al Nahrain
Date: / 10/2016

Member

Signature:
Name: Dr. Alaa Badr Hasan
Title: Assistant Prof
Address: Dep. of Physics – College of Education for Pure Science
Date: /10/2016

Supervisor

Signature:
Name: Dr. Mudhir Shihab Ahmed
Title: Instructor
Address: Dep. of Physics – College of Education for Pure Science
Date: /10/2016

Approved by the council of the college Education-Ibn Al-Haitham for pure science of Baghdad University

Signature:
Name: Dr. Khalid F. Ali
Title: Professor
The dean of Education College for Pure Science /Ibn Al-Haitham
Date: / /2016

Abstract

The current study included firstly the analytical solution of rate equations for optical fiber laser, that is process according to pump plan with four-levels system to find equation of lasing output power (P_{out}) by using the numerical emulation Secondly, calculating the (P_{out}) of Nd^{+3}-doped optical fiber laser as a typical example for the optical fiber laser, which is process according to this system. The required equations to calculate (P_{out}) was programmed by Matlab program (version8.1).

Two types of hosts were used in this simulation, the first type is Silica with four designs using commonly in the above mentioned, the four designs are Lycom (a), Lycom (b), York and IVA with lasing emission at the wavelengths (1064×10^{-9}m) and (1331×10^{-9}m). The second type of hosts is ZBLAN with only one design is Le Verre fluore, with lasing emission at two wavelengths (1048×10^{-9}m) and (1317×10^{-9}m).

The first step in this emulation was determining the value of numerical aperture (NA) for each design of special designs and at the special wavelengths for every host, which can obtain the highest values of lasing output power (P_{out}) and efficiency (η) at value of (NA).The second step was calculating the (P_{out}) corresponding to pump power (P_o) for each host according to the designs and the wavelengths related to the host, In case of the host Silica, for the two wavelengths of this host, it is found that the (P_{out}) was the highest value when the design (York) was used, while in case of the host (ZBLAN), it is found the highest value of (P_{out}) is when using the wavelength (1048×10^{-9}m).

For addition that, it is found that to obtain the highest values of (P_{out}) and (η) for this type of laser, it must be use the host Silica at the wavelength (1048×10^{-9}m). According to that, the third step was using this host and this wavelength to calculate the effect of the numerical aperture (NA), core radius (a), cladding radius (b), fiber length (L),reflection coefficients (R_2), Nd^{+3}- dopant concentration in the core (N_o), lifetime of upper laser level (T_2) and pump power (P_o) on the (P_{out}). The changing of the above mentioned coefficients values was determinate with its range which is finding in four designs related to the host Silica. It is found that the value of (P_{out}) decreased with the increase of the values of (NA, a, b, L and N_o), while increase with the increase of the values of (R_2 ,T_2 and P_o), through that, the optimal values of these coefficients which must be used to obtain the highest values of (P_{out}) and (η) for this type of laser.

CONTENTS

CONTENTS

List of Figures

List of Table

List of Symbols

Symbol	Description	Unit
n	Refractive index	-
c	Speed of light in free space	**m/sec**
v	Speed of light in a medium	**m/sec**
n_1	Core index of refraction	-
n_1	Cladding index of refraction	-
ε_r	Electrical relative permittivity	**f/m**
ε_o	Electrical permittivity of the vacumm	**f/m**
μ_o	Magnetic permittivity of the vacumm	**h/m**
Θ_c	Critical angle	**deg**
α_{max}	Acceptance angle	**deg**
NA	Numerical aperture	-
λ	Wavelength in vacumm	**m**
ν	Frequency	**Hz**
V	Normalized frequency at pumping wavelength	
M	Number of modes	-
N_1	Populations in level (2)	**ion/m**
N_2	Populations in level (2)	**ion/m**
E_1	Energy of level (1)	**J**
E_2	Energy of level (2)	**J**
H	Planck's constant	**J.sec**
B_{12}	Einstein's coefficient for stimulated absorption	m^3/sec^2. J

List of Symbols

Symbol	Description	Unit
ρ	Energy density per unit of frequency of the incoming photon	Kg/m^3
A_{21}	Einstein's coefficient for spontaneous emissiovn	1/sec
T_2	Fluorescence lifetime of level (2)	Sec
W_P	Pump rate	-
W_{21}	Probability per unit time for an induced transition	-
σ_p	Absorption cross – section at pumping wavelength	m^2
σ_L	Emission cross – section at lasing wavelength	m^2
I_L	Lasing intensity	W/m^2
v_L	Lasing frequency	Hz
v_p	Pumping frequency	Hz
R	Total number of atoms pumped up to level (2)	-
R_1	Reflectivity of mirror (1)	-
R_2	Reflectivity of mirror (2)	-
G	Gain coefficient	m^{-1}
G_{th}	Gain threshold	m^{-1}
L	Fiber length	m
N_o	Nd^{3+}- dopant concentration in fiber core	ion/m^3
Γ_L	Power filling factor at lasing wavelength	-
α	Core radius	m
w_L	Mode field radius at lasing wavelength	m
λ_L	lasing wavelength	m

List of Symbols

Symbol	Description	Unit
U	Normalized frequency at lasing wavelength	-
T_c	Cavity lifetime	sec
R_{th}	Total number of atoms pumped up to level (2) at threshold	W
λ_p	Pumping wavelength	m
I_p	Pumping intensity	W/m^2
α_L	Scattering loss at lasing wavelength	m^{-1}
α_P	Scattering loss at pumping wavelength	m^{-1}
Γ_p	Power filling at pumping wavelength	-
b	Cladding radius	m
A_{eff}	Cross – Sectional area of core	m^2
w_p	Mode field radius at pumping wavelength	m
γ	Single – Pass gain	m^{-1}
γ_{th}	Single – Pass gain threshold	m^{-1}
P_{th}	Threshold pumping	W
T	Transmission of mirror (2)	-
P_{out}	Lasing output power	W
P_{abs}	Absorbed pump power	W
I_s	Saturation intensity	W/m^2
η	Efficiency	-

List of Abbreviations

Abbreviation	Meaning
TIR	Total Internal Reflection
SM	Single – Mode
MM	Multi – Mode
SCF	Single – Clad Fiber
DCF	Double – Clad Fiber
RE	Rare – Earth
Nd	Neodymium
NDFL	Neodymium – Doped Fiber Laser
YAG	Yttrium Aluminum Garent
GGG	Godoliniom Gallium Garent
GSAG	Godoliniom Scandium Aluminum Garent
GSA	Ground State Absorption
ESA	Excited State Absorption
IR	Infrared
NIR	Near Infrared
VIS	Visible
UV	Ultra – Violet
LD	Laser Diode
PCF	Potonic Crystal Fiber
MCVD	Modified Chemical Vapor Deposition
SBS	Sitmulated Brillonin Scattering
LED	Light Emitting Diode

Chapter one

Background and Literature Review

(1.1) Introduction

In the early of 1960's, the first fiber laser that was doped with Neodymium ions was demonstrated. Since that time, lasers based on (Nd^{3+}) were the subject of intense research. Devices such as pulsed and Continuous-Wave (cw) lasers, super-fluorescence sources and amplifiers, were verified with (Nd^{3+}) - doped fibers. Besides, the first cladding-pumped fiber laser was also doped with (Nd^{3+}) [1,2]. In the current time, (Nd^{3+})-based lasers are still the attention of researchers, because of its four-level domination nature (1.1×10^{-6}m) transition, and because of the widely available, efficient, low cost and high-power laser diodes at (808×10^{-9} m) which can be used as pump sources. Recently Ueda et al. demonstrated a highly-multimode Neodymium-doped fiber laser with over (1×10^{-3} W) of output power [1,2].

This was an embedded fiber disk laser, and because of relatively low pump intensity, the low-threshold of the Neodymium-Doped Fiber Laser (NDFL) was essential. Details about (Nd^{3+})-spectroscopy, and (Nd^{3+})-doped lasers in general, are widely available in the literature [3]. The spectroscopy of (Nd^{3+}) is quite intricate, and careful investigations of spectroscopic properties like absorption and emission spectra, fluorescence lifetime, and laser performance with various glass hosts are required to optimize Neodymium-doped fiber lasers. [3,4].

(1.2) Optical fiber

In its simplest form, an optical fiber consists of a central single solid dielectric cylinder of radius (a) and refractive index (n_1), this cylinder is known as the core of the fiber. The core is surrounded by a solid dielectric cladding which has a refractive index (n_2) that is less than (n_1) [4].

Although, in principle, a cladding is not necessary of light to propagate along the core of the fiber, it serves several purposes. The cladding reduces scattering loss that results from dielectric discontinuities at the core surface, it adds mechanical strength to the fiber, and it protects the core from absorbing surface contaminants with which it could come in contact, [4,5] Figure (1-1) shows the cross section fiber

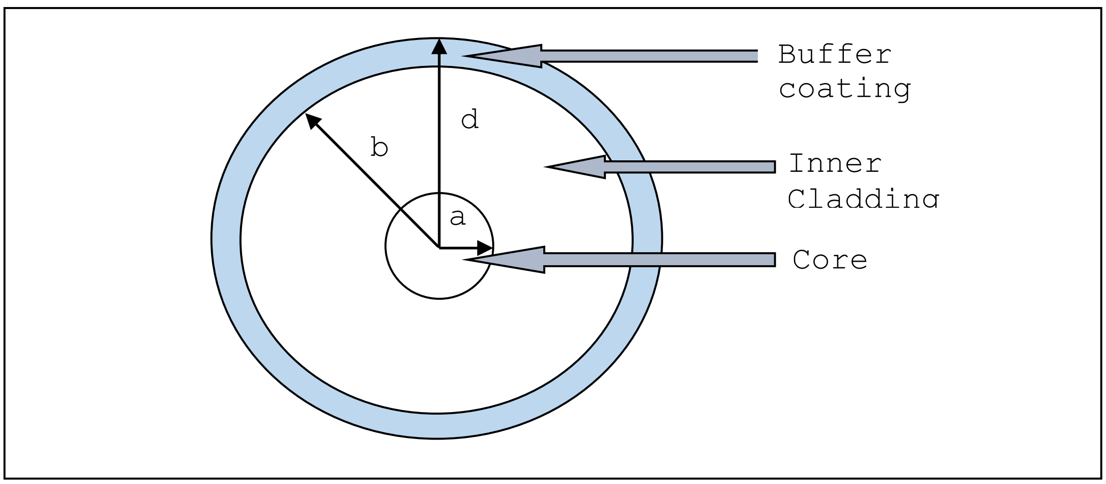

Figure.(1.1): Schematic illustration of the cross section of Single Clad Fiber (SCF).

In low–and medium–loss fiber the core material is generally glass and is surrounded by either a glass or a plastic cladding , Higher–loss plastic–core fibers with plastic cladding are also widely in use [4,6].

In addition, most fibers are encapsulated in elastic, abrasion plastic material [5]. This material adds further strength to the fiber and mechanically isolators or buffers the fiber from small geometrical irregularities distortions or roughness's of adjacent surfaces [5,6].

(1.2.1) Optical fiber types

Optical fibers are characterized by their structure and by their properties of transmission. They can be classified by the number of modes that propagate along the fiber into two types: single mode and multimode fibers. The basic structural difference between these two types is the core size, since core size is strictly related to the number of mode propagating in a fiber. Optical fibers can be also classified by the refractive index profile of the core/clad structure which determines the mode of propagation of the optical signal. The most common types are the step-index and graded-index fibers [5,7].

(1.2.1.1) Single mode and multimode fibers

The core size of single mode fibers is small. A fiber core of this size allows only the fundamental or lowest order mode to propagate around a ($1300*10^{-9}$m) wavelength. As already discussed, for single mode fibers (*V*) is less than or equal to (2.405). The number of modes propagating in a multimode fiber depends on the core size and (NA). As the core size and (NA) increase, the number of modes increases
‘Single mode fibers have many advantages as compared with the multimode: Small attenuation ; High transmission bandwidth ; Low fiber dispersion. However, due to smaller core size light coupling from an external source is more critical than in a multimode fiber[7,8]. As a consequence, single mode fibers typically require laser diodes while multimode can be coupled to Light Emitting Diodes (LEDs) that are less complex and cheaper than lasers None the less the use of multimode fibers has the disadvantage of modal dispersion that increases with the number of supported modes. This effect causes the light pulse to be spread during propagation in the fiber and thus decreases system bandwidth [7,9].

(1.2.1.2) Step-index and graded-index fibers

‘Step-index optical fibers have a refractive index profile of the core/clad structure characterized by a uniform refractive index within the core and a sharp decrease in refractive index at the core-cladding interface so that the cladding has a lower refractive index[4,6] Figure (1.2) shows the step-index and graded index fiber. The step-index profile corresponds to a power law index profile with the profile parameter approaching infinity. The step-index profile is used in most single mode fibers and some multimode fibers [7,9]. A Graded-Index Fiber means that the fiber core has a refractive index that decreases with the increase of radial distance from the optical axis of the fiber, as represented in Figure.(1.2,3). Because the part of the core closer to the fiber axis has a higher refractive index than the parts near the cladding, light rays follow sinusoidal paths down the fiber [8].

These types of fibers are designed to compensate for the difference in the propagation path length among various modes so that the distortion of the signal is minimized [9].

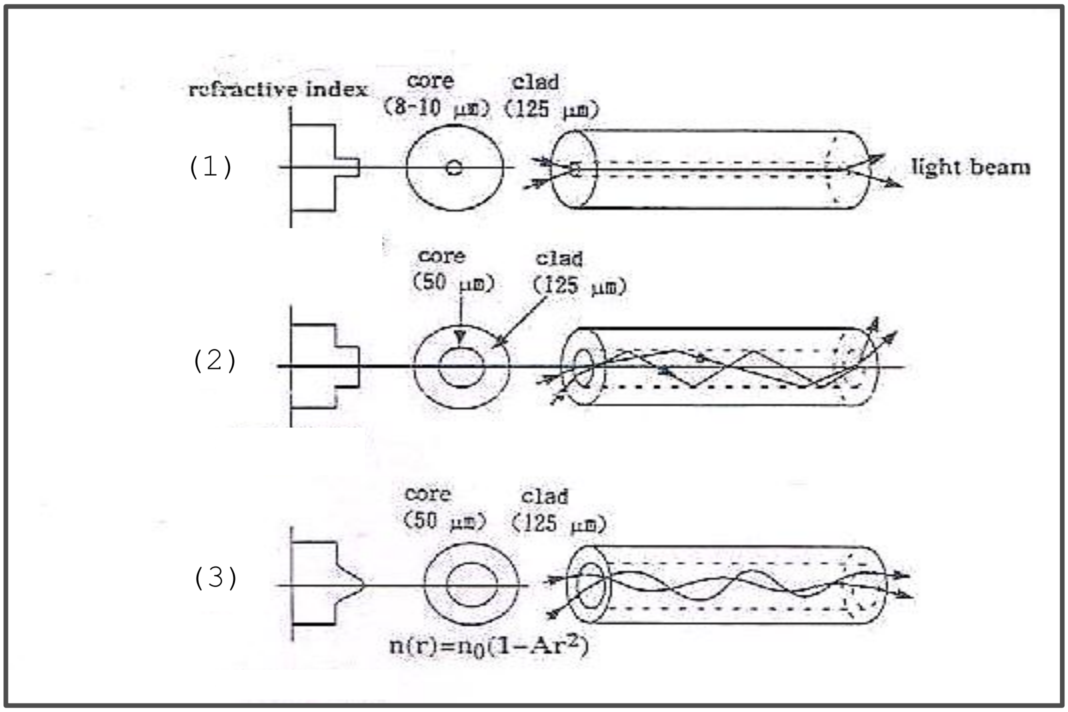

Figure (1.2). Typical structure of optical fiber for telecommunications: (1) single-mode fiber; (2) Multimode fiber of step-index type; (3) multi-mode fiber of graded-index type[5,7].

Multimode optical fiber can be manufactured with either graded-index or step-index. The advantage of the graded-index compared to step-index is the considerable decrease in modal dispersion [8].

(1.2.2) Refraction of light and total internal reflection

When a light ray encounters the boundary between two different transparent media, with different refractive index (n_1) and (n_2), part of ray is reflected back into the first medium while part of the ray is refracted.[4,5],Figure(1.2) shows reflection and refraction.The reflected ray follows the law of reflection which states that the angle of incidence (θ_1) is equal to the angle of reflect ion. The relationship between the incident and the refracted rays at the boundary is described by Snell's Law [5,6].

$$n_1 \sin \theta_1 = n_2 \sin\theta_2 \qquad (1.1)$$

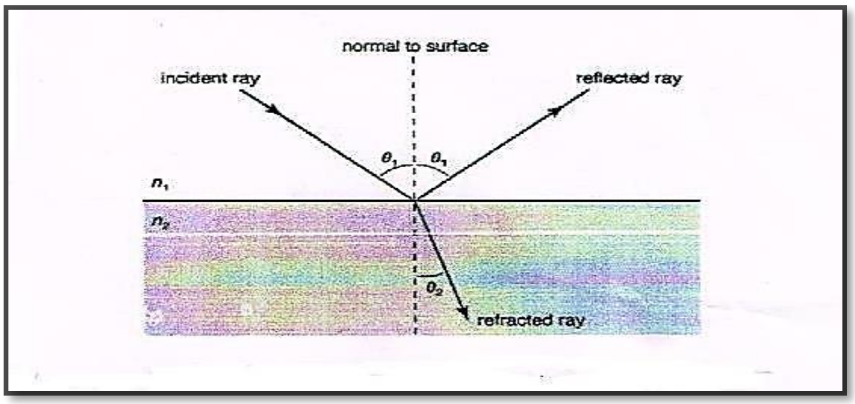

Figure (1.3). light reflection and refraction at a boundary between media of different refractive index[5].

Where (θ_1) is the angle of incidence and (θ_2) is the angle of refraction. If the wave passes from a less dense to a denser medium, it is bent toward the normal, and the angle of refraction is less than the angle of incidence. On the contrary, if the wave passes from a denser to a less dense medium, it bents away from the normal, and the angle of refraction is greater than the angle of incidence. As the angle of incidence (θ_1) becomes larger, the angle of refraction (θ_2) approaches (90°) until a point where no refraction is possible [6].

The light ray is then totally reflected back into the glass medium and no light escapes into the air. This condition is called Total Internal Reflection (TIR) and the angle θ_c at which (TIR) occurs is called the critical angle. The critical angle is determined by using Snell's Law and it is given by[5,6].

$$\sin \theta_c = \frac{n_2}{n_1} \quad \textbf{(1.2)}$$

The condition of total internal reflection is an ideal situation. However, in reality, there is always some light energy that penetrates the boundary. This situation is explained by the mode theory of light [6].

(1.2.3) Light propagation along an optical fiber

The transmission of light along an optical fiber can be described by two theories. The first is ray theory, This approach gives a clear picture of the propagation of light along the fiber and it is used to approximate the light acceptance and guiding properties of optical fibers [6]. The second is mode theory, or wave representation, approach where light is described as an electromagnetic wave. This theory describes the behavior of light within an optical fiber and it is useful to explain optical fiber properties like absorption, attenuation, and dispersion [7].

(1.2.3.1) Ray theory

Two types of rays can propagate along an optical fiber. The first type is made of rays that pass through the axis of symmetry of the fiber and are called meridional rays. [6]. The second type consists of rays that travel in a helical path through the fibers and never cross its axis; are called Skew Rays. Meridional rays can be classified as bound or unbound rays: bound rays remain in the core and propagate along the axis of the fiber by total internal reflection while unbound rays are refracted out of the fiber core [6].This in an ideal case where the core-cladding interface is perfect. However, imperfections at the core-cladding interface will cause part of the bound rays to be refracted out of the core into the cladding and escaping from the fiber [6]. In general, meridional rays follow the laws of reflection and refraction .In order to be guided along the optical fiber, a light ray incident on the fiber must be within a certain cone, known as the acceptance cone. The half-angle of this cone is called the acceptance angle;(a_{max}).Its value depends on fiber properties and transmission conditions[7].

Suppose that the incidence angle at the end of the fiber core is (a), and inside the fiber the ray makes an angle (θ) with the normal of the fiber axis. If the angle (θ) is smaller than the critical angle (θ_c), the ray will escape into the cladding; on the contrary, if (θ) is greater than the critical angle (θ_c)the ray will be guided along the fiber by(TIR) [6,7]. Figure (1.4) shows Total Internal reflection in fiber

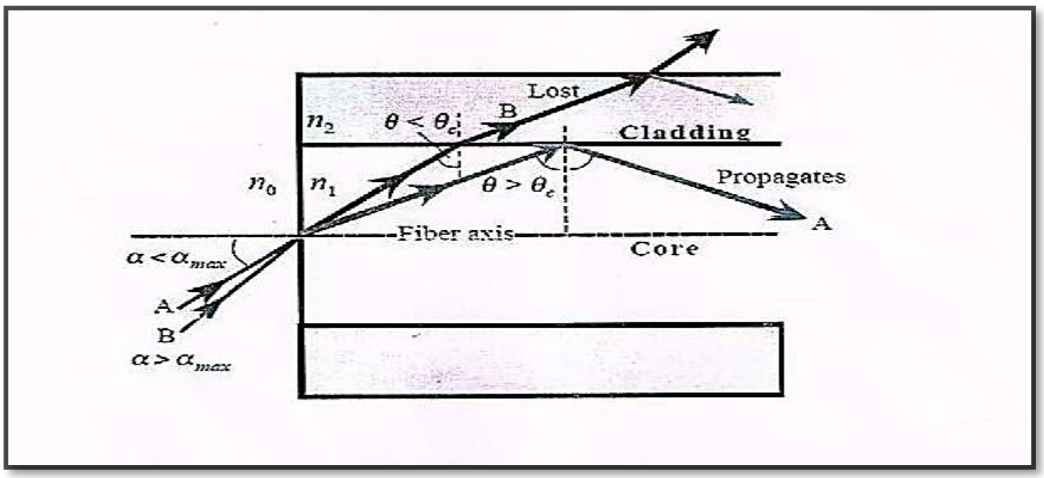

Figure (1.4). Acceptance angles of an optical fiber and total internal reflection [5].

Adapted the maximum value admitted for propagares (A) is the one for which ($\theta = \theta_C$).At the interface (n_0/n_1), from Snell law it can be written where (n_o) is the Refractive index of light in Vacuum [5,6].

$$\mathbf{n_o \bullet \sin \alpha_{max} = n_1 \bullet \sin(\frac{\pi}{2} - \theta_C)} \quad \textbf{(1.3)}$$

Being at the same time for TIR:

$$\mathbf{n_1 \bullet \sin \theta_C = n_2 \bullet \sin(\frac{\pi}{2})} \quad \textbf{(1.4)}$$

Thus by substituting for Θ_c:

$$\mathbf{\sin\alpha_{max} = \frac{(n1^2 - n2^2)^{1/2}}{no}} \quad \textbf{(1.5)}$$

The Numerical aperture *(NA)* of the fiber is a characteristic parameter defined by[5,6,7].

$$\boldsymbol{NA} = (n_1^2 - n_2^2)^{1/2} \qquad \textbf{(1.6)}$$

Where (NA) is the Maximum cone of light that can enter or exit the system

So in terms of (NA), the acceptance angle can be defined as [5].

$$\sin\alpha_{max} = \frac{NA}{no} \qquad \textbf{(1.7)}$$

the angle *(2*α_{max}*)* is called the total acceptance angle and depends on the (NA) of the fiber and the refractive index of the launching medium. This equation is strictly applicable only for meridional rays.

The (NA) is a convenient way to measure the light-gathering ability of an optical fiber. It can be used to measure the efficiency of light coupling between a source and a fiber[7].Skew Rays propagate without passing through the fiber axis. The acceptance angle for Skew rays is larger than the one of meridional rays, thus they increase the amount of light capacity of a fiber. They propagate in a helical motion, consequently they take- longer paths which increase their attenuation considerably. Skew rays tend to propagate in the annular region near the edge of the fiber core and so a large portion of them is considered to be leaky rays [6,7].

(1.2.3.2) Mode theory

Mode theory-uses electromagnetic wave behavior to describe the propagation of light along a fiber. It is useful for describing properties of light that ray theory is unable to explain. Light wave can be represented as a plane wave, which is described by its direction, amplitude, and wavelength of propagation. A plane wave is a wave whose wavefront is made of infinite parallel planes of constant amplitude normal to the direction of propagation. The wavelength of the plane wave is given by [7,8].

$$\boldsymbol{\lambda = \frac{c}{\nu n}} \qquad \textbf{(1.8)}$$

Where (c) is the speed of light in a vacuum, (ν) is the frequency of the light, and (n) is the refractive index of the medium. Figure (1.5) shows the direction and wavefronts of plane-wave propagation along the fiber. Not all wavefronts incident on the fiber at angles less than or equal to light acceptance angle propagate along the fiber. Wavefronts have to remain in phase for light to be transmitted along the fiber. If propagating wavefronts arc not in phase, they eventually disappear because of destructive interference. This interference is the reason why only a finite number of modes can propagate along the fiber [8].

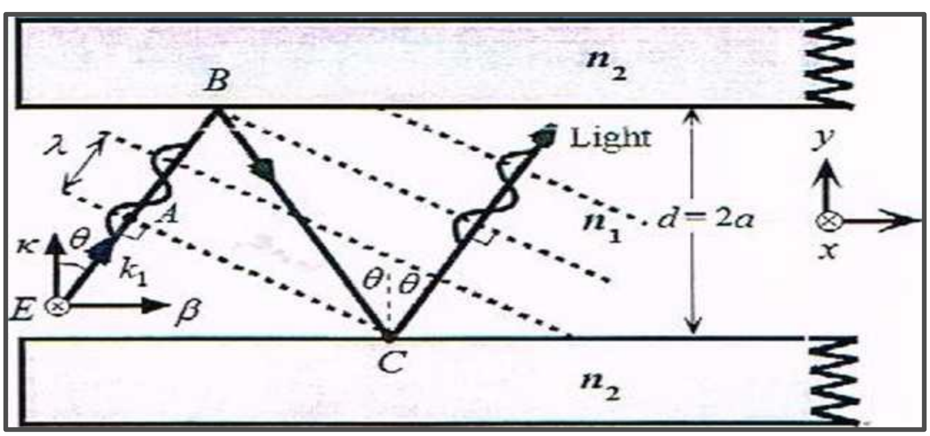

Figure (1.5).Wave front propagation along an optical fiber.The light ray must interfere constructively with itself to propagate successfully [5,6].

The modes of the fiber are then a set of guided electromagnetic waves in the optical fiber. Each mode of propagation is identified with a mode number (M=0,1,2,...) Figure 1.6 shows the electric field pattern of the first three modes (M= 0,1,2) traveling wave along the fiber[3,4].

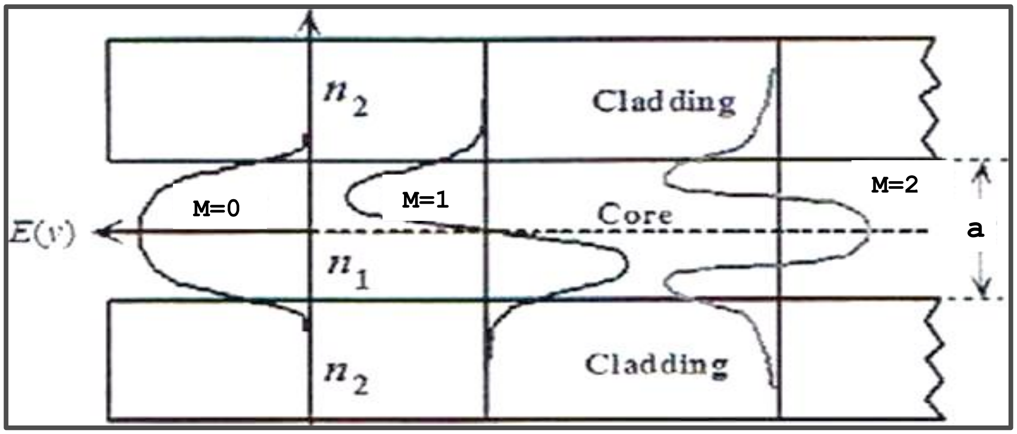

Figure (1.6). Electric field pattern of the first three modes (M=0,1,2) traveling wave along the fiber[5,6].

It can also be observed that the modes are not confined in the core of the fiber, but penetrate partially into the cladding material. While the low order mode are concentrated near the centre of the fiber, higher order modes are distributed more towards the external surface of the fiber. Thus a portion of light could be refracted out of the core and could be trapped into the cladding [7,8].

The order of the mode is also determined by the angle the wavefront makes with the axis of the fiber: high order modes cross the axis of the fiber at steeper angles compared to low order modes, while the lowest mode (M=0) travels nearly parallel to the fiber axis [7,8]. Figure (1.7) shows alight pulse traveling in a waveguide structure that enters a waveguide structure will thus be broken into various modes that propagate at different group velocity inside the guide. Therefore the signal emerging at the end of the guide will become broader than the input pulse [5,6].

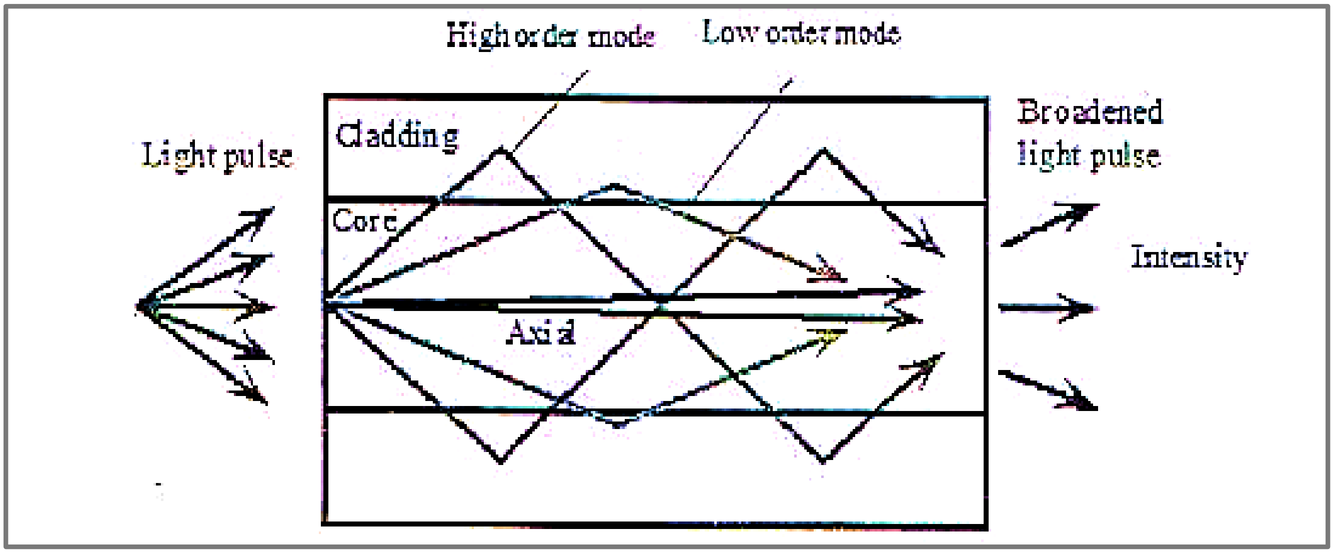

Figure (1.7). Schematic illustration of a light pulse travelling in a waveguide

Structure [5,6].

A last type of modes is the leaky mode that lose power as they propagate along the fiber. Generally, modes leaked into the cladding are lost in a few centimeters. However, leaky modes can carry a large amount of power in short fibers. There is an important parameter that describes how many modes a fiber can support: the normalized frequency *(V)*. It is a dimensionless quantity defined as[8,9].

$$\boldsymbol{V = \frac{2\pi a}{\lambda}(n_1^2 - n_2^2)^{\frac{1}{2}}} \qquad \textbf{(1.9)}$$

(a) is the core radius, and (λ) is the wavelength of light in air. For a given wavelength (λ) the *(V)* number depends on the waveguide geometry (a) and properties ($n_1$and n_2), so it is a characteristic parameter of the optical fiber. It can be demonstrated that for ($V \leq 2.405$) only the fundamental modes propagates along the fiber, while high order modes are lost in the cladding.this kind of fiber is called Single-Mode *(SM)* [7,8].

For low (*V)* values most of the power is propagated in the cladding material and it is easily lost at fiber bends. Hence, the value of (*V)* should remain near the (2.405) value.

When (*V*> 2.405), the number of modes propagating along the fiber increases sharply, This kind of fiber is called Multi-Mode *(MM)*. For large values, the number of supported modes of a fiber can be calculated approximately as [8,9].

$$M=\frac{4}{\pi^2}V^2 \tag{1.10}$$

(1.3) The Hosts

Since the first demonstration of laser emission from a ruby crystal in (1960), hundreds of crystals and glassed doped with rate-earth ion have been fabricated and utilized in solid-state laser to generate coherent emissions at different wavelengths. In contrast to crystals, glasses do not only have broad laser transition which are essential conditions for wavelength tuning and ultrashort pulses generation but also have broad absorption spectra that relieve the wavelength tolerance for the pump source. Most importantly, single-mode optical fiber, as the most flexible and compact gain media for high efficiency and excellent beam-quality laser generation, are mostly drawn from glasses[10,11].

Although crystalline fiber can be drawn using techniques of edge-defined film-fed growth, micro pulling-down, and laser heated pedestal growth, their cores can not be precisely controlled to small enough to ensure exclusive single-transverse-mode guiding and their length are also technically limited[10,11].

To date, silicate, phosphate, ZBLAN and chalcogenide glasses can be drawn into single-mode fiber. A variety of lasers have also been demonstrated in these glass fiber. The spectral rang of glass fiber lasers can cover from ultraviolet (UV) to mid-infrared [11,12]. In contrast to other laser, the attractive features of fiber laser include outstanding heat-dissipating capability beam quality, high optical conversion efficiency, simplicity and compactness, high single-pass gain, low laser threshold, broad gain bandwidth Silicate glasses are outstanding hosts for rate-earth ions and most of recent fiber lasers and constructed with silica fibers due to their low loss, high tenability, and strong strength. Phosphate glass as the host for the fiber lasers has a high solubility that enables extremely high doping high-gain fibers[12,13]. ZBLAN and chalcogenide glasses have drawn much attention because they are found to have low phonon energy and mid-infrared transparency. These glasses are excellent regions where emissions are hard to be optained from silicate and phosphate fiber [12, 13, 14].

Comparing to chalcogenide fiber, ZBLAN fiber have been studied for lasing actions with more significant efforts due to their high allowable doping levels, relatively high strength, high stability, and low background loss[11, 15]. Though there are some studies on rare-earth doped chalcogenide fiber lasers and amplifiers, their efficiencies and output powers are relatively low due to the low available rare-earth doping level, the large background loss, and the fragility of chalcogenide glass[16,17].

The composition of silica is [(0.1) O_3 – (1) Al_2O_3 – (98.9) SiO_2] and ZBLAN is [(53%) ZrF_4 – (20%) BaF_2 – (4%) La F_3 – (3%) AlF_5 – (20%) NaF], physical properties of silica and ZBLAN glass are listed in Table (1.1) [18,19].

Obviously, the mechanical, optical, and thermal resistibility of ZBLAN glass is much lower than that of silica glass. As a result, output levels of ZBLAN fiber lasers would be much lower than those of silica fiber lasers [18,19].

Table (1.1). Composition of basic properties of silica and ZBLAN glass [19].

Glass property	Silica	ZBLAN
Transmission rang (µm)	(0.16 – 4)	(0.22 – 8)
Phonon energy (cm^{-1})	1100	600
Transition temperature (c^{o})	1175	260
Specific heat ($J/g.k^{o}$)	0.179	0.151
Thermal conductive ($W/cm.k^{o}$)	1.38	0.628
Density (g/cm^{3})	2.20	4.33
Refractive index (at 0.589 µm)	1.458	1.499

(1.4) Rare earth doped solid-state laser

A solid-state laser is a laser with a gain medium that is a solid, such as crstalline or glass material, doped with Rare Earth RE or transition metal ions,that can be made in the form of bulk lasers, fiber lasers, or other types of waveguide lasers. Semiconductor based lasers are also solid-state devices, but are generally considered as a separate class of lasers. The host material must have good optical, mechanical, and thermal properties to withstand the severe operating conditions of practical lasers[20].Other important properties include hardness, chemical inertness, absence of internal strain and refractive index variations, resistance to radiation-induced colour centres and ease of fabrication. For crystalline host, several interactions between the host crystal and the dopant ion restrict the number of useful material combinations[20].

In particular the size and valence of the dopant ion should match that of the host ion to replace. The most common crystal hosts are: Sapphire, Vanadates, Fluorides and Synthetic garnets like yttrium aluminum garnet (YAG), gadolinium gallium garnet (GGG) and gadolinium scandium aluminum garnet (GSGG), glass is an important class of host material for solid-state laser, especially doped with RE ions. Glass is easy to manufacture, versatile and less expensive than crystal[20,21].

It allows a homogenous distribution or RE ions, and these ions in glass show a large inhomogeneous broadening of the absorption and emission cross section, due to the lack of a unique and well-defined crystalline field surrounding the individual active ions[21]. Moreover, glass possesses a particular viscosity-temperature relationship that allows for fiber drawing. However, glass has a much lower thermal conductivity than most crystalline hosts and this causes, for laser rods, large thermally induced birefringence and optical distortion when they are operated at high average powers. Besides, a low thermal conductivity causes a lower thermal shock resistance than crystals [22].

In the following, the discussion will be limited to RE doped solid slate lasers based on glass material, and specifically phosphate glass [21,22]. In order to obtain an active material for solid-state laser, host material must be doped with an active ion, which must have sharp fluorescent line, broad absorption bands and high quantum efficiency for the wavelength of interest. ‘These characteristics are generally shown by solids that incorporate a small amount of active ions, in which the optical transitions can occur between states of inner incomplete electron shells. RE ions have been the most extensively used active ions, because they exhibit a wealth of sharp fluorescent transitions representing almost every region of the visible and near-infrared portions of the spectrum. [22].

(1.4.1) Rare earth

The rare earths atoms are divided into two groups: the Lanthanides that begin with cerium (Ce, Z=58) and end with lutetium (Lu, Z = 71) and the Actinides from thorium (Th, Z = 90) to lawrencium (Lr, Z = 103). Despite their name, (RE) elements are relatively plentiful in the Earth's crust,[22]. Only the lanthanides are considered here, because they are of greater than importance in lasers and amplifiers; many actinides, in fact, have no isotopes stable enough to be used in such devices, only promethium (Pm) has a short half-life. Let us consider a classic description of atom as an inner nucleus surrounded by shells of electrons, which are gradually filled as one moves along the periodic table. In general, the radius of each shell is larger than the previous one, but at the atomic number (Z = 57), an abrupt contraction takes place. [23]. This latter instead of having a larger radius than the (*5S*) and (5*P)* shells actually contracts and becomes shielded from the environment by these shells. This effect is called Lanthanide Contraction and is the reason of RF [22,23]. peculiar optical and electronic properties. The most common and stable form of RE elements in condensed matter is the ionic form, in particular the trivalent (3+) state [22,23]. When a trivalent ion is formed, the RE atom gives up its outermost electrons and the electronic configuration is Nd^{3+}**:**[Xe] $4f^4$ $6s^2$,where Xe :$1s^2$,$2s^2$ $2p^6$,$3s^2$ $3p^6$,$4s^2$ $3d^{10}$ $4p^6$,$5s^2$ $5p^6$ [24].

(1.4.2) Nd^{3+}- doped optical fiber

This section describes basic characterization measurements performed on most fibers fabricated for this work, including the (Nd^{3+})-doped fibers. This involved measurements of fluorescence lifetime, absorption spectra for light in core and inner cladding, and coupling efficiency of available diode pump lasers[25]. Background loss was often measured too. A knowledge of those parameters is a prerequisite for the further development of fiber lasers . When a new fiber has been fabricated and its’ refractive index profile has been, measured by the fabricator, the first step is typically to measure the absorption in the core and inner cladding. Absorption spectra for light launched into the inner cladding of double-clad fibers are simply measured with a white light source and a spectrum analyzer [25]. The fiber can be cut back for improved accuracy. However, different me is with different overlaps with the core are absorbed at different rates. Therefore, unless complete and rapid mode- mixing occurs in the fiber, the absorption is not unique, but depends on the launch, the fiber length, and the geometric arrangement of the fiber. To measure the absorption of light travelling in the core of a cladding-pumped fiber with a low-index polymer outer cladding, the following procedure was used [26].

Sometimes a very short fiber length must be used owing to a high core-absorption and the limited dynamic range of the measurement system. The fiber was stripped of its outer cladding, at least at its ends. Index matching fluid with a higher index of refraction relative to that of the inner cladding of the fiber was applied to strip cladding-modes, at least at the ends of the fiber. In some cases, stripping the fiber and covering it with index-matching oil through most of the mid-section, or otherwise intermittently throughout the mid-section, helped to strip cladding-modes more thoroughly [26]. This improves the dynamic range of the measurement, which would be limited by any light propagating through the cladding. The core absorption was then measured using the white light source and a spectrum analyzer [26].The measurement can be repeated after the fiber is cut back for better accuracy. In case the tested fiber was too short to effectively strip cladding-modes, [26]. The lifetime of neodymium metastable ($^4F_{3/2}$) level was measured with pulsed excitation by a diode laser. The diode laser was on-off modulated either directly via the current or externally with a mechanical chopper. To have an accurate measurement, stimulated emission and reabsorption must be negligible. Lifetime shortening via stimulated emission was avoided by using low pump levels. Furthermore, in double-clad of NDFs, reabsorption is quite weak and does not affect the measured lifetime under typical measurement conditions, since most detected fluorescence propagates in the inner cladding and interacts only weakly with the Nd^{+3}-ions in the core[26,27].

(1.4.2.1) Neodymium energy levels

A partial energy level diagram, with the relevant transitions for the pump bands and the fluorescence bands of (Nd^{3+}) is shown in Figure (1.8).The numbers indicate the approximate wavelengths of the Nd^{3+} laser transitions, spanning the range from (0.9×10^{-6} to1.3×10^{-6})m[28].

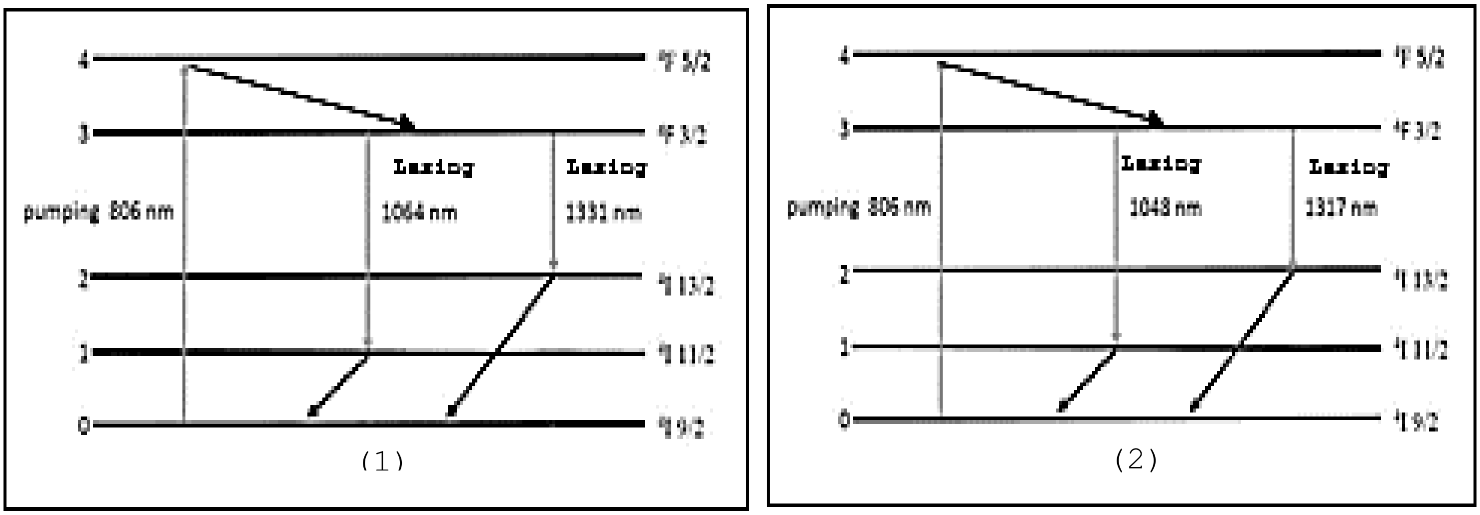

Figure (1.8): Partial energy level diagram of (Nd^{+3})-doped 1-silica and 2-ZBLAN fiber laser.

Figure 1.8- Partial energy level diagram of (Nd^{3+})-doped silica and ZBLAN host fiber showing the pump at (806×10^{-9}m) and the lasing wavelengths in silica(1064×10^{-9}m and 1331×10^{-9}m) and in ZBLAN (1048×10^{-9}m and 1317×10^{-6}m). The wave lines indicate rapid non-radiative transitions. (Nd^{3+})-ions have many energy levels, but the most important ones are the metastable$^4F_{3/2}$ level[28].

The pump level ($^4F_{5/2}$) and the fluorescence terminal levels ($^4I_{13/2}$,$^4I_{11/2}$, and $^4I_{9/2}$) (the ground state). Furthermore, the ($^4I_{9/2} \longrightarrow {}^4F_{5/2}$) transition corresponds to absorption of a pump photon from the ground level[29].Laser emission is most commonly, and easily,obtained on the($^4F_{3/2} \longrightarrow {}^4I_{11/2}$) transition at ($\sim1100\times10^{-9}$ m).The ($^4F_{3/2} \longrightarrow {}^4I_{9/2}$) emission line is centred at ($\sim 900\times10^{-9}$m), and the ($^4F_{3/2} \longrightarrow {}^4I_{13/2}$) transition emits in the range (1300×10^{-9} -1400×10^{-9} m). Some wavelengths that suffer from excited-state absorption from the metastable ($^4F_{3/2}$) state are also indicated [29,30].Figure (1.9) shows a emission cross section spectra of Nd^{3+} -ion for representative glass compositions

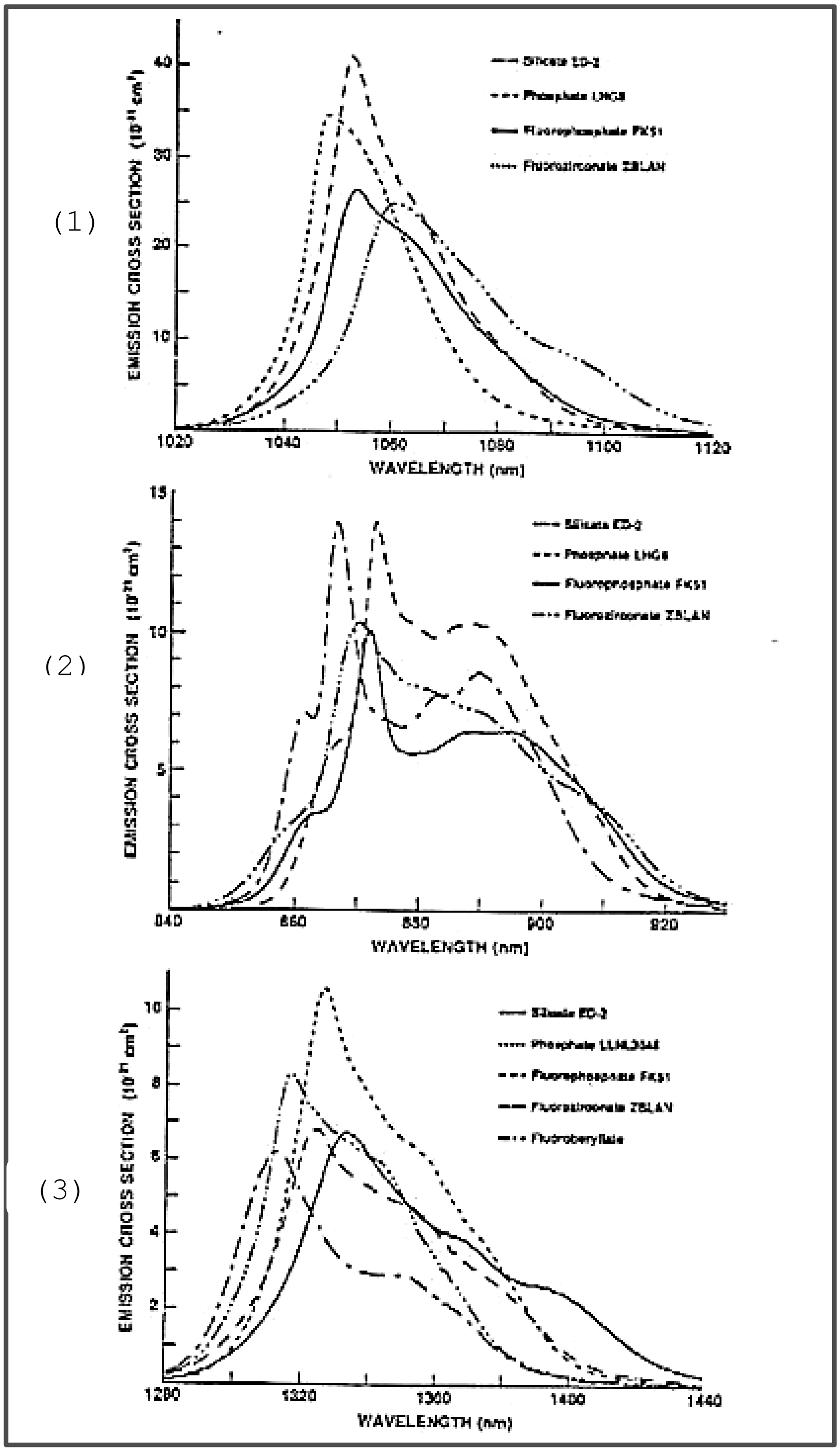

Figure(1.9):The emission cross section spectra of Nd^{3+}ion for representative glass compositions[22].

(1.4.2.2) Radiative transitions

the (N) electron state configuration of the RE ions is not sensitive to the environment, on the contrary the transition probability between these electron states is sensitive to the surrounding ions, both radiatively and nonradiatively.If we assume the host medium as a collection of charged particles, the elastic displacement of the electronic charge distribution to the nucleus causes a collection of induced electric-dipole moments. Classically, a light wave consists of electric and magnetic fields which vary sinusoidally at optical frequency. Since a light wave interaction with a material induces a charge displacement, its effect can be expressed in terms of the field induced electric-dipole moment [27]. The likelihood of transitions between electronic levels in an atom is governed by certain selection rules. However, for ions in a glass, internal electric and magnetic fields can break certain symmetries, so that originally dipole-forbidden transitions become possible by mixing of states with different parity. Such processes, however, exhibit a small probability to occur [31]. The resulting transitions are called Weakly Allowed Transitions. Whereas typical upper-state lifetimes are of the order of a few nanoseconds for allowed transitions for spontaneous emission, weakly allowed transitions for ions in glasses are typically between micro second sandmilli seconds. ‘Such long-lived levels are called metastable states. Optical transitions in RE ions have been found to be predominantly electric-dipole in nature, and thus, since no change of parity is involved, mixing of higher lying states of opposite parity into the (4F) configuration, introduces a degree of electric dipole strength into the (F $\longrightarrow$ F) transitions .Magnetic dipole and electric quadrupole transitions are allowed by the selection rules but their contributions to radiative decay arc generally small or negligible[31].

(1.4.2.3) Nonradiativer relaxations

In addition to the interaction with (EM) radiation through emission and absorption of photons, RE ions in glass can interact with vibration of If the energy gap (ΔE) between the electronic levels is of the order of one or two phonons, for example the Stark components of a multiplet, the transitions will occur rapidly. This leads to thermal occupation of levels above the ground state or metastable excited state if the separations are on the order of the thermal energy, When the energy- gaps (ΔE) are much larger than (κT),[31,32].

Where (T) is the Temperature of the host material in (Kelvin) an (K) is Boltzmann constant

For the energy conservation it is required that [31].

$$\rho\, \hbar\omega_{Ph} = \Delta E \qquad \textbf{(1.11)}$$

The nonradiative decay rate (W_{nr}) is inversely proportional to the exponential of the energy gap separating the two levels[31,32].

$$W_{nr} = W_0 \exp[-\alpha \Delta E] \qquad \textbf{(1.12)}$$

Where (α) is the correlated to phonon vibration (ω_{Ph})

From the equations (1.12) follow that the nonradiative decay rate (W_{nr}) has not only an exponential dependence on ΔE but also on the phonon vibration (ω_{Ph}).In practice (W_0),($\hbar\omega_{Ph}$) are considered as empirical parameters that are host-dependent, but insensitive to the RE ion and energy levels involved.-Their values were measured for several glasses and crystalline materials. Table (1.2). lists the maximum phonon energy of various glasses that corresponds to the stretching vibrations of the glass network formers[32].

Table (1.2). Maximum phonon energy of various glasses [32].

Glass type	Phonon energy($\hbar\omega_{ph}$) (cm^{-1})
Borate	1400
Silica	1100
Phosphate	1200
Germinate	900
Tellurite	700
Flurozirconate	500
Chalcogenide	350

(1.5) Optical resonator

The most common fiber laser resonator ıs the Fabry-Perot Figure. (1.10) shows the fiber resonators. formed by ordinary dielectric mirrors in close contact with the ends of the doped fiber Figure. (1.10,1) Pump light is launched from the left-hand side, through the dichroic mirror, into the doped fiber. Laser light is generated in the fiber through a stimulated emission process, and it is extracted on the right-hand side. A variation of this design is possible by depositing dielectric reflector directly on fiber ends, usually with some evaporation method [22].

The Fresnel reflection from a bare fiber end face is often sufficient for the output coupler of a fiber laser, especially in lasers based on a high gain transition.

For commercial products, it is common to avoid the use of free space optics and all- fiber Fabry-Perot resonator designs are preferred. Figure (1.10,2). shows a resonator in which the optical feedback is provided by two Signal fiber loops, one at each end of the doped fiber. Each loop is made of a length of doped fiber closed by a coupler. They have a typical insertion loss of less than 0.3 dB, so that the loss of this resonator is quite low [22].

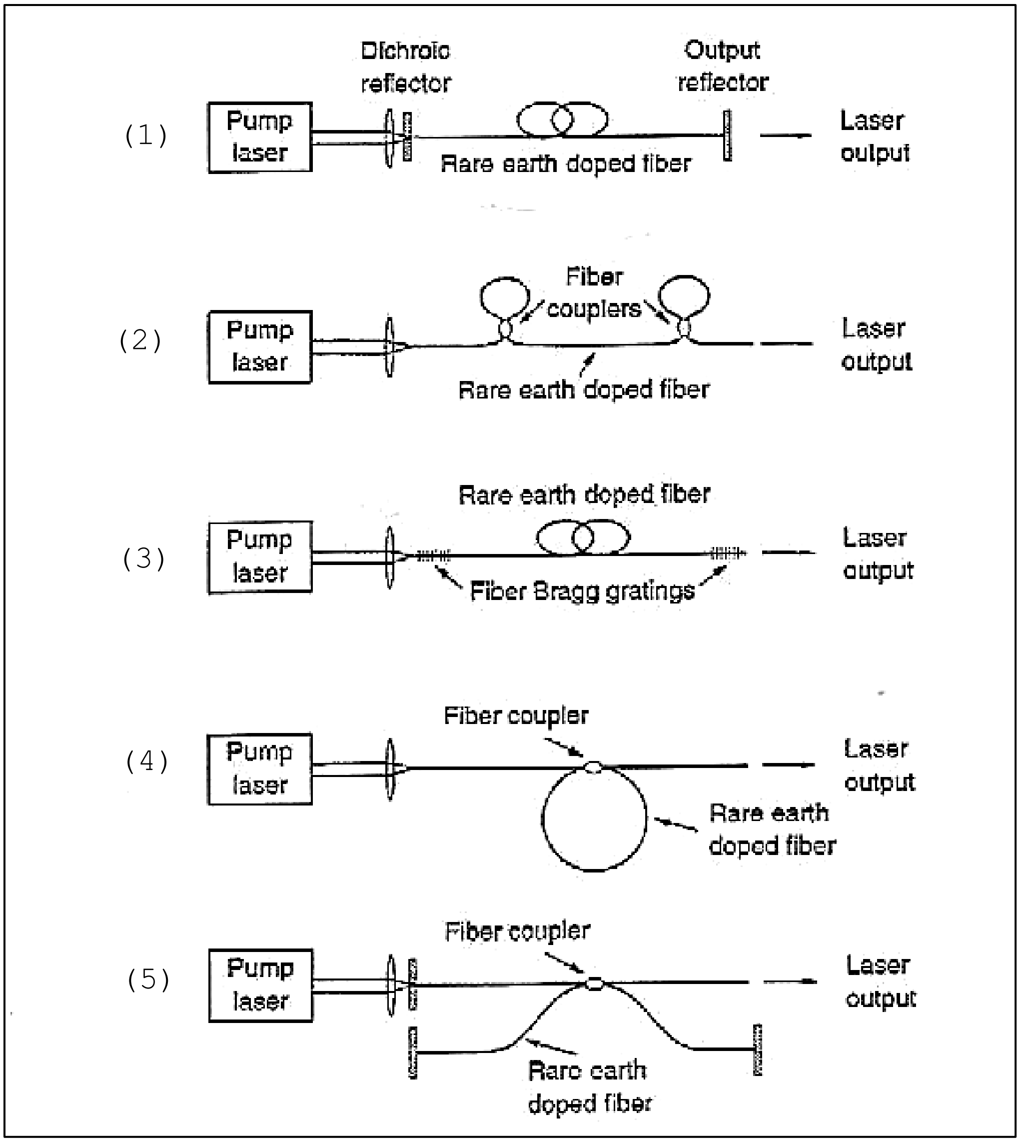

Figure (1.10). Step of various fiber resonators : (1) fabry-perot with dielectric reflector ; (2) fabry-perot with all-fiber reflector ; (3) fabry-perot with fiber Bragg gratiangs ; (4) ring ; and (5) fox-smith [22].

Another solution is provided by the use of fiber Bragg gratings Figure. (1.10,3) that can be either spliced to the fiber end or, if possible, directly written in the doped fiber, reducing the number of splice and consequently the loss a particular benefit of this design is the possibility to use as pump source a fiber Apigtailcd laser diode that can be spliced directly to the fiber laser, thus reducing coupling loss[22,23].

Alternative setup for fiber laser is the all-fiber ring resonator Figure.(1.10,4), which consists in a loop of doped fiber with a low loss fused fiber coupler. The displayed ring laser resonates in both directions and, therefore, has a bidirectional output. This means that its conversion efficiency is only half compared to the one of Fabry-Perot cavity. It is possible to overcome this limitation by introducing an optical isolator in the ring[22], which forces unidirectional operation. However, this element introduce also a small loss, thus unidirectional ring fiber lasers require higher threshold.

A less commonly used solution is the Fox-Smith resonator Figure. (1.10,5), which consists in a standard Fabry-Perot resonator coupled through a fiber coupler, to a third branch with a mirror at its end. ‘The doped fiber is positioned in one of the arms and pumped through one of the reflectors[22,23].

(1.6) Pumping Sorics

Consider two energy level schemes for obtaining apopulation inversion, in both schemes, ahigher state is excited directly by the pumping mechanism, and this state decays quikly and nonradiatively to the upper laser level, stimulated emission then occurs from upper to lower laser levels, which is the optical gain transition [1,2].

The difference between the two schemes is in the position of the lower laser level, for the three-level system, the lower laser level is in the ground state, whereas for the four- level system the lower laser level is excited stste of the system [1,2,3].

In the three-level system requires that at least half the atoms be pumped of the ground state, which agood deal of pump energy, whereas for the four-level system can achieve population inversion with only a small number of atoms raised out of the ground state, therefor, it is easiest to obtain amplification and lasing with a four-level system because not as much pump energy must be wasted in removing atoms from the ground state [3,21].

Generally,the pumping sorics are used in optical fiber lasers are (Nd^{3+}-YAG ,GaAs, ALGaAs, InGaAs, Ar^{3+}ions, dye Laser), in this study used the ALGaAs laser is pumping sorics for the output power (0-10)W [3,21].

(1.7) Advantages of fiber laser

Optical fiber lasers have several key advantages over conventional bulk solid state laser:

1-Outstanding heat-dissipation capability thanks to their high surface area-to-volume ratio and the distribution of the thermal load over a considerably long length, resulting in excellent heat dissipation. Thermal distortion of the beam is thus negligible, and the beam quality depends primarily on the physical design of the fiber. Tight confinement of both pump and laser light, resulting in a low threshold and high optical conversion efficiency [33,34].

2-Excellent beam quality, quite insensitive to thermal and mechanical perturbations. Single mode fiber laser exhibits a diffraction-limited Gaussian beam that is a beam that can be focused to the smallest spot possible for a given wavelength, i.e. the beam quality is ideal. For a given optical power, a diffraction-limited beam has also the highest brightness[33,34].

3-Simplified beam handling and beam delivery that enables to transport higher levels of power inside the laser, using higher brilliance to deliver more useful power at the work piece[33,34].

Possibility of pumping with low cost reliable diode lasers.

4-Scalability to high power level through modularity. Commercial devices at 10^{-3}W level commonly employ more sophisticated architecture than a single stage laser resonator. They often use one or more high power amplifier stages that are seeded by a medium or even high power fiber oscillator[33,34].

Possibility to realize the whole laser resonator only using fiber components, all-fiber setup, such as fiber Bragg gratings and fiber couplers. This configuration avoids the use of free-space optics that can be critical in presence of vibrations or large temperature variations; in addition light in fibers is totally confined within the core cladding structure and thus completely shielded from the environment. Using an all-fiber setup, a robust and compact system design is possible, thus enabling the usability of fiber lasers outside the laboratory [33,34].

(1.8) Literature Review .

Fiber lasers are nearly as old as the glass laser itself the first demonstration of a fiber laser dated back to the (1960’s) when C.J. Koester and E. .Snitzer developed a flash lamp pumped Neodymium-doped optical fiber with a large core-however, after these pioneering efforts, work in fiber lasers essentially stopped until (1985), when D.N. Payne and co-workers at Southampton university, reawakened interest in fiber laser announcing the fabrication of the first low-loss single fibers containing (Nd) and (Er)[1,3].

In that period, fiber lasers were investigated mainly for their applications in telecommunication field, as optical amplifier for path long-haul (1.5×10^{-6}m) and local area network (1.3×10^{-6}m). They were mostly single-mode devices with average of (10^{-3}w). The next significant step forward in fiber laser evolution was introduction in (1980) of double clad fiber structure, that leads to a gradual increase in fiber laser output power in the intervening decode, thanks also to the increase of pump diode powers and brightness, as well as decreasing cost per watt[1,3].

In the past few years, (cw) µw-level silica fiber using length of tens of meters to provide effective absorption of pump power. Power scaling of these sources is eventually limited by stimulated Brillonin scattering (SBS) and photo – darkening, which can limit the maximum attainable output power or induce output power degradation over time [2,3].

M.J.F. Digonnet and C.J. Gaceta. [1985] [34]: “unsing the formalism of mode overlap, a theoretical analysis of optically pumped fiber laser amplifiers oscillators is developed. Simple and accurate closed-from expressions are derived for the gain of fiber amplifiers and the threshold and energy conversion efficiency of fiber laser oscillators in terms of the fiber and laser material parameters and the pump and single modes, when applied to step-index Nd^{3+} - doped fiber lasers, this study predicts optimum fundamental mode oscillation in fiber with a (V) number of (5-25) with submilli watt thresholds and nearly quantum-limited conversion efficiencies**"**

P. Alcock.et.al.[1986][35]: " Amenomode silica fiber doped with Nd^{3+} has allowed the first demonstration of (CW) laser action on the ($^4F_{3/2} \longrightarrow {}^4I_{9/2}$) transition of Nd^{3+} in a glass host, with tuning over the range (900×10^{-9}-945×10^{-9}) m"

D.C.et.al. [1987][36]: " Recent studies of monomode silica fiber which has rare-earth impurity ions incorporated into the core region have shown that it can exhibit laser action with low threshold and high efficiency when end pumped by on external laser source. We described the first demonstration of Q-switching Nd^{3+} transition at (10.9×10^{-6}m) using a fiber laser of this type. In Q-switched operation an introcavity acousto-optic modulator was needed to generate pulses of (200×10^{-9}s) duration and (8.8w) peak power at repetition rates up to (1×10^{3}HZ) "

M.W.Phillips.et.al .[1987][37]: "Modulated pumping of Nd^{3+} doped silica monomode fiber laser has been investigated experimentally. For small modulation depths the laser exhibits a resonance of the relation oscillation frequency , providing pulses of a few microseconds duration at a repetition rate in the region of (10×10^{3}HZ), dependent on the average pump level above threshold".

G.Geister and R.Ulrich. [1988][38]: "A $LINbo_3$; T_i intrgrated-optic phase modulator is inserted into the cavity of a Nd^{3+}-doped fiber laser operating near (λ_L=1080×10^{-9} m). Active mode-locking was achieved at the fundamental frequency (29×10^{6}HZ) of the cavity and at higher harmonics thereof, using sinusoidal modulating voltages of (5-15) V_{rms} . the laser output is a stable periodic train of pulses, having lengths ($\leq90\times10^{-12}$ sec) energies ($\geq1.5\times10^{-12}$J) and a repetition rate (29×10^{6} HZ) "

" P.R.Morrel.et.al.[1988][39]: "The spectral variation of gain and excited absorption have been measured for Nd^{3+}-doped silica fiber co-doped with Germania and alumina. The results show that an observed excited state absorption peak at (1300×10^{-9}m) is considerably reduced47 in the alumina co-doped fiber"

M.S. Osullivan. [1989][40]: "A narraw linewidth ,(cw) Nd^{3+} -doped fiber laser is described for application to the excitation of the (1092×10^{-9}m) ,(5p) $^2p_{1/2}$-$(4d)^2$ $D_{3/2}$ transition in Sr^+ .The laser incorporates a gradient – index lens as an intra-cavity beam collimator and employs agroting together with a series of etalons as frequency selective and tuning elements .Tunable laser output in the region of (940×10^{-9}m) is also described"

M.Ledig. [1991][41] : "A (cw)-pumped Nd^{3+} -deped silica fiber laser is mode –loked by feeding back the light from linear external mode –loked by feeding mirror.The duration of laser pulses is measured in dependence on the mismatch between the lengths of main and external cavity .The shortest pulses have a full width at half maximum (FWHM) of (32×10^{-12}sec).They are generated if the laser cavity is (3.2×10^{-9}m) shorter than the external cavity"

M.Le.Flohic.et.al. [1991][42]: " describe both experimentally and theoretically the two –stage process of the transient buildup of emission in Nd^{3+}-doped fiber lasers. After switching on the pump, spontaneous emission increases first until the gain becomes suffeicient to compensate for the cavity losses; then the laser field develops and reaches the steady state after more or less regular oscillations .During this second stage ,an almost chaotic spiking is obtained either for high pumping rates and /or at low temperature"

P. R . Morkel .et. al. [1992][43]: "A high – power , laser –diode pumed , Q . switched Nd^{3+} – doped fiber laser operating at (1.053×10^{-9}m) is described which is suitable for use in time – multiplexed fiber sensor applications . The laser emits (>1 $\times10^3$W) pulses at (1.053×10^{-9}m) with (2×10^{-9}sec) duration at up to (1×10^3Hz) repetition rakes for an absorbed pump power of only (22×10^{-3}W) at (810×10^{-9}m) with (2×10^{-9}sec) duration at up to (1×10^3Hz) repetition rakes for an absorbed pump poer of only (22×10^{-3}W) at (810×10^{-9}m) "

M.D. Selker and J .L .Dallos. [1992][44]: " We have demonstrated simultaneous lasing and self-frequency doubling of a Neodymium and Germanium doped Silica fiber laser at (1.064×10^{-9}m) . The doubling action is provided by a self-organized phase matching grating in the fiber .The laser was mode-locked using a linear external cavity which produced (600×10^{-12}sec)pulses a (1.664×10^{-9}m) "

". P. R Morkel .et .al [1993][45] : " The operation of a short-pulse , Q-switched , Neodymium-doped fiber laser operating at (1.054×10^{-6}m) is described experimentally and theoretically . The laser is efficiently pumped with a single-stripe AlGaAs laser diode and emits ($>1\times10^{3}$w) pulses . It is seen that due to high gain , short pulses with high energy extraction efficiency can be obtained . The feature of broad emission lines associated with rare-earth-doped glass is exploited to demonstrate tunable , Q-Switched operation over a (40×10^{-9}m) tuning rang "

U.Gheara.et.al.[1994][46]:"Laser made of regular (i.e.non .polarization-maintaining) rare-earth doped single mode fibers have birefringence which is randomly diotriuted along the length of the gain medium This property and its consequences are examined in detail , together with applications tunable laser , as well as to lasers capale of simulataneously lasing in a number of discrete spectral lines"

"H.Ammann.et.al.[1994][47]: "have investigated experimentally and theoretically the propagation and amplification characteristics of short optical pulses at (1.3×10^{-6}m) in a Neodymium –doped flourozirconate fiber . We have found that pulses(4×10^{-12}sec) with Sub-NJ eneries can be propagated and amplified without appreciable temporal and spectral rashaping . The propagation and amplification of Sub-psec pulse (300×10^{-15}sec) of comparable energy , however , is significantly affected by the diopersive and nonlinear properties of the fiber . The comparison between experimental and numerical results allows to identify the pulse shaping mechanisms involved which is important in order to assess Nd^{3+} doped fluoride fiber amode-locked fiber laser"

F. Sanchez . et . al . [1995] [48]: **"**A simple theoretical modeling of a fiber laser that ineludes distributed losses and inhomogeneous pumping which pressented distributed closed-from expressions for both the output and backward at the input mirror intensities are obtained . The model is based on an extended formulation of the Rig red's theory .In particular , we show that for long (short) lasers optimal output power is achieved with low output-coupler reflectivity"

J. Wang. et. al. [1995] [49]: "The fabrication of a highly efficient Nd^{3+}-doped single-mode fiber laser operating at (1.064×10^{-6}m) described . The Nd^{3+} is introduced by doping (Nd_2O_3) into a multicomponent lead-silicate glass host . A fabrication technique for doping rare-earth evenly into commercial optical glasses is demonstrated . Spectroscopic properties relevant to laser operation in Nd^{3+}-doped lead-silicate glass fibers were measured and influence of Pb^{3+} ions on the spectral properties was analyzed , Owing to the long lifetime and large absorption emission cross-section of Nd^{3+} this lead-silicate glass host , a high-performance Nd^{3+}-doped lead-silicate fiber laser device operating at (1.064×10^{-6}m)”.

M. Wegműller. et. al [1996] [50]: ."A diode pumped Nd^{3+}. ZBLAN Auoride fiber laser operating at (1.05×10^{-6}m) Experiment and theory reveal that the fiber gain is strongly saturated which leads to an improved stability when the fiber laser is passively mode-locked with a multiple quantum well storable absorber pulse of (9×10^{-12}sec) duration with a pubc energy of (70×10^{-12}J) are routinely obtained from a simple and compact set-up without dispersion compensation . On the other hand band width limited (2×10^{-12}sec) pulses are obtained for a slightly anomalous total intracavity dispersion"

T. Chartier. et. al [1996][51]: "A detailed experimental and theoretical of optical feedback effects in Nd^{3+}-doped fiber lasers is presented . of particular interest is an output-intensity reduction attributed to broadband nature of the laser spectrum with a mode-selection mechanism of external Fabry-Perot cavity . The theoretical approach on a simple multimode rate-equation model , provides on excellent description of experimental results"

".Y. C. Hool and H. B. Ahmad. [1996] [52]: "Operating characteristics of a Q-Switched Nd^{3+}-doped single-mode silica fiber with a mechanical chopper as a Q-switching device are presented . peak powers as high as self-mode-locking in Nd^{3+}-doped fiber is also reported . An output power of (312 W) with a centre pulse duration of (4×10^{-9}sec) is observed"

R. Hofer. et.al. [1997][53]: " report mode-locked operation of a Nd^{3+}-doped fiber laser at a wavelength of (920×10^{-9}m) . The moving mirror technique was used as a starting mechanism and mode-locking was self-sustaining by nonlinear polarization evolution . Nearly transform limited pulses of (53×10^{-15}sec) duration with output energies of (500×10^{-12}J) were generated "

R. Bőhm. et.al. [1997][54]: "The optical nonlinearity , saturation of the lower laser level , and spontaneous emission modify the relaxation oscillations in a Nd^{3+}-doped fiber laser . A novel four-level rate_equation model correctly describes the modified laser dynamics and allows the determination of the second-order susceptibility of the fiber , lifetimes of upper and lower levels , cavity loss . and the number of oscillating modes by monitoring relaxation oscillations "

J.M.Lee. et. al. [1997] [55]: "The start-up of passive mode-locking with a moving mirror was demonstrated in a Nd^{3+}doped glass fiber laser pumped by a single-stripe laser diode and pulses with a duration of (250×10^{-15}sec) were generated . A relatively long fiber was used to lower the mode-locking threshold by increasing the kerr effect in the fiber and variation of the threshold for the start-up of mode-locking was investigated by changing the length of the fiber from (0.74 – 2) m"

K. Ueda and A. Liu [1998][56]: "Possible designs of high-power fiber lasers are discussed in work related to the future power delivering system in laser material processing factories.High efficiency operation of (73 %) was demonstrated by clod pumping schem using homogeneous absorption regime of Nd^{3+}-doped rectangular double clad fibers.Fiber-embedded lasing dis and tube are proposed for the high-power laser that produces more than (1×10^{3}w)for a single core of (50×10^{-6}m) in diameter"

J.Hűnkcmeier. et. al. [2000][57]: " Diode-pumped Nd^{3+}-and Yb^{3+} multimode fiber lasers with external cavities allow sensitive measurements of inter a cavity absorption in the spectral ranges of (0.9×10^{-9} – 0.945×10^{-9})m . The sensitivity is characterized by effective absorption path length and is derived from the spectral dynamics of the lasers with intracavity atmospheric absorption , and calibrating the emission spectra with HIIRAN database . The highest sensitivity is achieved with a (cw) Nd^{3+}-doped fiber laser ; it corresponds to a (140×10^{3} m) effective path length of absorption"

N. S. Kim. et. al. [2000][58]: "Numerical analysis is investigated for the high-power double-clad fiber lasers and experimental results using different microscope objectives for focusing into Nd^{3+}-doped rectangular double-clod fiber also performed . The numerical analysis includes dependence of output power an output mirror reflectivity absorbed pump power, losses, and fiber length and pump power distribution for the cases of one-end and two-end pumps with 20 dB/km loss.Calculated conversion efficiencies are 76.36 % , 69.73 % and 63.84 % for lossless , two-end pump and one-end pump fiber lasers respectively "

H. S. Seo. et. al. [2002][59]:" created a design for an Nd^{3+}doped clad-pumped silica fiber laser to enhance the pump absorption and lasing efficiency for a butt-eoupled end-pumped scheme Two concatenated a diabetic tapers formed within the laser cavity simultaneovely removed higher order mode and were spliced to conventional single-mode fibers .We theoretically analyzed mode along the composite cavity and caper achieved continuous wave (cw) oscillation in the (LP_{o1}) mode at (1.064×10^{-6}m) and a laser output power of over 820×10^{-3}w with a efficiency of (27 %)"

D.B.S.soh.et.al. [2004][60]:"A tunable high –power cladding –pumped Nd^{3+}-doped aluminosilicate fiber laser is demonstrated .The maximum power reached was (2.4 w) with a slope efficiency of (41%) and a threshold pump power of (1.68 w),both with respect to launched pump power ,when cladding pumped by two (808×10^{-9}m) diode pump sources at both fiber ends .The tuning range changed from (922×10^{-9}-942×10^{-9})m for a (25m) fiber length to (908×10^{-9}-938×10^{-9}) m with a (14m) fiber length , because of reabsorption effects. The filtered out the unwanted and competing strong transition at (1.064×10^{-9}m) while guidance of (0.9×10^{-6}m) remained intact"

"T.J.Kane.et.al.[2004][61]: "A cladding –pumped Nd^{3+}-aoped fiber with a fundamental – mode cut-off near (100×10^{-9}m) was used to build an amplifier with gain ever a range near (920×10^{-6}m) .pulses from an Nd:YVO_3 passively Q- switched laser were amplified and then frequency doubled in (LBO) to produce bule with (3w) average power"

"M.rusu.et.al. [2004][62]: " demonstrate a practical ultrafast Nd^{3+} - doped fiber laser operating in the (894×10^{-9}-909×10^{-9}) m spectral range. Using purposely designed semiconductor storable operation with clean transform- limited (360×10^{-15} sec) pulses was a chieves,"

J.Swiderski .et.al. [2005][63]: "A Q switched operation of a (1064 nm)Nd^{3+} -doped eliding –pumped silica a fiber laser using an electron apace modulation has been presented .The laser developed woplsnd at the temptation rate of up to(10×10^{3}Hz) .for a (5m) along double- clad fiber of (3m) length . pulses with the energy of (0.36×10^{-3}g)and the pulse duration of (84×10^{-9}sec) have been obtained, for the same fiber of (3m) length.Pulses of (154×10^{-3}g) energy and (48×10^{-9} sec) duration have been achieved"

M. Meenster.et.al.[2005][64]: " demonstrate femtoserond operation of a Nd^{+3} doped microstructure fiber laser .The fiber Provides and anomalous dispersion at lasing wave length of (1.064×10^{-6}m) and canes the construction of shert and simple cavity designs of a saturable absorber mirror ,fiber nonlinearity,and diopersion and produces transform limted sub (400×10^{-15} sec) pulses with a pulse with a pulse energy as high as (100×10^{-12} J) "

L.B.Fu.et.al. [2005][65]: " present a compact high power continuous wave tunable Nd^{3+}-doped double cladding fiber a prating on three-level $^4F_{3/2} \rightarrow {^4I_{9/2}}$ tansition with a maximum slope efficiency of (49.3 %) against absorbed (808×10^{-9} m) tuning range is achieved "

E. Yahel.et.al. [2006] [66]: "High-power continues-wave Nd^{3+} - Yb^{3+} co-doped fiber laser (NYDFL) are analyzed, based on a rate-propagation equation model, The model takes into account energy transfer between Nd^{3+} and Yb^{3+}, as well as cross relaxation between Nd^{3+} ions, and contributions from high-order modes to the Amplified spontaneous emission. Examples of cladding-pumped NYDFLs with distributed Bragg reflector at either end are presented**"**

R. A. Martin and Jonathan C. Knight. [2006][67]: " have fabricated a neodymium-doped phosphate glass fiber with a silica cladding and used it to form a fiber laser. A bulk phosphate glass of composition $(Nd_20_3)_{0.011}$ $(La_2O_3)_{0.259}$ $(P_2O_5)_{0.725}$ $(Al_2O_3)_{0.005}$ was prepared and the resultant material was transparent, free from bubbles and visibly homogeneous. The bulk phosphate glass was drawn to a fiber while being jacketed with silica and the resultant structure was of good optical quality, free from air bubbles and major defects. The attenuation at a wavelength of $1.06\times10^{-12}m$ was 0.05 dB/cm and the refractive index of the core and cladding at the pump wavelength of488×10^{-9} m were 1.56 and 1.46, respectively**"**

A.E. Siegman.et.al. [2006][68]: "The authors report laser oscillation in what appears to be a single transverse mode with very large mode area in optical fibers having heavily Nd-doped 100×10^{-6}m diameter cores with refractive index significantly lower in the core than in the surrounding cladding. Since fibers of this type cannot support conventional index-guided modes, their results appear to confirm a recent analysis which predicts gain-guided single-mode propagation in index antiguided fibers, provided the gain coefficient in the core exceeds a threshold value**"**.

H.Kalayciogly.et.al. [2008] [69]: "have achieved, for the first time to our knowledge, lasing in a new type of telluride – tungstate glass host doped with neodymium : Nd^{3+} : (0.8) Teo_2-90.2) WO_3. Lasing was obtained at 1065×10^{-9} m with two samples containing (0.5 mol%) and (1.0 mol% Nd_2O_3). During gain-switched operation , slope efficiencies of (12%) and (10%) were obtained with (0.5 mol%) and (1.0 mol%) doped samples, respectively, at a pulse repetition rate of 1000Hz. Judd-ofelt analysis was further employed two determine the emission cross section σ_e at 1065×10^{-9}m from the absorption spectra and life time data. The emission cross section from the Judd-ofelt analysis came to ($3.23\mp0.09\times10^{-20}$ cm^2), in reasonable agreement with the value of ($2.0\mp0.13\times10^{-20}$ cm^2) obtained from the analysis of laser threshold data "

J. Azkargorta.et.al. [2008][70]: "In this work we present a detailed study about the influence of the host matrix in the spectroscopic and laser properties of Nd^{3+} in three different fluoride glasses. Stimulated emission experiments performed under selective wavelength laser pumping show the existence of dichromatic emission from two distinguishable site distributions for Nd^{3+} in fluoride glasses. This result can be explained by the moderate inter-site energy transfer among Nd^{3+} ionsfound in these systems"

A.Peled.et.al. [2008][71]:" Report the design, fabrication, and characterization of a monolithic tapered rib waveguide laser made of Nd doped silica hafnia sol-gel. The laser has a (604×10^{-9} m) thick guiding layer. (CW) pumping was coupled in via a grating which also coupled out the lasing signal output, while reflection gratings supported the feedback. A lasing threshold of (20×10^{-3} W) and an output power of (2.45×10^{-3} W) were measured in a (3×10^{-2}m) long device. "

Z. Fan.et.al. [2008][72]: "A global optimization method - niche hybrid genetic algorithm (NHGA) based on fitness sharing and elite replacement is applied to optimize (Nd^{3+}-$Yb^{3+)}$ co-doped fiber lasers (NYDFLs) for obtaining maximum signal output power. With an objective function and different pumping powers, five critical parameters (the fiber length, L; the proportion of pump power for pumping (Nd^{3+}),

(Nd^{3+}) and (Yb^{3+}) concentrations,Results show that dividing equally the input pump power among 808×10^{-9} m (Nd^{3+}) and 940×10^{-9} m (Yb^{3+}) is not optimal choice and the pump power of (Nd^{3+}) ions should be kept around (10 - 13.78%) of the total pump power.Three optimal schemes are obtained by NHGA and the highest slope efficiency of the laser is able to reach 80.1%"

P.Dallocchio.et.al. [2009][73]: " present a compact Nd:silicate laser pumped by a single 1-W high-brightness commercial laser diode that generates pulses as short as (88×10^{-15} s) (nearly Fourier limited) when passively mode-locked with a saturable absorber mirror. We also tested a prismless cavity setup employing a single Gires-Toumois mirror, yielding 100×10^{-15}-s pulses. These setups are significantly simpler and more compact than those reported previously for short pulse Nd:silicate lasers."

C. N. Santos,et.al.[2009][74]:"In this work we performed a thorough spectroscope and thermo-optical investigation of yttrium aluminoborate glasses doped with neodymium ions. A set of samples, prepared by the conventional melt-quenching technique and with Nd_2O_3 concentrations varying from (0.1 to 0.75 mol %), were characterized by ground state absorption, photoluminescence, excited state lifetime measurements, and thermal lens technique, For the neodymium emission at (1064×10^{-9}m)($^4F_{3/2}\rightarrow 4I_{11/2}$ transition), no significant luminescence concentration quenching was observed and the experimental lifetime values ranged around (70×10^{-6}s). The obtained values of thermal conductivity and diffusivity of approximately ($10.3 \text{ X } 10^{-3}$ W/cm K)and ($4.0 \text{ X } 10^{-3}$ cm^2/s), respectively, are comparable to those of commercial laser glasses.Moreover, the fluorescence quantum efficiency of the glasses, calculated using the Judd-Ofelt formalism and luminescence decay, lies in the range from (0.28 to 0.32), larger than the typical values obtained for Nd^{3+} doped $YAl_3(BO_3)_4$"

E. Ramsay.et.al. [2010][75]: " report single-transverse mode laser oscillation from waveguides inscribed in a commercially available Nd-doped silicate glass substrate using an ultrafast fiber laser operating at 1064×10^{-9} m. When pumped at 808 nm, laser action was observed at (1062×10^{-9} m), With a slope efficiency of (15.0%) and a maximum output power of (7.5×10^{-3} W). Analysis of the laser performance implied a waveguide loss of (0.17 ± 0.06 dB cm^{-1}).

I.Iparraguirre,[1].et.al.[2011][76]:"The influence of the host matrix on the spectroscopic and laser properties of Nd^{3+} in a K-Ba-Al phosphate glass has been investigated as a function of rare-earth concentration. Site-selective time resolved laser spectroscopy and stimulated emission experiments under selective wavelength laser pumping show the existence of a very complex crystal field site distribution of (Nd^{3+}) ions in this glass. The peak of the broad stimulated ($^4F_{3/2}\rightarrow{}^4I_{11/2}$) emission shifts in a non monotonous way up to (3×10^{-9}m) as a function of the excitation wavelength. The best slope efficiency obtained for the laser emission was 40%."

M. Hughes.et.al. [2011][77]:"The internal quantum efficiencies under sunlight and laser excitation were measured directly by an integrating sphere method for tellurite, borosilicate and fluoride glasses. The radiative quantum efficiency was also obtained by Judd-Ofelt analysis. The radiative quantum efficiency was almost (100%) for tellurite and fluoride glasses and (50%) for borosilicate glasses. The quantum efficiency under laser excitation was (86%),(34%) and (88%) for tellurite, borosilicate and fluoride glasses at a low (Nd^{3+}) content and decreased by concentration quenching. The quantum efficiency under sunlight excitation was up to (33%, 21%) and(70%) for tellurite borosilicate and fluoride glasses. Nd^{3+}-doped fluoride glass is a promising candidate for solar pumped laser applications since it has the high quantum efficiency under sunlight excitation. "

M. Klimczak and R. Piramidowicz. [2012][78]:"in this work the short-wavelength emission properties are investigated for the highest observed 4f metastable energy level ($4F_{5/2}$) of (Nd^{3+}) tens In fluorozirconate ZBLAN glass.Various dopant concentrations, ambient temperatures and excitation conditions have been considered throughout the study. Distinct spectral features were observed under pulsed and cw excitation at (514×10^{-9} m). In particular, pulsed pumping enabled recording of ($4F_{5/2}$)

emission spectra, not observable under (cw) excitation, as well as the level fluorescence decay dynamics and its evolution with temperature and dopant concentration. According to the best of the authors' knowledge, neither the fluorescence lifetime of ($4F_{5/2}$) of (Nd^{3+}) in ZBLAN, nor its concentration dependent evolution were reported before".

N.Oliveira.et.al.[2013][79]:"The optical properties of trivalent neodymium embedded in a P_2O_5-Al_2O_3- Na_2O K_2O phosphate glass system, synthesized by the fusion method, are studied. Absorption, luminescence, lifetime, and Raman spectroscopy measurements were performed and the Judd-Ofelt theory was applied to determine optical parameters such as die quantum efficiency and the stimulated emission cross section of the Nd^{3+}-doped glass system. This structure has high quantum efficiency at low Nd^{3+} concentrations, comparable to the efficiency of a commercial YAG:Nd^{3+} crystal".

A. Ryasnyanskiy.et.al. [2014][80]:"The first demonstration, to the best of our knowledge, of distributed Bragg reflector (DBR) and monolithic distributed feedback (DFB) lasers in photothermoreffactive glass doped with rare-earth ions is reported. The lasers were produced by incorporation of the volume Bragg gratings into

the laser gain elements. A monolithic single-frequency solid-state laser with a linewidth of(250×10^{3}Hz) and output power of (150×10^{-63}w) at (1066×10^{-9} m) is demonstrated. "

M.Venkateswarlu,.et.al.[2014][81]:"Lead Tungsten Tellurite (LTT) glasses doped with different concentrations of Nd^{3+} ions were prepared by using the melt quenching technique to study the absorption, emission and decay spectral profiles with an aim to understand the lasing potentialities of these glasses. The emission spectra recorded for LTT glasses give three emission transitions ($^4F_{3/2} \rightarrow {}^4I_{9/2}$) ($^4F_{3/2} \rightarrow {}^4I_{11/2}$) and ($^4F_{3/2} \rightarrow {}^4I_{13/2}$)for which effective band widths ($\Delta\lambda_P$) and stimulated emission cross-sections (σ_{se}) are evaluated. Branching ratios (β_R) measured for all the ITT glasses show that ($^4F_{3/2} \rightarrow {}^4I_{11/2}$) transition is quite suitable for lasing applications. The intensity of emission spectra increases with increase in the concentrations of Nd^{3+}up to (1.0 mol%) and beyond concentration quenching is observed. From the absorption, emission and decay spectral measurements, it was found that (1.0 mol%) of (Nd^{3+}) ion concentration is aptly suitable for LTT glasses to give a strong NIR laser emission at (1062×10^{-9}m). "

C.Tian.et.al.[2015][82]:"A detailed investigation on (1.06×10^{-6} m) spectroscopic properties as a function of (Nd^{3+}) ions concentration in bismuth silicate glasses is reported. Judd-Ofelt analysis indicated that (Nd^{3+}) has no substantial influence on glass structure. Based on the Judd-Ofelt intensity parameters, several radiative properties such as radiative transition probability, radiative lifetime, branching ratio and emission cross-section of (Nd^{3+}) ions have been derived. The (1.06×10^{-6} m) emission intensity increases firstly and then attains maximum at (0.5 mol%) Nd_2O_3 and decreases with further increase of dopant concentration.The luminescence quenching behavior at higher Nd^{3+} concentration has been ascribed to the hopping migration assisted cross relaxation mechanism. The high emission cross section ($233\ x\ 10^{-20}$ cm^2) and large quantum efficiency (90.7%) suggest their potential for compact (1.06×10^{-6} m) lasers applications. "

.IL.Leconte.et.al. [2015][83]:"High-power and tunable operation of Nd-doped fiber lasers at wavelengths as short as (872×10^{-9} m) is reported. Using a reflective VBG, we showed a narrow line width (~35pm) laser emission with a maximum output power of (22W) **"**

(1.9) Thesis Layout

This thesis included four chapter, the first chapter is Background and Literature Riview, which is description the active medium of studied laser through the topics Optical fiber, Optical fiber type, Refraction of light and total internal reflection, Light propagation along on optical fiber, The Host, Rare-earth doped solid-state laser, Rare-Earth, Nd^{3+}- doped optical fiber, Neodymium energy levels, Radiative transitions, Nonradiative**r** relaxations, Optical resonator, Pumping Sorics , and Advantages of fiber laser, also in this chapter, number of researchers studies related this research was reviewed.

The title of chapter two is Theoretical Treatment, which is study the topics; Principle of laser action, Rate equations, Threshold condition Efficiency and Lasing output power.

Results and Discussion is the title of chapter three, which is introduced a comprehensive presentation of a numerical solution results for Lasing output power equation in case of using the host of types Silica and ZBLAN, and study the effect all the coefficients related this Laser design on lasing output power calculation, and determine the optimal values of these coefficients to obtain the highest value of lasing output power and efficiency for laser consideration study.

The title of chapter four is Conclusion and Future works, ‘which is included a number of derived conclusion from this study, addition to that, this chapter included a number of proposed future projects, which are complementary to the current study.

(1.10) Aim of the present work

The aim of this work is using the analytical solution of modified equations for optical fiber laser, which works according to pump plan with four – levels system to find the equation of lasing output power (p_{out}), and using the numerical solution to calculate (P_{out}) of (Nd^{+3}) doped optical fiber laser as a model example for optical fiber laser, which is working according to this system. Two types of hosts included Silica and ZBLAN with using a different designs.

In addition to that, the study was achieved to know the effectiveness of the numerical aperture (NA), core radius (a), cladding radius (b), fiber length (L), reflection coefficient of mirror(2) (R_2), (Nd^{+3})-dopant concentration in the fiber core (N_o),lifetime of upper laser level (T_2) and pump power (P_o) up on the (P_{out})for the host type Silica when the emission of laser with wavelength is ($1064*10^{-9}$m).

Chapter two

Theoretical treatment

(2.1) Introduction

Light in the core of an optical fiber is trapped by total internal reflection, and this provides a natural way of confining the lasing mode laterally. Light can be confined in the longitudinal direction by a mirror on each end of the fiber [22]. The mirrors in this case can be flat, because the optical mode is defined by the fiber rather than the mirrors. In this type of laser cavity, light can be confined to a small lateral size for an arbitrarily long cavity length, subject only to attenuation losses in the fiber. Gain in the cavity is provided by rare earth ions, which are doped into the fiber core. A device of this type is termed a fiber laser [22].

To obtain gain in the fiber laser, the rare earth ions need to be optically pumped with a suitable light source. The first fiber lasers, proposed and developed by Snitzer in the early 1960s, were lamped pumped from the side. However, this pump scheme does not take advantage of the long fiber lengths that are possible, and fiber lasers today are nearly always end pumped[85]. One way to end pump the laser is to send pump power through a dichroic mirror at the fiber end. This mirror is highly transmitting at the pump wavelength(λ_p) which allows the pump power to be coupled into the core of the fiber, but it is highly reflecting at the lasing wavelength (λ_L), so it can serve as a high reflector in the laser cavity. This pumping arrangement is generally used for experimentation and setting up prototypes, since the cavity can be easily altered [22,85]

(2.2) Principle of laser action.

The interaction between electromagnetic (EM) radiation and matter causes change in the energy states of the electrons in matter.

To simplify the discussion, let us consider an idealized material with just two nondegenerate energy levels (E_1) and (E_2) having populations of (N_1) and (N_2), respectively. The total number of electrons in these two levels is assumed to be constant[21,22].

$$N_1 + N_2 = N_o \qquad \textbf{(2.1)}$$

We can identify three types of interaction between (EM) radiation and a simple two-level atomic system (see Figure.2.1).

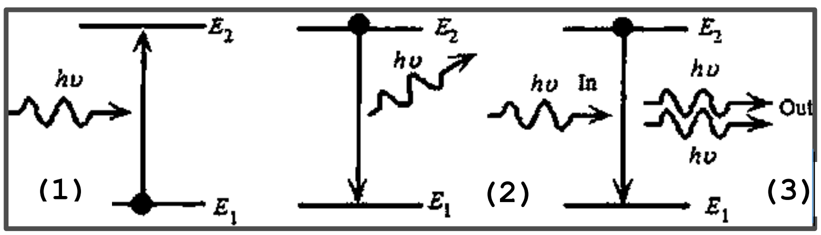

Figure (2.1). Interaction of radiation with matter .
(1) Absorption (2) Spontaneous emission (3) Stimulated emission

Absorption: when a electromagnetic (EM) wave of frequency (ν) enters a material, electrons can be raised from lower energy level (E_1) to higher energy level(E_2), if the photons energy equals the energy difference between the two levels[21,22].

$$h\nu = E_2 - E_1 \qquad \textbf{(2.2)}$$

The population of lower level will be depleted at a rate equals to:

$$d N_1/ dt = - B_{12}\ \rho\ N_1 \qquad \textbf{(2.3)}$$

Where (B_{12})is the Einstein's coefficient for stimulated absorption, (N_1) is the population in lower state and(ρ) is the energy density per unit of frequency of the incoming photons.

Spontaneous emission: after an electron has been raised to the upper energy level by absorption, there is a probability that it will return to the lower energy state emitting, in a random direction, a photon of energy equals to the energy difference between the two levels. The population of the upper level will be depleted at a rate equals to[21,22].

$$dN_2/dt = -A_{21} N_2 \quad \textbf{(2.4)}$$

Where (A_{21}) is the Einstein's coefficient for spontaneous emission.

It can be observed that this spontaneous decay of the upper level takes place in absence of an (EM) field. It is purely a statistical phenomenon related with time and space and is dependent on the lifetime of the excited state. If the transition lifetime is very large, it is considered as a forbidden transition.

If we consider a large number of spontaneously emitted photons, there is no phase relationship between them, thus they are incoherent.

Equation (2.4) has a solution equals to[21,22].

$$N_2(t) = N_2(0) \exp(-t/T_{21}) \quad \textbf{(2.5)}$$

where (T_{21}) is the lifetime for spontaneous radiation of level (2). This radiation lifetime is equal to the reciprocal of the Einstein coefficient[21].

$$T_{21} = A_{21}^{-1} \quad \textbf{(2.6)}$$

In general, the reciprocal of the transition probability of a process is called its Lifetime and has the dimension of time. The shorter the spontaneous lifetime, the greater is the probability that spontaneous emission will occur. In certain materials, there are energy levels which have the spontaneous lifetime of the order of microseconds to a few milliseconds.

These levels are known as metastable levels. The probability of transitions involving metastable levels is relatively low [21].Stimulated emission: emission takes place not only spontaneously but also under stimulation by (EM) radiation of the appropriate frequency (ν), that satisfies equation (2.2).

In this case the emitted photon is in phase with the incoming photon, it is in the same direction, it has the same polarization and the same energy.

The population of the upper level will be depleted at a rate equals to[22].

$$dN_2 / dt = -B_{21} \rho N_2 \qquad \textbf{(2.7)}$$

Where (B_{21}) is the Einstein's coefficient for stimulated emission and (ρ) is the energy density per unit of frequency of the incoming photons.

The useful parameter for laser action is the (B_{21}) coefficient; the (A_{21}) coefficient represents a loss term and introduces a noise source in a laser.

Considering an ideal material in thermal equilibrium, where absorption, spontaneous emission and stimulated emission take place, it can be written [21,22]

$$B_{21} \rho N_2 + A_{21} N2 = -B_{21} \rho N_2 \qquad \textbf{(2.8)}$$

Using Boltzmann statistical black body radiation law, it is possible to demonstrate that[21,22].

$$A_{21} / B_{21} = 8\pi\nu^2 h\nu / c3 \qquad \textbf{(2.9)}$$

$$B_{21} = B_{12} \qquad \textbf{(2.10)}$$

These equations are known as Einstein’s relations.

From eq. (2.9) it is possible to observe that the ratio of the probability of spontaneous to stimulated light emission depends directly on the frequency of emission. Hence, stimulated emission is more probable than spontaneous in the microwave region, while in the optical region, spontaneous emission is more likely than stimulated emission and this gets worse as we go into the (UV) region of the spectrum [22].

Eq. (2.10) states that the Einstein coefficients for stimulated emission and absorption are equal. This means that, in steady state, the two processes have the same probability to happen [22].

$$\left(\frac{N_2}{N_1}\right) = \exp\left(-\frac{E_2-E_1}{KT}\right) \qquad \textbf{(2.11)}$$

Where (T) is the Temperature of the host material in (Kelvin) an (K) is Boltzmann constant

(2.3) Rate Equation

Consider the four – level scheme as shown in Fig (3.2) .

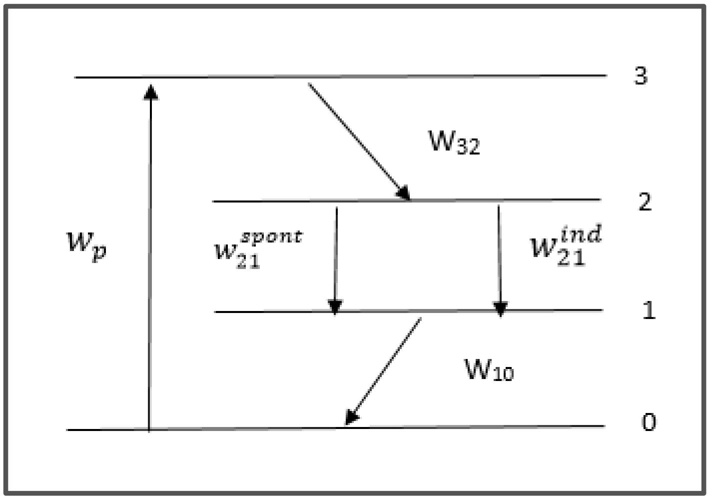

Figure (2.2). The scheme of a four – level system.

In this scheme , a higher state level (3) is excited directly by the pumping mechanism , and this state decays quickly and nonradiatively to the upper laser level (2) . Stimulated emission then occurs from level (2) to level (1) , which is the optical gain transition . In contrast , the four – level system can achieve population inversion with only a small number of atoms raised out of the ground – state . Generally , it is easy to obtain amplification and lasing with a four – level system because not as much pump energy must be wasted in removing atoms from the ground state[30,82].

Where ($N_1 = N_3 \cong 0$) , population inversion is therefor , readily obtained , since ($\Delta N \cong N_2$), which is positive for any rate of pumping . It is also clear level (2) is in effect being directly populated by the pump .

With the above approximations , only a single rate equation is required to describe the level populations in the four – level system . The rate of change of the upper laser state population can be written as[30,82].

$$\frac{dN_2}{dt} = N_o W_p - N_2 W_{21}^{ind} - \frac{N_2}{T_2} \quad \textbf{(2.12)}$$

Where (T_2) is the fluorescence lifetime of level (2) and the approximation ($N_1 \ll N_2$) has been used. The rate (W_P) is the pump rate, defined as the probability per unit time that an atom is promoted by the pump from the ground state up to level (3). (N_o) is the Nd^{3+}-dopant concentration in fiber core .The rate (W_{21}^{ind}) is, as before, the probability per unit time for an induced transition and are geien by [82,83].

$$W_p = \frac{I_p \sigma p}{h\upsilon_p} \quad \textbf{(2.13)}$$

$$W_{21}^{ind} = \frac{I_L \sigma_L}{h\upsilon_L} \quad \textbf{(2.14)}$$

Where (σ_P) ,(σ_L) are absorption and emission cross – section at pumping and lasing wavelength , and (I_L) is the lasing intensity that is resonant with the Level (2) → Level(1) transition .

Using eq. (2-13 and 2 - 14), the rate equation of eq. (2-12) can be written as.

$$\frac{dN_2}{dt} = R - N_2 \left(\frac{I_L \sigma_L}{h\upsilon_L} + \frac{1}{T_2}\right) \quad \textbf{(2.15)}$$

$$R = N_o W_P \quad \textbf{(2.16)}$$

Where (R) is the total number of atoms pumped up to level (2) per unit volume per unit time .

The equation (2.15) relates the excited – state population (N_2) to the lasing intensity (I_L) , and to understand the operation and behavior of lasers[86] .

(2.4) Threshold condition

The conditions under which lasing will occur can be determined by considering the simple laser cavity shown in Fig (2.3).

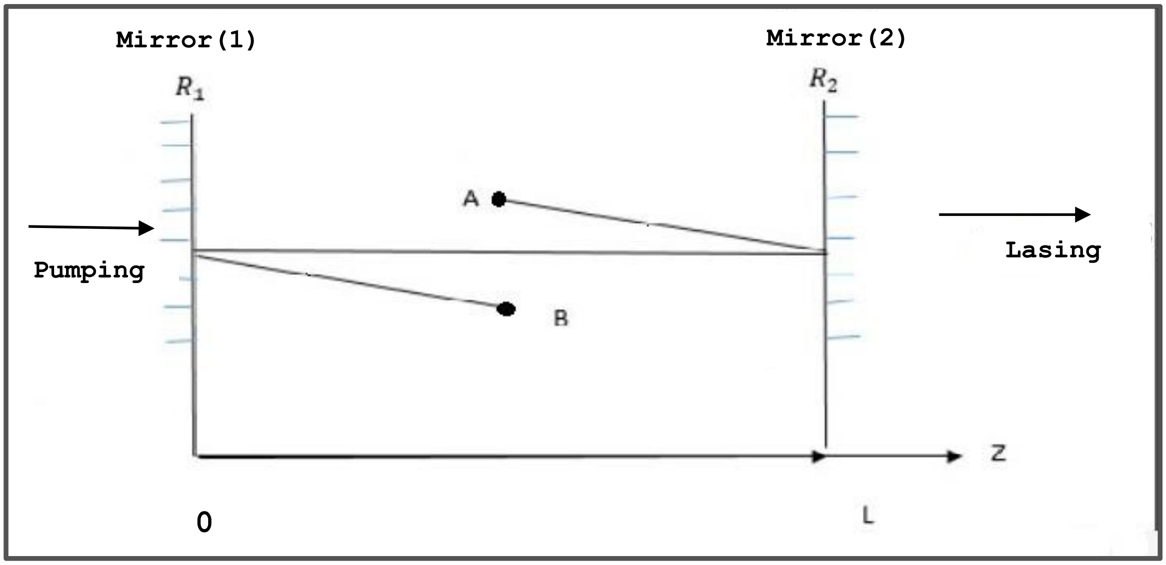

Figure (2.3). Laser cavity.

A uniform gain medium fills the region between two cavity mirrors which are separated by distance (L) and have reflectivities (R_1) and (R_2) . Let us consider that there is a small amount of lasing intensity at point (A) that happens to be moving in a direction toward mirror (2) , as shown . As the lasing makes a round – trip through the cavity from point (A) to point (B) it is amplified with again coefficient (G) while at the same time being attenuated by the loss coefficient at lasing wavelength . After reflection from mirror (2) , the losing intensity is reduced by a factor (R_2) and similarly for mirror (1) . The intensity of lasing arriving at point (B) , the (I_B) can be written as[86].

$$I_L(B) = R_1 R_2 e^{2(G-\propto_L)L} I_L(A) \quad \textbf{(2.17)}$$

Where (I_A) is the intensity of lasing originating at point (A) .If ($I_B < I_A$) then the lasing intensity will become progressively smaller with each round – trip , and lasing output will not occur .

For lasing output to occur , it is necessary that ($I_B > I_A$).The threshold condition for laser oscillation then becomes[21,86,88].

$$R_1 R_2 e^{2(G-\propto_L)L} \geq 1 \quad \textbf{(2.18)}$$

The smallest vlaue of (G) that satisfies this inequality is the threshold gain coefficient and is denoted (G_{th}) ,taking the log of eq. (2.18) gives[21,86,88]:

$$G_{th} = \propto_L + \frac{1}{L} \ln \frac{1}{\sqrt{R_1 R_2}} \quad \textbf{(2.19)}$$

So that the condition for threshold can be written ($G > G_{th}$) .The Scattering loss at lasing wavelength is given by[15].

$$\propto_L = N_o \Gamma_L \sigma_L \quad \textbf{(2.20)}$$

Where (Γ_L) is the power filling factor at lasing wave length (λ_L) is defined by [86].

$$\Gamma_L = 1 - \exp\left[-2\left(\frac{a}{w_L}\right)^2\right] \quad \textbf{(2.21)}$$

(w_L) is the mode field radius , for a fundamental mode (w_L) is defined by[93].

$$W_L = a\left[6.616 + \frac{1.660}{\sqcup^{1.5}} + \frac{0.987}{\sqcup^{6}}\right] \quad \textbf{(2.22)}$$

Where ($\sqcup$) is the normalized frequency at lasing wavelength is defined by:

$$\sqcup = \frac{2\pi a N_A}{\lambda_L} \quad \textbf{(2.23)}$$

Where (a) is the radius of core fiber .

The net fractional increase in intensity of lasing after propagating a distance (ΔZ) is ($G - G_{th}$) ΔZ , this fractional increase occurs in a time ($\Delta t = \frac{\Delta Z}{c}$) , since the beam is moving with speed (c) .

The fractional increase in intensity of lasing can then be written[86].

$$\frac{\Delta I_L}{I_L} = (G - G_{th})\, c\, \Delta t \quad \textbf{(2.24)}$$

At ($\Delta N = N_2$) , the(G)and the cavity lifetime(T_c) has been defined by[21,86] :

$$G = \sigma_L N_2 \tag{2.25}$$

$$T_c = \frac{1}{cG_{th}} \tag{2.26}$$

The eq. (2-24) become :

$$\frac{\Delta I_L}{\Delta t} = c\, \sigma_L N_2 I_L - \frac{1}{T_c} \tag{2.27}$$

Taking the limit($\Delta t \rightarrow 0$) in eq. (2-27) gives an equation for the rate of change of lasing intensity , then yields of differential equation relation (I_L).

$$\frac{dI_L}{dt} = c\, \sigma_L N_2 I_L - \frac{1}{T_c} \tag{2.28}$$

In the steady state , eq.s (2-15) and (2-28) become[21,86].

$$0 = R - N_2 \left(\frac{I_L \sigma_L}{h\upsilon_L} + \frac{1}{T_2}\right) \tag{2.29}$$

$$0 = c\, \sigma_L N_2 I_L - \frac{1}{T_c} \tag{2.30}$$

The solutions for (N_2) and (I_L) both above and below threshold can be found in the following way . Below threshold , (I_L) is very small , so $\left(\frac{I_L \sigma_L}{h\upsilon_L}\right)$ can be neglected compared to ($\frac{1}{T_2}$) in eq. (2-29) . The excited state population is then[86,91] :

$$N_2 = R\, T_2 \tag{2.31}$$

Which increases linearly with the excitation rate I_L .

When I_L reaches the threshold value :

$$R_{th} = \frac{N_{2th}}{T_2} = \frac{1}{c\sigma_L T_c T_2} \tag{2.32}$$

Laser action begins , with eq. (2-28) giving (dI_L / dt ≥ 0) .

The lasing intensity (I_L) builds up rapidly , but is prevented from going to infinity by saturation of the population inversion (N_2)[91] .

A further increase in (I_L) does not result in any additional increase in (N_2) , because the steady – state condition of eq. (2-28) would then be violated . Instead , (N_2) becomes pinned at the threshold value[86,91].

$$N_2 = N_{2th} = R_{th}\, T_2 \qquad \textbf{(2.33)}$$

Although (N_2) does not increase above threshold , the lasing intensity (I_L) does increase with increasing (R).

This can be seen by combining eqs (2-33) and (2-29) :

$$R = R_{th}\left(\frac{I_L \sigma_L T_2}{h\upsilon_L} + 1\right) \qquad \textbf{(2.34)}$$

And solving for (I_L) to give :

$$I_L = \frac{h\upsilon_L}{\sigma_L T_2}\left(\frac{R}{Rth} - 1\right) \qquad \textbf{(2.35)}$$

The Lasing intensity (I_L) is increased linearly with excitation rate (R) , this linear increase in lasing intensity above threshold , along with the pinning of the population inversion , are key identifying features of laser action[86,91] .

(2-5) Threshold Lasing power

The pump power is absorbed as it propagates down the fiber core , and this causes the pump intensity to vary with position along the fiber .

Consider pump power of intensity (I_p (o)) and wave length (λ_p) that is coupled into the core of fiber of length (L) .

The core has cross – sectional area (A_{eff}) and is doped with (N_o) rare earth ions per unit volume .

In this case , the pump intensity decays exponentially with(Z) according to Beer's a law [21].

$$I_{p(Z)} = I_{p(0)}\, e^{-\propto_p Z} \quad \textbf{(2.36)}$$

Where ($\propto_p$) is the scattering loss at pump wave length is given by[22].

$$\propto_p = \Gamma_p\, N_o\, \sigma_p \quad \textbf{(2.37)}$$

If (Γ_p) is the power filling at pumping wave length (λ_p) is defined by[90].

$$\Gamma_p = \frac{A_{eff}}{A_{clad}} \quad \textbf{(2.38)}$$

Where :

$$A_{clad} = \pi b^2 \quad \textbf{(2.39)}$$

(b) is the radius of cladding and (A_{eff}) in Multi – Mode fiber defined by[90].

$$A_{eff} = \pi a^2 \quad \textbf{(2.40)}$$

The A_{eff} in a Single – Mode fiber defend by[90].

$$A_{eff} = \pi\, w_p^2 \quad \textbf{(2.41)}$$

Where (w_p) is the mode field radius at pumping wave length , for a fundamental mode is defined by[90].

$$W_p = a\left[0.761 + \frac{1.237}{V1.5} + \frac{1.429}{V6}\right] \quad \textbf{(2.42)}$$

$$V = \frac{2\pi a N_A}{\lambda_p} \quad \textbf{(2.43)}$$

The gain coefficient varies with (z), we first express it in terms of the level populations as [22,86.87].

$$G_{(Z)} = [N_{2\,(Z)} - N_{1\,(Z)}]\, \sigma_L \tag{2.44}$$

Where ($N_1 \ll N_2$) has been assumed for the four – level transition .

$$G_{(Z)} = N_{2(Z)}\, \sigma_L \tag{2.45}$$

By using eqs. (2-13), (2-16) , (2-31) and (2-37) the eq. (2-45) can be written as[87].

$$G_{(Z)} = \frac{\propto_p \sigma_L T_2}{\Gamma_p h\upsilon_p} I_{P(Z)} \tag{2.46}$$

This result shows that the gain coefficient ($G_{(Z)}$) varies with (z) in the same manner as the pump intensity $I_P(z)$.

The gain coefficient gives the fractional increase per unit length of lasing intensity at lasing wave length (λ_L) .

For the small section (dz) of fiber , the increment in lasing intensity is [87].

$$dI_L = I_L\, G_{(Z)}\, dz \tag{2.47}$$

By using eqs. (2 - 46) and (2 - 36) can be integrating over the fiber length , we obtain

$$\int_{I_{L1}}^{I_{L2}} \frac{dI_L}{I_L} = \frac{\sigma_L T_2}{\Gamma_p h_{\upsilon p}} I_{P(0)} \int_0^L \propto_P e^{-\propto_P Z} dz \tag{2.48}$$

Where I_{L1}, I_{L2} is the intensity at the mirror (1) and (2) respectivly

$$\mathrm{Ln}\, \frac{I_{L2}}{I_{L1}} = \frac{\sigma_L T_2 I_{p(0)}}{\Gamma_p h\upsilon_p} (1-e^{-\propto_p L}) \tag{2.49}$$

The single – pass gain was denoted previously as [21,86].

$$\gamma = \frac{I_{L2}}{I_{L1}} \tag{2.50}$$

By using eq. (2-50) the eq. (2-49) can be written as :

$$\ln \gamma = \frac{\sigma_L T_2 I_{p(0)}}{\Gamma_p h\upsilon_p} [1-\exp(-\propto_p L)] \tag{2.51}$$

the threshold Lasing power (p_{th}) can be evaluated using[86,87].

$$I_{P(0)} = \frac{P_{th}}{Aeff} \tag{2.52}$$

$$\ln \gamma = \ln \gamma_{th} = G_{th}\, L \tag{2.53}$$

$$P_{th} = \frac{A_{eff}\, h\upsilon_p \Gamma_p G_{th} L}{\sigma_L T_2 [1-\exp(-\propto_p L)]} \tag{2.54}$$

(2.6) Lasing output power

The output power from the laser can be determined by referring to Fig (2.4) .

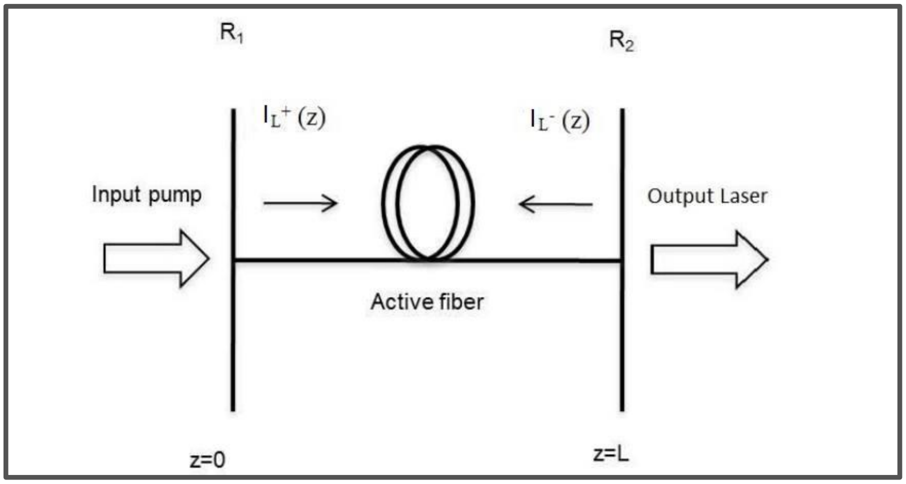

Figure. (2.4) : Schematic of end-pumped linear-cavity.

The two counter. Propagating beam of intensities (I_L^-) only the (I_L^+) beam is transmitted through the mirror (2) to give laser output.

The wave inside the resonator has the form of a standing wave , which is equivalent to the superposition of two counter propating beams of intensities (I_L^-) and (I_L^+) as showed[86,92] .

Each of these has half the intensity (I_L) of the wave in the cavity, So ($I_L^- = I_L^+ = I_L/2$) . Assume for simplicity that the left mirror (R_1), and that the other mirror has a transmission (T) , so ($T = 1 - R_2$) . wave will then have the cavity only through the right mirror (R_2) , with an intensity ($T\, I_L^+ = \frac{1}{2} T I_L$) , the power exiting the laser becomes[86,87] .

$$P_{out} = \frac{1}{2} I_L T\, A_{eff} \qquad \textbf{(2.55)}$$

By using eq. (2-35) , the eq . (2-55) become :

$$P_{out} = \frac{1}{2} \frac{h\upsilon_L}{\sigma_L T_2} T\, A_{eff} \left(\frac{R}{R_{th}} - 1\right) \qquad \textbf{(2.56)}$$

Where the saturation intensity (I_s) is defiend as[21,86,92] :

$$I_s = \frac{h\upsilon_L}{\sigma_L T_2} \quad \textbf{(2.57)}$$

The input power to laser (p_{in}) can be taken as the absorbed pump power (p_{abs}) is given by[86,87,92].

$$P_{in} = P_{abs} = Rh\nu_p \, Aeff \, L = P_o \, [1\text{-}\exp(-\propto_p L)] \quad \textbf{(2.58)}$$

And the lasing threshold can be written as :

$$P_{th} = R_{th} h\nu_p A_{eff} \, L = \frac{A_{\,eff} \, h\upsilon_p \Gamma_p G_{th} L}{\sigma_L T_2 [1 - \exp(-\propto_p L)]} \quad \textbf{(2.59)}$$

Combining eqs. (2-57) , (2-58) and(2-59) with eq. (2-56) yields :

$$P_{out} = \frac{1}{2} \, Aeff \, \frac{TI_s}{P_{th}} \, [P_{in} - P_{th}] \quad \textbf{(2.60)}$$

(2.7) Efficiency

Eq. (2-60) can be further manipulated the simple form [21,22,86].

$$P_{out} = \eta_s \, [P_{abs} - P_{th}] \qquad \textbf{(2.61)}$$

Combining eq. (2-60) with eq. (2-61) , the slope efficiency giving :

$$\eta_s = \frac{1}{2} A_{eff} \, T \, \frac{I_s}{P_{th}} \qquad \textbf{(2.62)}$$

By using eqs. (2-57), (2-59) and (2-26) the eq. (2-62) become :

$$\eta_s = T \, \frac{h\upsilon_L}{h\upsilon p} \, \frac{cT_c}{2L} \qquad \textbf{(2.63)}$$

Where :

$$\frac{cT_c}{2L} = \frac{1}{2\ln\gamma_{th}} \qquad \textbf{(2.64)}$$

Then the eq. (2-63) becomes :

$$\eta_s = T \, \frac{h\nu_L}{h\nu_p} \, \frac{1}{2\ln\gamma_{th}} \qquad \textbf{(2.65)}$$

Chapter three

Results and discussion

(3.1) Introduction

There is a growing interest in the optical fiber lasers, especially in desired applications in low threshold pumping, Compared to other lasers, it can reach the threshold of the laser emission due to the fact that the size of a very small core of optical fiber. In these lasers, the core of the optical fiber has been fed by one of rare earth elements, as each of the absorption cross-section, emission cross-section and the energy levels life-time that control the intensity of laser emission depending on how the distribution of ions of these elements within the host, in which a core of the optical fiber is made up.

In the current study, the Silica and ZBLAN have been chosen as a model example of hosts that represented the full common flight attendant use in optical fiber laser that is being vaccinated by Neodymium element.

(3.2) Simulation of lasing output power

After the equation laser output power (p_{out}) was derived in the two chapter and equation (2-61), we will calculate the output power and study the effect of all coefficients in this equation on P_{out} value, by Matlab (version8.1) (see.AppindaxA).

In the current study, as in case of host type (silica),it has been adopted different designs, the first design is Lycom (Denmark) with two types, that are indicated by two symbols (d1) and (d2) respectively,the second design is York (England) which has been indicated by the symbol (d3), while the third design is IAV (Germany) which is indicated by the symbol(d4)[64]. For this host, the laser transitions with largest intensity for Nd^{+3}, including wavelength (1064×10^{-9}m) which is indicated by the symbol (Nd1) and the wavelength of (1331×10^{-9}m) indicated by the symbol (Nd2).

For the case of the host type (ZBLAN), the design Le Verre Fluore (France) has been adopted, which is indicated by symbol (d5) [64] ,for the case (Nd^{+3}), the largest intensity laser transitions are wavelengths (1048×10^{-9}m), which are indicated by symbol (Nd3) and (1317×10^{-9}m) which are in turn indicated by symbol (Nd4). According to above symbols, the results of output power are as follows:

(3.2.1)The host is silica

Table (3.1).shows all required coefficients to calculate the laser output power for each of the four designs which are related to the optical fiber laser that has been doped by (Nd).

Table (3.2).shows the coefficients related the two wavelengths (Nd1) and (Nd2) when pumping source has been used. Therefore, the results of the two wavelengths (Nd1) and (Nd2) will be reviewed respectively.

Table (3.1). Default value for used parameters[64].

Parameters	d_1	d_2	d_3	d_4	unit
N_o	11.5×10^{25}	5.6×10^{25}	5×10^{25}	5×10^{25}	ion/m^3
T_2	430×10^{-6}	485×10^{-6}	460×10^{-6}	480×10^{-6}	sec
T_3	15×10^{-9}	9.5×10^{-9}	12×10^{-9}	10.5×10^{-9}	sec
L	75×10^{-2}	135×10^{-2}	54×10^{-2}	46×10^{-2}	m
a	1.35×10^{-6}	1.85×10^{-6}	1.85×10^{-6}	2.75×10^{-6}	m

Table (3.2). default value for used parameters[93,94].

Parameters	Nd_1	Nd_2	Unit
λ_p	806×10^{-9}	806×10^{-9}	m
σ_p	2.5×10^{-24}	2.5×10^{-9}	m^2
λ_L	1064×10^{-9}	1331×10^{-9}	m
σ_L	2×10^{-24}	0.256×10^{-24}	m^2

(3.2.1.1) (Nd_1)-wavelength

1- Determination of NA

The first step in calculations was to determine the hole of the numerical aperture (NA), then the highest laser output power will be obtained for each of the four designs. Tables (3.1, 3.2, 3.3 and 3.4). show the values of (P_{out}) corresponding to the values of (NA) respectively. According to these results, table (3.7). shows the value of (NA) for each design, that the highest laser output power has been obtained.

Table (3.3). The values of (P_{out}) vs (NA) for a design (d1) at (Nd_1) wavelength.

NA	P_{out}(W)
0.045	6.797222
0.057	4.634369
0.063	1.299336
0.079	0.2902448
0.092	0.083342
0.103	0.032241
0.115	0.016089
0.127	0.009765
0.138	0.006823
0.150	0.005256

Table (3.4). The values of (P_{out}) vs (NA) for a design (d2) at (Nd_1) wavelength.

NA	P_{out}(W)
0.035	6.619543
0.048	2.065099
0.061	0.232754
0.073	0.045107
0.086	0.015858
0.099	0.008388
0.117	0.005663
0.124	0.004394
0.137	0.003697
0.150	0.003268

Table (3.5). The values of (P_{out}) vs (NA) for a design (d3) at (Nd_1) wavelength.

NA	P_{out}(W)
0.035	6.90901905
0.048	3.811524
0.061	0.616297
0.073	0.125056
0.086	0.044313
0.099	0.023496
0.117	0.015878
0.124	0.012327
0.137	0.010375
0.150	0.009173

Table (3.6). The values of (P_{out}) vs (NA) for a design (d4) at (Nd_1) wavelength.

NA	P_{out}(W)
0.025	6.772212
0.039	1.065229
0.053	0.090138
0.067	0.027297
0.081	0.015662
0.094	0.011741
0.108	0.009961
0.122	0.008902
0.136	0.008278
0.150	0.007867

Table (3.7). The values of (NA) will be obtained highest (P_{out}) for each of the four designs at (Nd_1) wavelength.

Design	NA
d_1	0.045
d_2	0.035
d_3	0.035
d_4	0.025

2- calculation of (P_{out})

In this step, for the four designs, the laser output power (P_{out}) corresponding to pump power (P_o) were calculated respectively.

Table (3.8). shows all the coefficients which are not affected when the pump power increased, that were calculated from the equations ((2-43),(1-14),(2-41), (2-38),(2-21),(2-37) ,(2-20),(2-65),(2-54) and (2-19)) as indicated in the table above.

Table (3.9). shows the absorption power in optical fiber (P_{abs}) that were calculated from the equation (2-58) corresponding the pumping power of the four designs.

Figure (3.1). shows the laser output power that is corresponding to pumping power of the four designs, from this figure, it has been noted that

$P_{out}(d_3) > P_{out}(d_1) > P_{out}(d_4) > P_{out}(d_2)$.

Table (3.8). The values of parameters are not affected when the (P_o) increased at (Nd1) wavelength.

parameters	Value				
	d_1	d_2	d_3	d_4	unit
V	0.473576	0.504759	0.504759	0.535942	-
M	0.090896	0.103259	0.103259	0.116411	-
A_{eff}	9.860152×10^{-8}	8.828149×10^{-8}	8.828149×10^{-8}	9.796919×10^{-8}	m^2
Γ_p	0.160000	0.160000	0.160000	0.160000	-
Γ_L	9.001193×10^{-6}	1.911504×10^{-5}	1.911504×10^{-5}	3.865782×10^{-5}	-
α_p	36.799999	17.919999	15.999999	16.000000	m^{-1}
α_L	0.002588	0.002676	0.002389	0.004832	m^{-1}
η%	69.343005	67.283569	70.178938	68.986909	-
P_{th}	0.197682	0.161724	0.163507	0.176975	W
G_{th}	36.870240	17.959022	16.097556	16.114522	m^{-1}

Table (3.9). The values of (P_{abs}) vs (P_o) for each of the four designs at (Nd1) wavelength.

P_o (w)	P_{abs} (w)			
	d_1	d_2	d_3	d_4
1	0.999999	0.999999	0.999823	0.999363
2	1.999999	1.999999	1.999646	1.998728
3	2.999999	2.999999	2.999469	2.998091
4	3.999999	3.999999	3.999292	3.997455
5	4.999999	4.999999	4.999116	4.996819
6	5.999999	5.999999	5.998939	5.996183
7	6.999999	6.999999	6.998762	6.995547
8	7.999999	7.999999	7.998585	7.994910
9	8.999999	8.999999	8.998408	8.994274
10	9.999999	9.999999	9.998231	9.993638

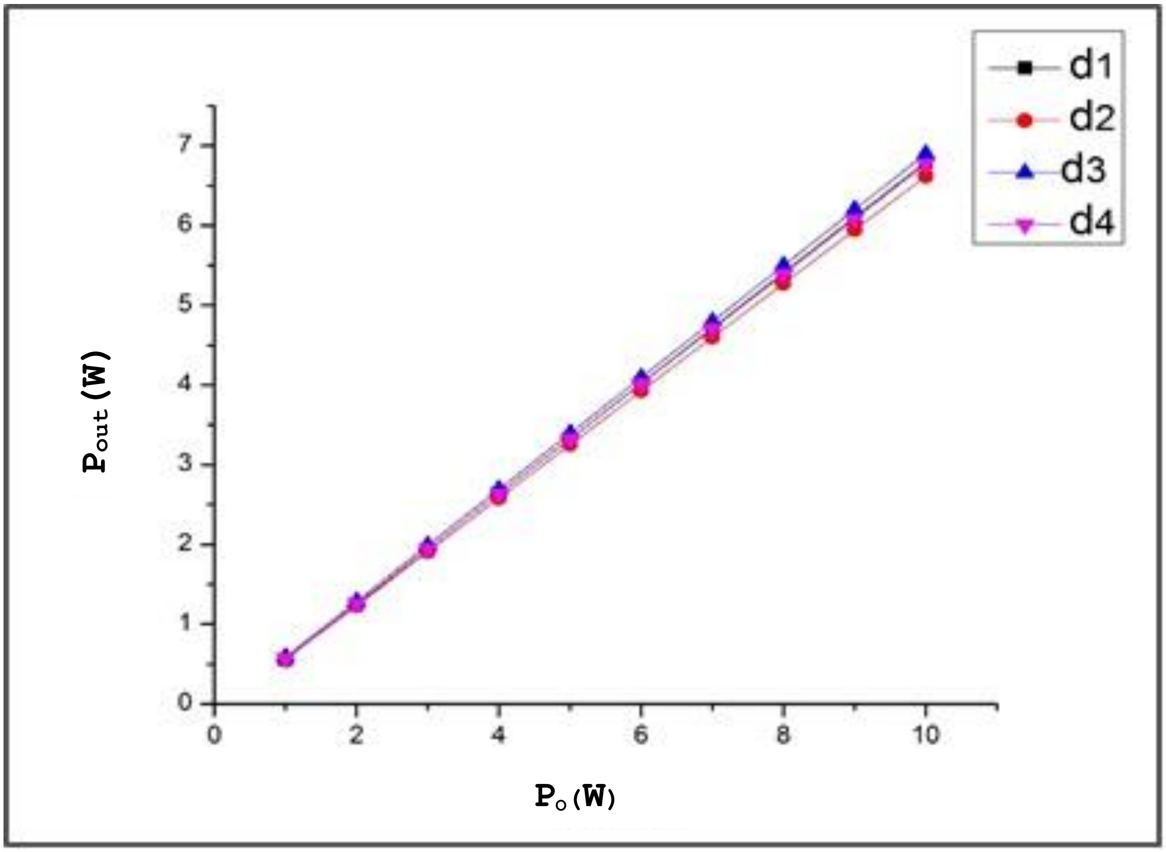

Figure. (3.1). Lasing output power versus input pump power for each of the four designs at (Nd1) wavelength

(3.2.1.2)(Nd_2)-wavelength

1- Determination of (NA)

Tables (3.10, 3.11, 3.12. and 3.13). show the (P_{out}) values that correspond to (NA) values that are in turn correspond to (NA) values of this wavelength for the four designs according to these results. Table (3.14) shows the greatest (NA) values for each design that a highest laser output power has been obtained.

Table (3.10). The values of (P_{out}) vs (NA) for a design (d1) at (Nd_2) wavelength.

NA	P_{out} (W)
0.060	5.660532
0.070	5.476400
0.080	4.697795
0.090	3.172767
0.100	1.681684
0.110	0.817666
0.120	0.415843
0.130	0.232746
0.140	0.144330
0.150	0.981566

Table (3.11). The values of (P_{out}) vs (NA) for a design (d2) at (Nd_2) wavelength.

NA	P_{out} (W)
0.045	5.641061
0.057	5.037636
0.068	2.760123
0.079	0.93833
0.092	0.335527
0.103	0.153292
0.114	0.087822
0.127	0.059445
0.138	0.045081
0.150	0.036879

Table (3.12). The values of (P_{out}) vs (NA) for a design (d3) at (Nd_2) wavelength.

NA	P_{out} (W)
0.045	5.672673
0.057	5.467722
0.068	4.144123
0.079	2.030603
0.092	0.850425
0.103	0.409864
0.114	0.239605
0.127	0.163662
0.138	0.124706
0.150	0.102301

Table (3.13) The values of (P_{out}) vs (NA) for a design (d4) at (Nd_2) wavelength.

NA	P_{out} (W)
0.035	5.626989
0.048	3.852399
0.061	1.091129
0.073	0.358863
0.086	0.184210
0.099	0.125066
0.112	0.985190
0.124	0.084184
0.137	0.075459
0.150	0.697090

Table (3.14). The values of (NA) will be obtained highest (P_{out}) for each of the four designs at (Nd_2) wavelength.

Design	NA
d_1	0.060
d_2	0.045
d_3	0.054
d_4	0.035

2- Calculation of (P_{out})

Table (3.15) shows all the coefficients which don't affect to the pumping power increasing, while table (3.16) shows (P_{abs}) values corresponding of pumping power in this case while Figure (3.2) shows the laser output power coresponding to pumping power for the the four designs. It can be noted that:

P_{out} (d_3)> P_{out}(d_1)>P_{out} (d_2)>P_{out}(d_4) .

Table (3.15) The values of parameters are not affected when the (P_o) increased at (Nd2) wave length.

parameters	Value				Unit
	d_1	d_2	d_3	d_4	
V	0.631437	0.648977	0.648977	0.750318	-
M	0.161592	0.170694	0.170694	0.228166	-
A_{eff}	3.802732×10^{-9}	5.325131×10^{-9}	5.325131×10^{-9}	2.706331×10^{-9}	m^2
Γ_p	0.160000	0.160000	0.160000	0.160000	-
Γ_L	1.911661×10^{-5}	2.639386×10^{-5}	2.639386×10^{-5}	1.431108×10^{-4}	-
α_p	36.799999	17.919999	15.999999	16.000000	m^{-1}
α_L	5.637609×10^{-4}	3.789736×10^{-4}	3.383693×10^{-4}	0.001835	m^{-1}
η%	57.017838	54.922205	57.276355	56.568718	-
P_{th}	0.072270	0.089897	0.094192	0.046471	W
G_{th}	36.870240	17.959022	16.097556	16.114522	m^{-1}

Table (3.16) The values of (P_{abs}) vs (P_o) for each of the four designs at (Nd2) wavelength.

P_o (W)	P_{abs}(W)			
	d_1	d_2	d_3	d_4
1	0.999999	0.999999	0.999823	0.999368
2	1.999999	1.999999	1.999646	1.998428
3	2.999999	2.999999	2.999469	2.998091
4	3.999999	3.999999	3.999292	3.997455
5	4.999999	4.999999	4.999116	4.996819
6	5.999999	5.999999	5.998939	5.996183
7	6.999999	6.999999	6.998762	6.995547
8	7.999999	7.999999	7.998585	7.994910
9	8.999999	8.999999	8.998408	8.994274
10	9.999999	9.999999	9.998231	9.993638

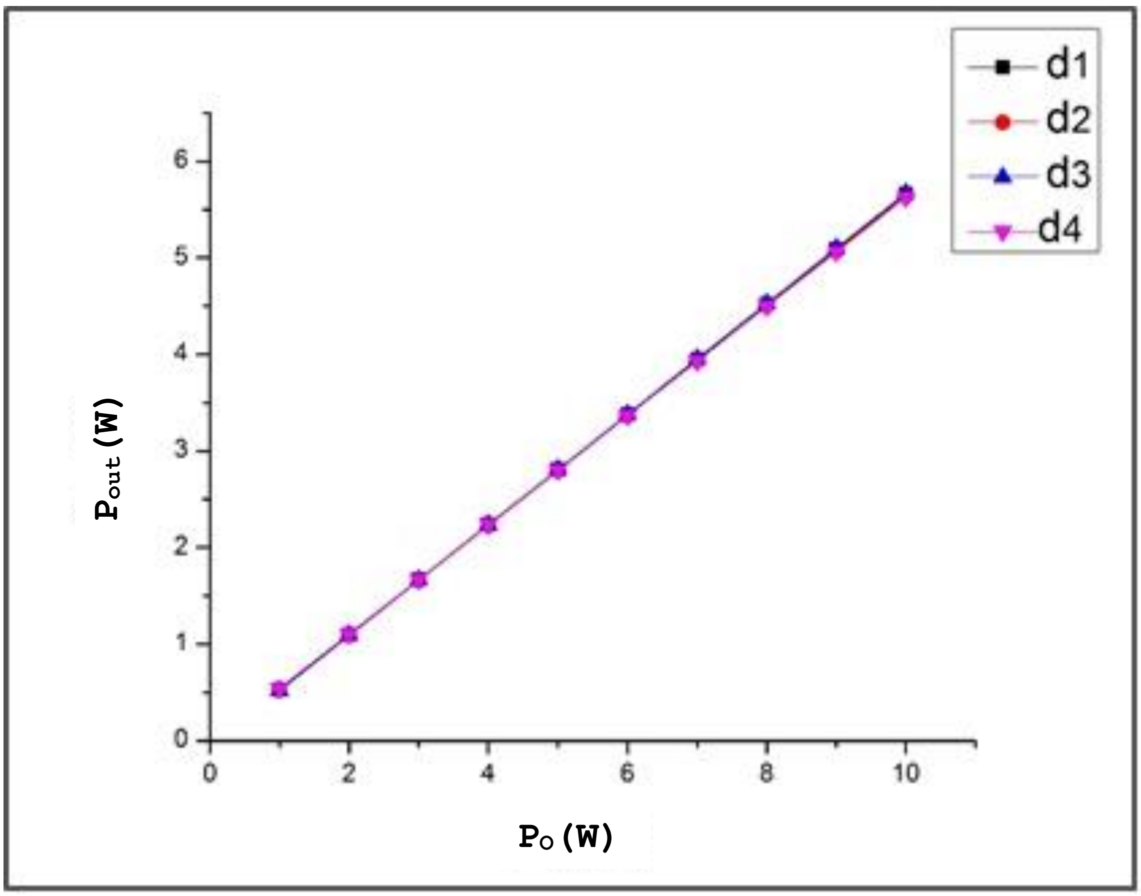

Figure.(3.2): Lasing output power variation versus pump power for each of the four designs at (Nd_2)wave length.

(3.2.1.3) comparing between the wavelength (Nd_1) and (Nd_2)

Figures (3.3, 3.4, 3.5 and 3.6) show the laser output power corresponding to pumping power of the two wavelength (Nd_1) and (Nd_2) for each designs of the four design from the all figures was noted that: **P_{out} (Nd1)> P_{out}(Nd2)**

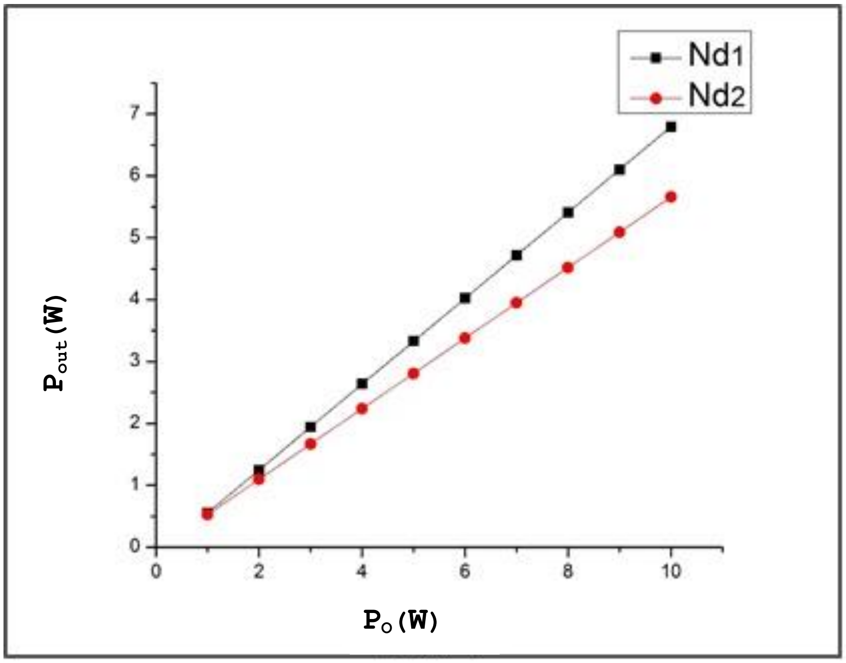

Figure (3.3). Lasing output power vs pump power at design(d1)

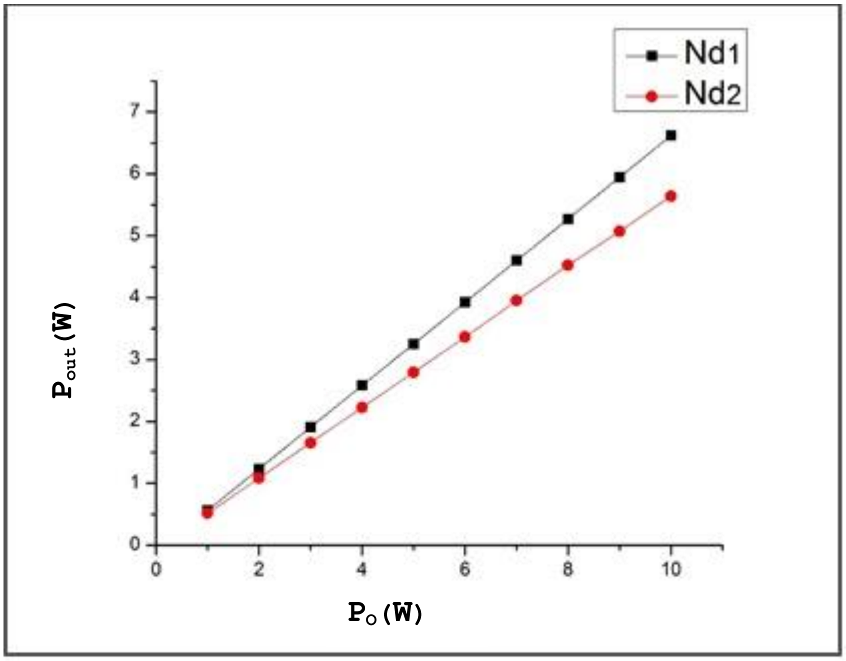

Figure (3.4).Lasing output power vs pump power at design (d2)

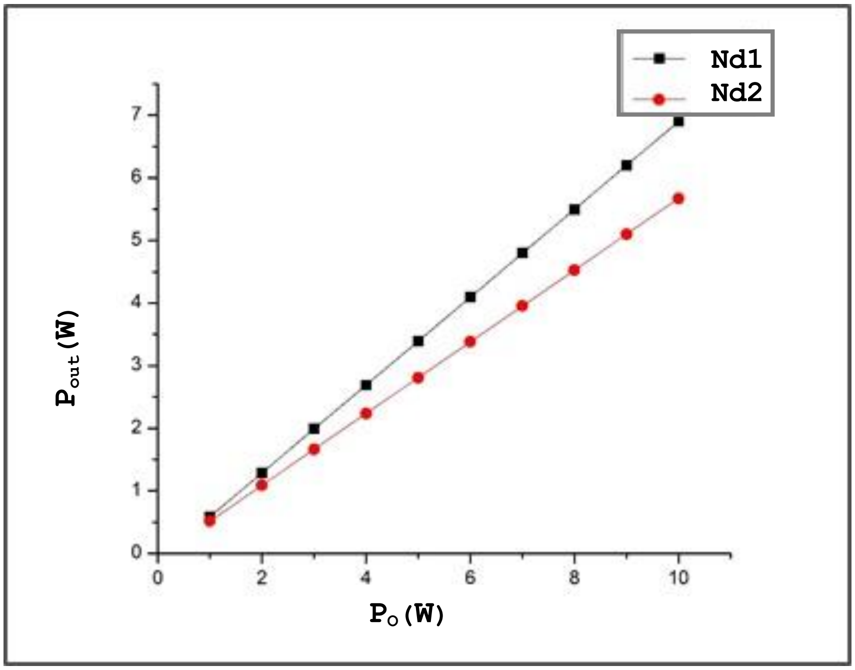

-

Figure (3.5). Lasing output power vs pump power at design (d3).

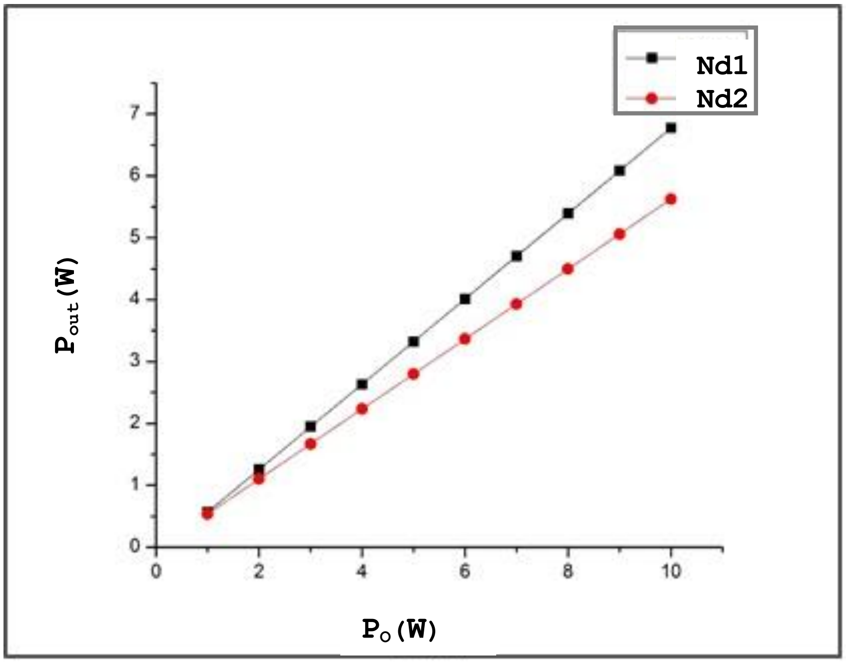

Figure (3.6).Lasing output power vs pump power at design (d4)

(4.2.2) The host ZBLAN

Table (3.17) shows all the required coefficients to calculate the laser output power design (d5) specialized for this host. Table (3.18). shows the coefficient of the two wave length (Nd3) and with pumping source (diode laser), the result of (Nd3) and (Nd4) in this case are as follows:

Table (3.17). default value for used parameters[64].

Parameters	Value	Unit
N_o	20×10^{25}	ion/m^3
T_2	445×10^{-6}	sec
T_3	11×10^{-9}	sec
L	116×10^{-2}	m
a	1.9×10^{-6}	m

Table (3.18) default value for used parameters[93,94].

Parameters	Value		unit
	Nd_3	Nd_4	
λ_p	806×10^{-9}	806×10^{-9}	m
σ_p	2.5×10^{-24}	2.5×10^{-24}	m^2
λ_L	1048×10^{-9}	1317×10^{-9}	m
σ_L	34.515×10^{-25}	8.28×10^{-25}	m^2

1- Determinations of (NA)

Tables (3.19). and (3.20). show (P_{out}) values corresponding to (NA) for the two waves length (Nd3) and (Nd4) respectively according to these results, table (3.21). Shows (NA) value for each wave length that is the highest laser output power has been obtained.

Table (3.19). The values of (P_{out}) vs (NA) for a design (d5) at (Nd_3) wavelength.

NA	P_{out}(W)
0.030	6.371059
0.043	1.098634
0.057	0.072241
0.069	0.011178
0.083	0.003590
0.097	0.001852
0.0109	0.001249
0.0123	0.000975
0.137	0.000826
0.150	0.000735

Table (3.20). The values of (P_{out}) vs (NA) for a design (d5) at (Nd_4) wavelength.

NA	P_{out}(W)
0.040	5.705477
0.052	4.80164
0.064	1.848423
0.077	0.443471
0.089	0.135116
0.101	0.058004
0.113	0.032652
0.126	0.022129
0.138	0.016906
0.150	0.013956

Table (3.21). The values of (NA) will be obtained highest (P_{out}) for the design (d5).

Lasing wavelength	NA
Nd_3	0.030
Nd_4	0.040

2- calculations of (P_{out})

Table (3.22). Shows all the coefficients which aren't affected by pumping power increasing (Nd3) and (Nd4), table (3.23). shows the (P_{abs}) values corresponding to pumping power for two wavelengths while Figure (3.17) shows the (P_{out}) values corresponding of pumping power for (Nd3) and (Nd4) then it can be noted that

P_{out}(Nd3)> P_{out}(Nd4).

Table (3.22). The values of parameters are not affected when the (P_o) increased for design (d5) at (Nd3) and (Nd4)wavelength.

Parameter	Value		Unit
	Nd_3	Nd_4	
V	0.444344	0.592459	-
M	0.080020	0.142258	-
A_{eff}	4.119856×10^{-7}	1.512309×10^{-8}	m^2
Γ_p	0.160000	0.160000	-
Γ_L	5.061683×10^{-6}	1.020951×10^{-5}	-
α_p	63.999999	15.99999	m^{-1}
α_L	0.003494	4.229798×10^{-4}	m^{-1}
η%	67.780540	57.549975	-
P_{th}	0.600459	0.086048	W
G_{th}	64.045414	16.045414	m^{-1}

Table (3.23). The values of (P_{abs}) vs (P_o) for design (d5) at the wavelength (Nd3) and (Nd4).

P_o (W)	P_{abs} (W)	
	Nd_3	Nd_4
1	1	0.999999
2	2	1.999999
3	3	2.999999
4	4	3.999999
5	5	4.999999
6	6	5.999999
7	7	6.999999
8	8	7.999999
9	9	8.999999
10	10	9.999999

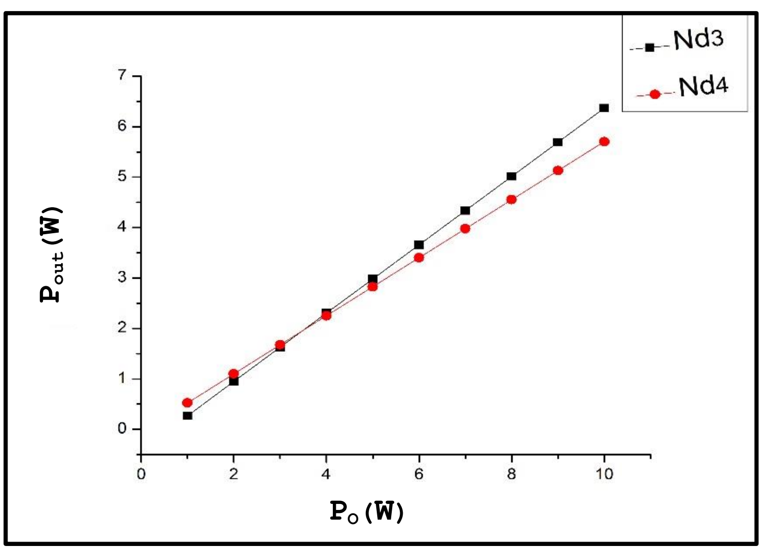

Figure (3.7) Lasing output power variation vs pump power at design (d5)

(3.2.3) Highest value of laser output power

According to the results that are demonstrated, it can be noted that to obtain the highest value of laser output power, must be used the wave length (Nd1) and the host is Silica for the design (d3), then this step of all the coefficients will be calculated which included the laser output power and these coefficients are (NA, a, b, L, R_2, N_o, T_2 and P_o**)** respectively,As in table (3.1), in order to determine the range that each coefficient changes, the effectiveness of these coefficients will be presented as bellow:

(3.2.3.1) The effects of (NA)

Table (3.24). shows the all coefficients that are not effected by increasing the numerical aperture (NA) while table (3.25). shows all the coefficients which their values change by increasing (NA).

Figure (3.8). illustrated the change of (P_{th}) with (NA) increasing, it is noted that (P_{th}) value decreased gradually by (NA) increasing , and increased gradually too, the reason of this behavior belongs to the exponential factor in equation(2-54) , figures (3.9). and (3.10). illustrated the largely decreasing of the efficiency and laser output power respectively with (NA) increasing, it is noted that the highest laser output power value , obtained with (NA= 0.045).

Table (3.24). The values of coefficients that are not effected by increasing (NA).

Parameter	Value	Unit
Γ_p	0.160000	-
α_p	15.999999	m^{-1}
P_{abs}	9.993638	W
G_{th}	16.114522	m^{-1}

Table (3.25). The values of coefficients that are changed by increasing (NA).

NA	α_L (m^{-1})	Γ_p	$A_{eff}\times10^{-12}$ (m^2)	M	V
0.045	0.001125	0.000009	0.986015	0.090896	0.473577
0.057	0.016739	0.000134	0.071004	0.144136	0.596357
0.063	0.138269	0.001106	0.009857	0.209596	0.719136
0.079	0.725016	0.005800	0.002327	0.287275	0.841916
0.092	2.6335	0.020803	0.000844	0.377173	0.964695
0.103	6.767334	0.054139	0.000422	0.479289	1.087474
0.115	13.585265	0.108682	0.000263	0.593626	1.210254
0.127	22.395012	0.179160	0.000189	0.720182	1.333033
0.138	32.054444	0.256436	0.000149	0.858951	1.455813
0.150	41.604508	0.332836	0.000125	1.009950	1.578590

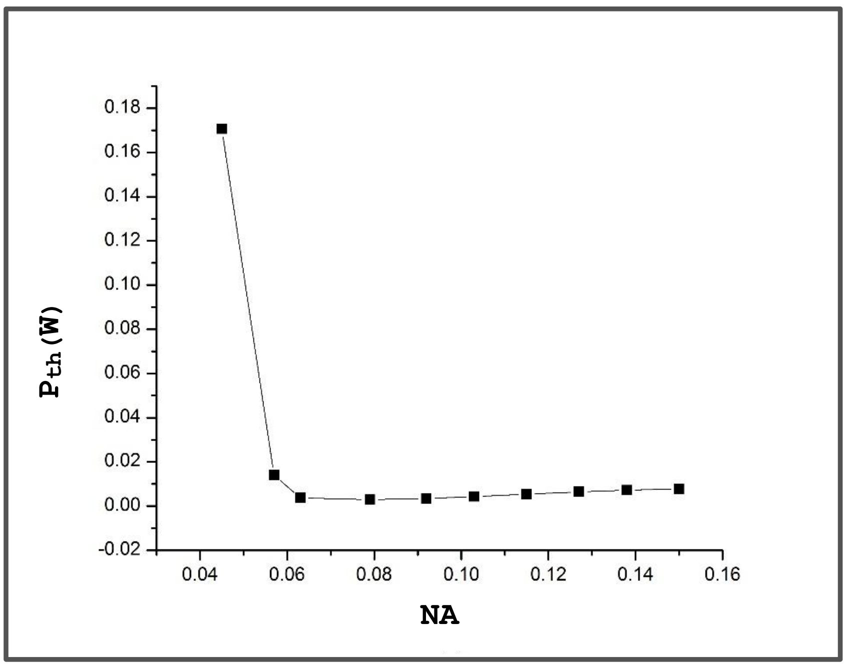

Figure (3.8). Lasing threshold power vs Numerical aperture.

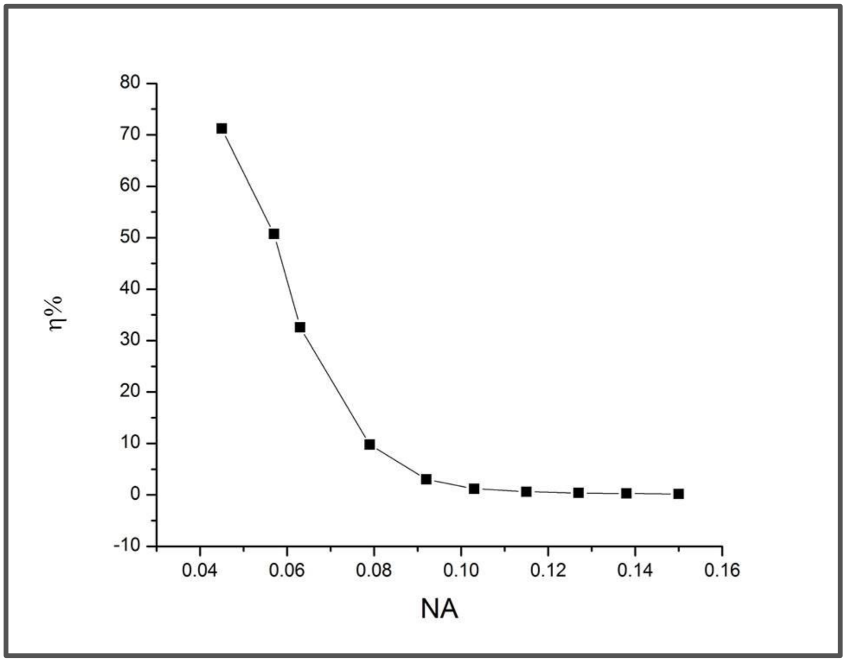

Figure (3.9). Efficiency vs Numerical aperture.

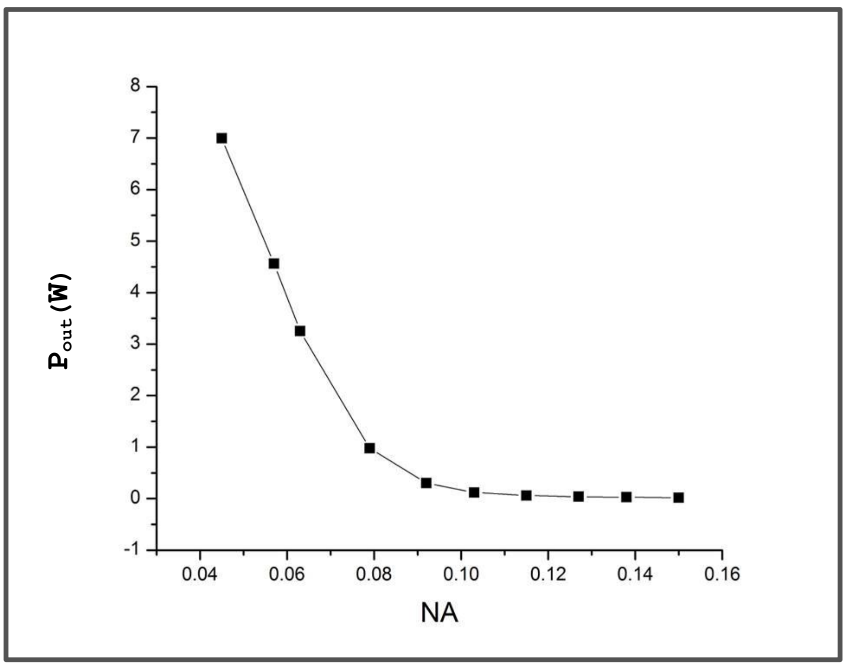

Figure (3.10). Lasing output power vs Numerical aperture.

(3.2.3.2)The effect of (a)

Table (3.26) shows all the coefficients which cannot be effected by increasing of the laser optical fiber core radios (a) while table (3.27). Shows all the coefficients which can be affected by this increase.

Table (3.26) The values of coefficients that are not effected by increasing (a) .

Parameters	Value	Unit
Γ_p	0.160000	-
α_p	15.999999	m^{-1}
P_{abs}	9.993638	W
G_{th}	16.114522	m^{-1}

Table (3.27). The values of coefficients that are changed by increasing (a).

$a*10^{-6}$ (m)	α_L (m^{-1})	Γ_L	A_{eff} (m^2)	M	V
1.350	0.001125	0.000009	0.986015	0.090896	0.473578
1.500	0.004069	0.000033	0.347203	0.113049	0.528146
1.661	0.012810	0.000102	0.138989	0.137617	0.582715
1.817	0.035816	0.000287	0.062360	0.164598	0.637283
1.972	0.090254	0.000722	0.031052	0.193993	0.691852
2.128	0.207171	0.001627	0.017029	0.225802	0.746421
2.283	0.436652	0.003493	0.010216	0.260024	0.800989
2.439	0.850435	0.006803	0.006655	0.296659	0.855558
2.594	1.538881	0.012311	0.004671	0.335709	0.910126
2.750	2.600331	0.020802	0.003502	0.377173	0.964695

Figure (3.11). illustrated the decreased (P_{th}) gradually with increasing (a), and after that starting increasing gradually ,while Figures (3.12) and (3.13) illustrated how the efficiency and laser output power increased largely when the (a) increased, respectively. The highest laser output power can be obtained at a=1.35x10 $^{-6}$m.

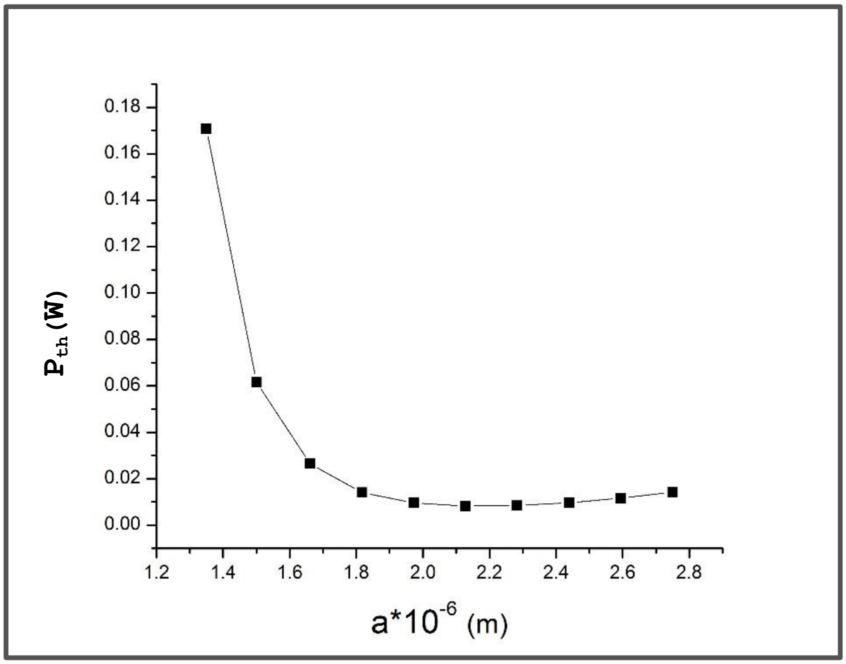

Figure (3.11). Lasing threshold power vs core radius.

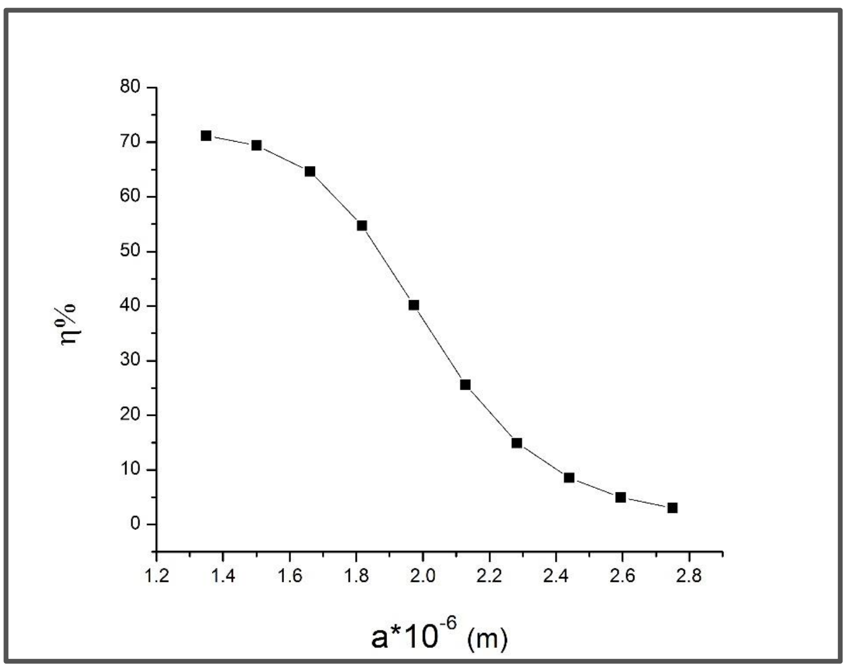

Figure (3.12). Efficiency vs core radius.

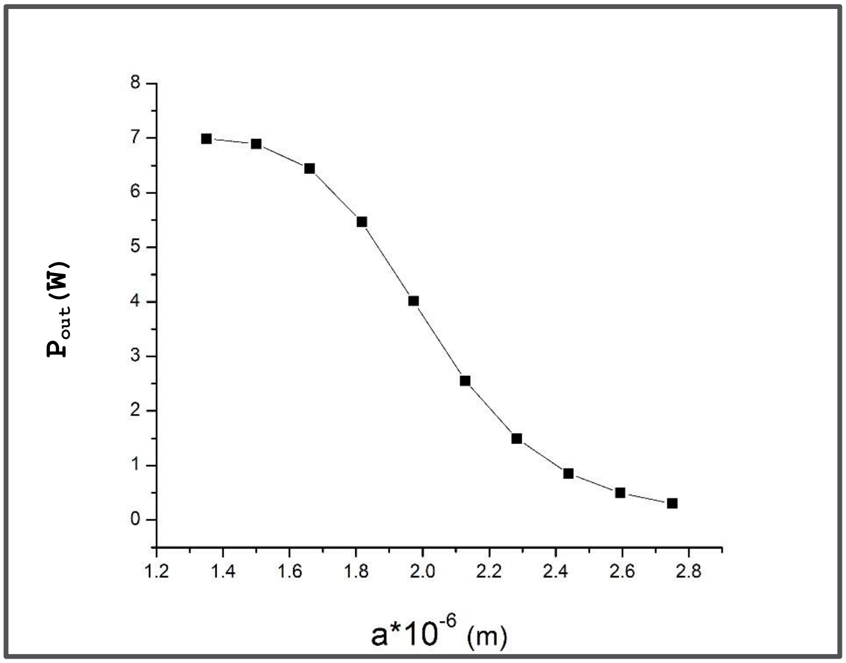

Figure (3.13). Lasing output power vs core radius.

(3.2.3.3)The effect of (b)

Table (3.28) shows all the coefficients which cannot be affected when the protection clad radios (b) increases, while table (3.29). shows all the coefficients that their values can be changed with this increase.

Table (3.28). The values of coefficients that are not effected by increasing (b).

Parameters	Value	Unit
V	0.473578	-
M	0.090896	-
A_{eff}	9.860152×10^{-8}	m^2
Γ_L	9.0011929×10^{-6}	-
α_L	0.001125	m^{-1}
$\eta_{\%}$	71.198285	-

Table (3.29). The values of coefficients that are effected by increasing (b).

$b*10^{-6}$ (m)	G_{th} (m^{-1})	α_p (m^{-1})	Γ_p
3.375	16.114522	15.999999	0.160000
4.050	11.225633	11.111111	0.111111
4.725	8.277787	8.163265	0.081633
5.400	6.34522	6.250000	0.062500
6.075	5.052794	4.938272	0.049382
6.750	4.114522	4.000000	0.040000
7.425	3.420307	3.305785	0.033058
8.100	2.892300	2.777777	0.027777
8.775	2.481386	2.366864	0.023668
9.450	2.15539	2.040816	0.020408

Figures (3.14 and 3.15) and 3.16). Show the (P_{th}), (P_{abs}) and (P_{out}) respectively, which decreased when (b) is increased, the highest laser output power can be obtained at (b= 2.5 a).

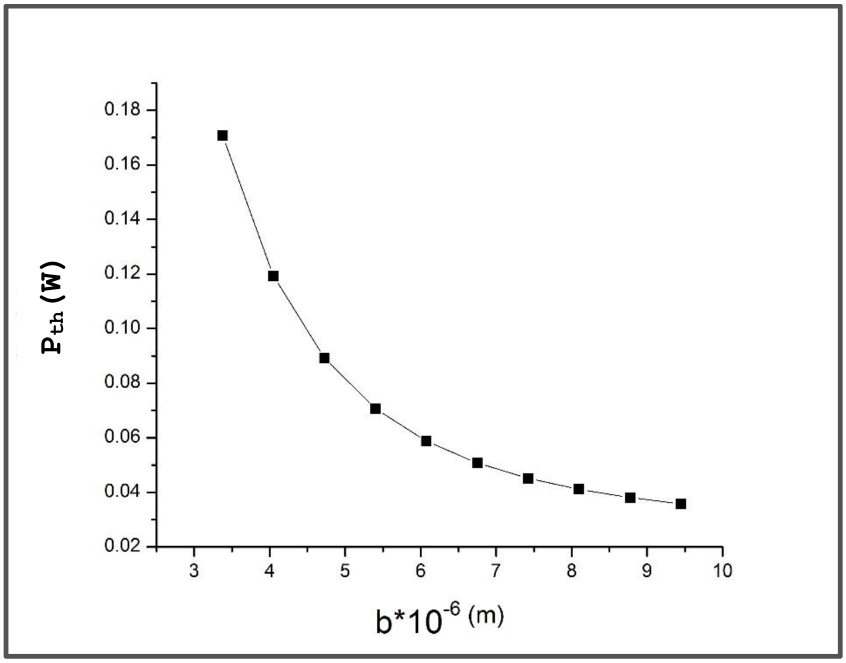

Figure (3.14). Lasing threshold vs cladding radius.

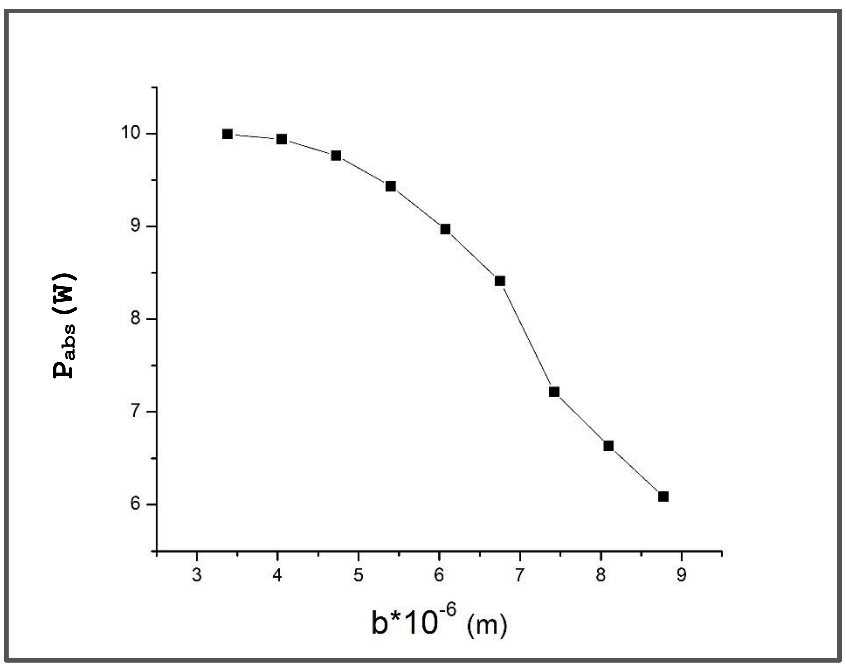

Figure (3.15). Absorbed pump power vs cladding radius.

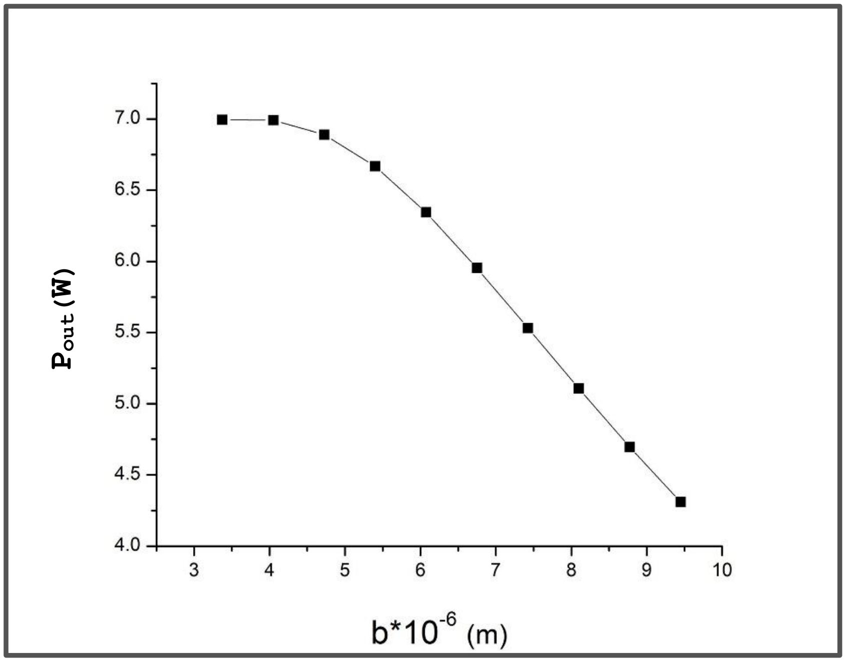

Figure (3.16). Lasing output power vs cladding radius.

(3.2.3.4) The effect of (L)

Table (3.30). Shows all the coefficients that cannot be affected when the optical fiber length (L) increased, while table (3.31). Shows the increased (G_{th}) slightly with this increase.

Table (3.30). The values of coefficients that are not effected by increasing (L) .

Parameters	value	Unit
V	0.4335778	-
M	0.090896	-
A_{eff}	9.560151×10^{-8}	m^2
Γ_p	0.160000	-
Γ_L	9.001193×10^{-6}	-
α_p	15.999999	m^{-1}
α_L	0.001125	m^{-1}

Table (3.31). The values of (G_{th}) vs (L).

L ×10^{-2} (m)	G_{th} (m^{-1})
45.000	16.114522
55.889	16.094258
65.778	16.080088
75.667	16.069621
85.556	16.061574
95.444	16.055195
105.333	.16.050013
115.22	16.045721
125.111	16.042721
150.000	16.039022

Figures (3.17). and (3.18). illustrated (P_{th}) and (P_{abs}) values that increased slightly when (L) increased. Figures (3.19 and 3.20). illustrated the decrease of (η) and (P_{out}) with this increase, the highest output power can be obtained at (L= 46x10 $^{-2}$ m).

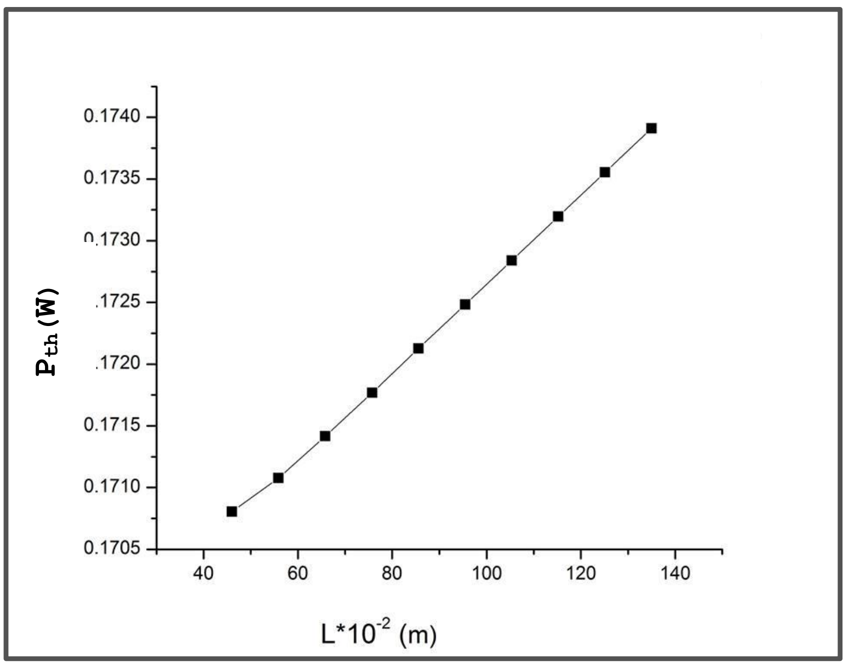

Figure (3.17). Lasing threshold vs fiber length.

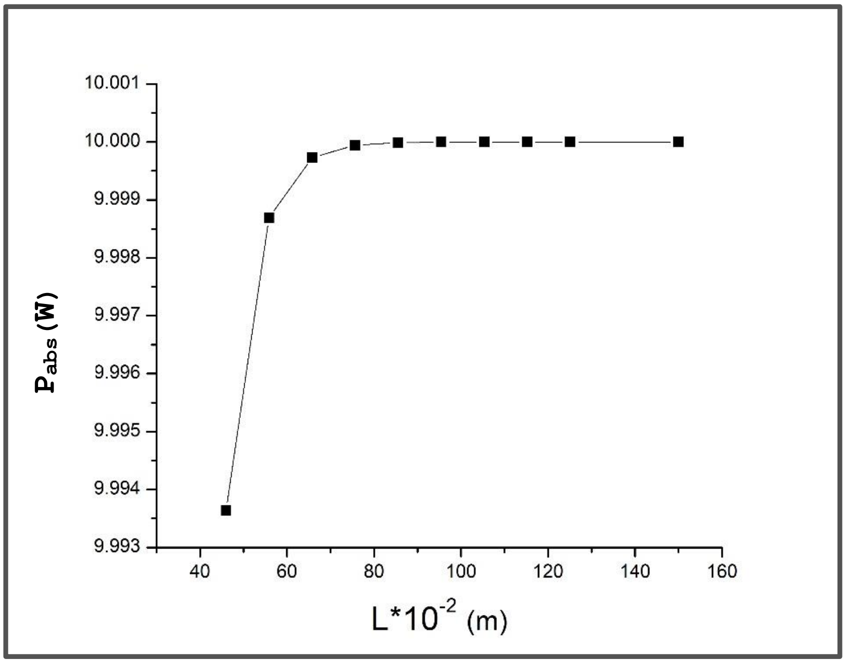

Figure (3.18). Absorbed pump power vs fiber length.

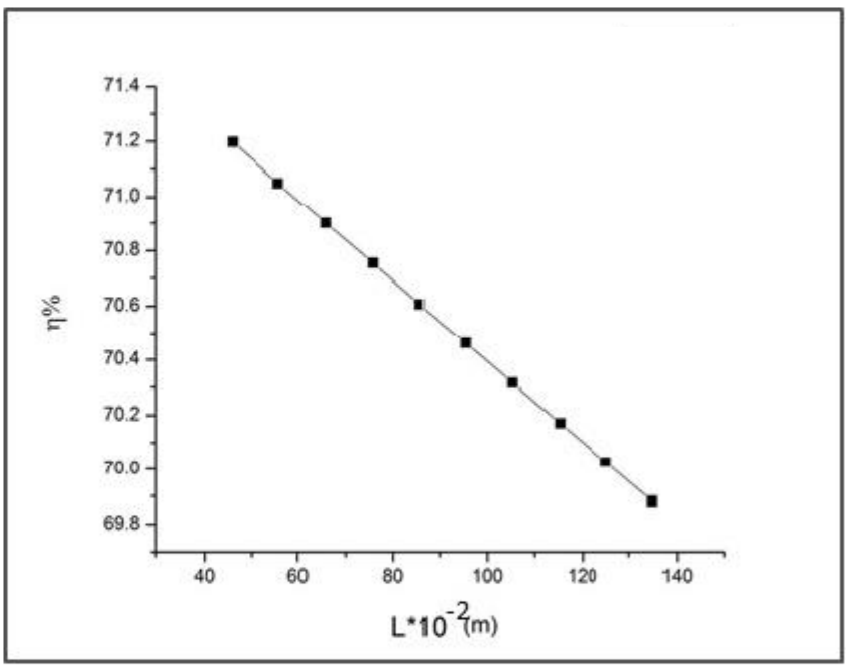

Figure (3.19). Efficiency vs fiber length.

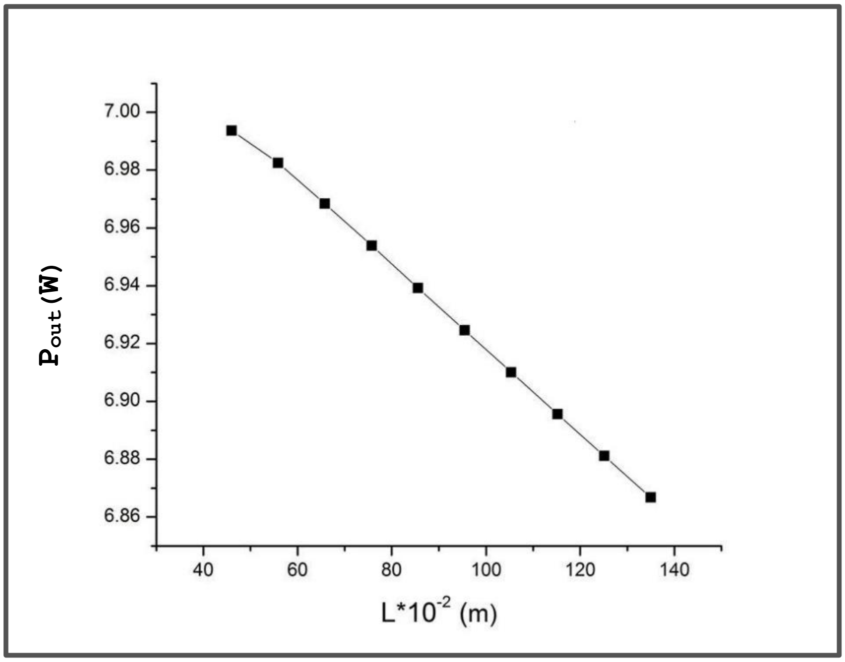

Figure (3.20). Lasing output power vs fiber length.

(3.2.3.5) The effect of (N_o)

Table (3.32). shows all the coefficients that cannot be affected with the increasing of the(Nd^{+3}) concentration in the core of optical fiber (N_o) while table (3.33). shows all the confidents that can be changed with this increase.

Table (3.32). The values of coefficients that are not effected by increasing (N_o).

Parameters	Value	Unit
V	0.473578	-
M	0.090896	-
A_{eff}	9.860152×10^{-8}	m^2
Γ_P	0.160000	-
Γ_L	9.001193×10^{-6}	-

Table (3.33). The values of coefficients that are effected by increasing (N_o)

N_o*10^{25} (ion/m^2)	G_{th} (m^{-1})	α_p (m^{-1})	α_L (m^{-1})
5.000	16.114522	15.999999	0.001125
5.722	18.425633	18.311111	0.001288
6.444	20.736744	20.622222	0.014502
7.167	23.047855	22.933333	0.001613
7.889	25.358966	25.244444	0.001775
8.611	27.670077	27.555555	0.001938
9.333	29.981189	29.866666	0.002100
10.056	32.292299	32.177777	0.002263
10.778	34.603411	34.488888	0.002425
11.500	36.914522	36.799991	0.002588

Figures (3.21 and 3.22). illustrated the increase of (P_{th}) and (P_{abs}) respectively when (N_o) increased, while figures (3.23 and 3.24). illustrated the increase slightly with this increase, the highest value of laser output power can be obtained at (N_o = 5x10 ^{25}) ion/ m^3.

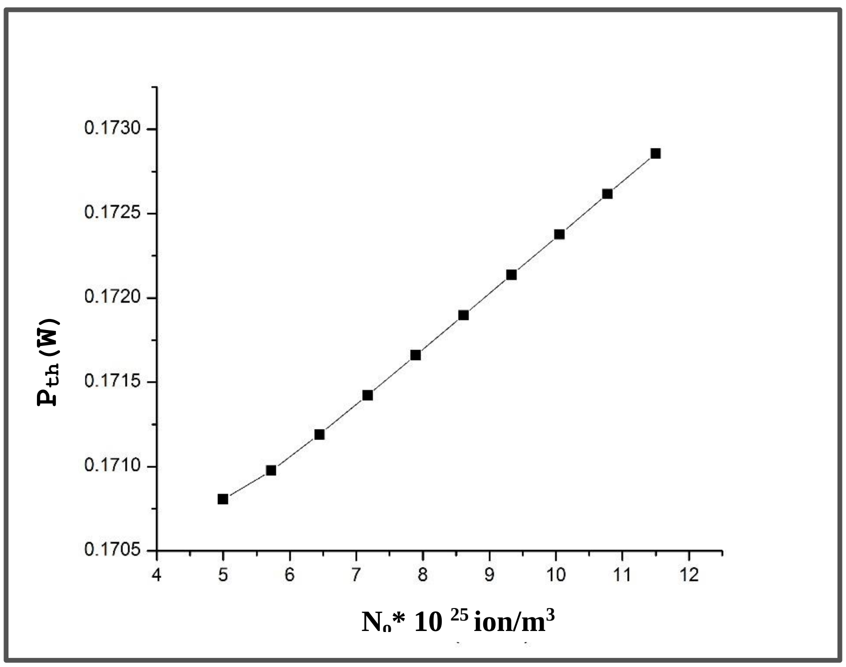

Figure (3.21). Lasing threshold power vs concentration.

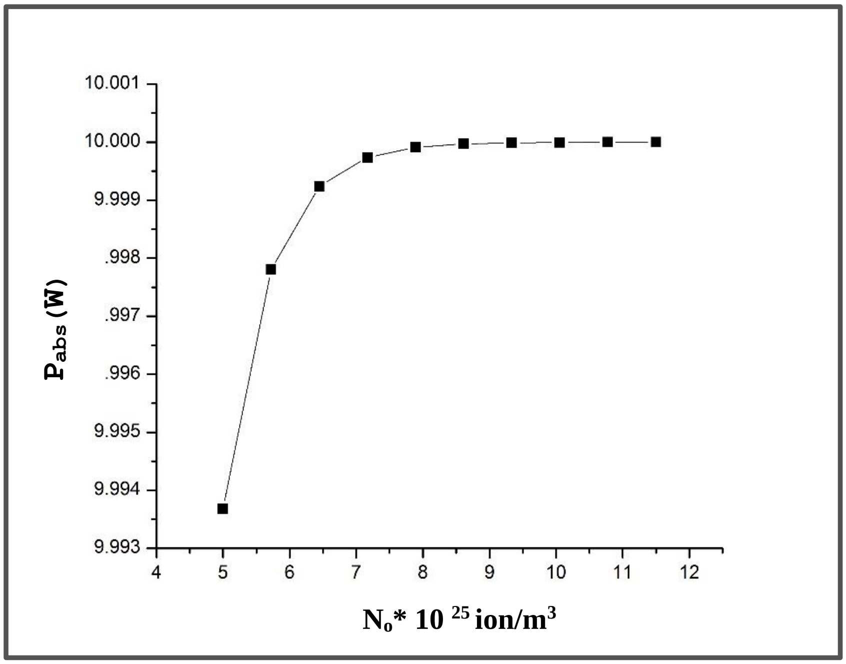

Figure (3.22). Absorbed pump power vs concentration.

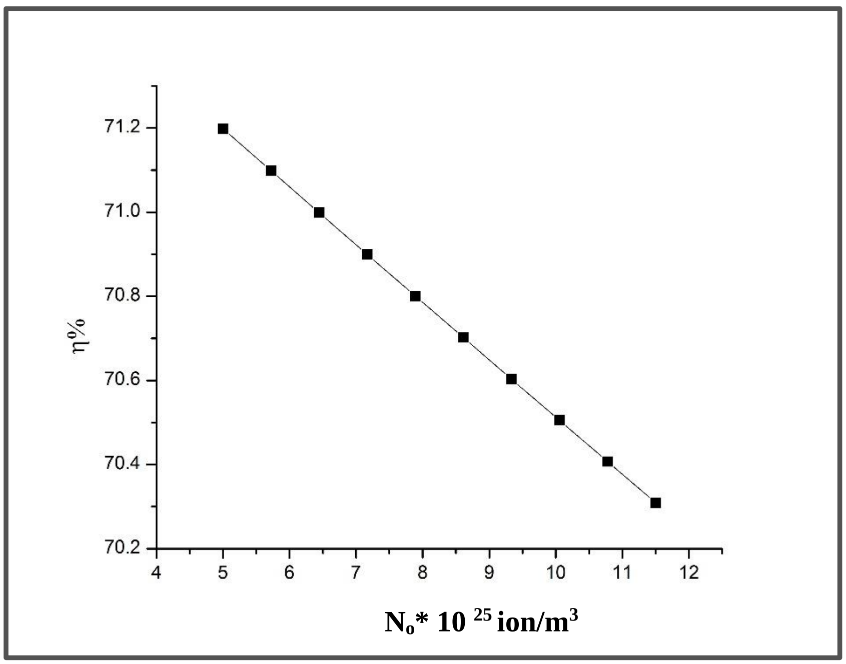

Figure (3.23). Efficiency vs concentration.

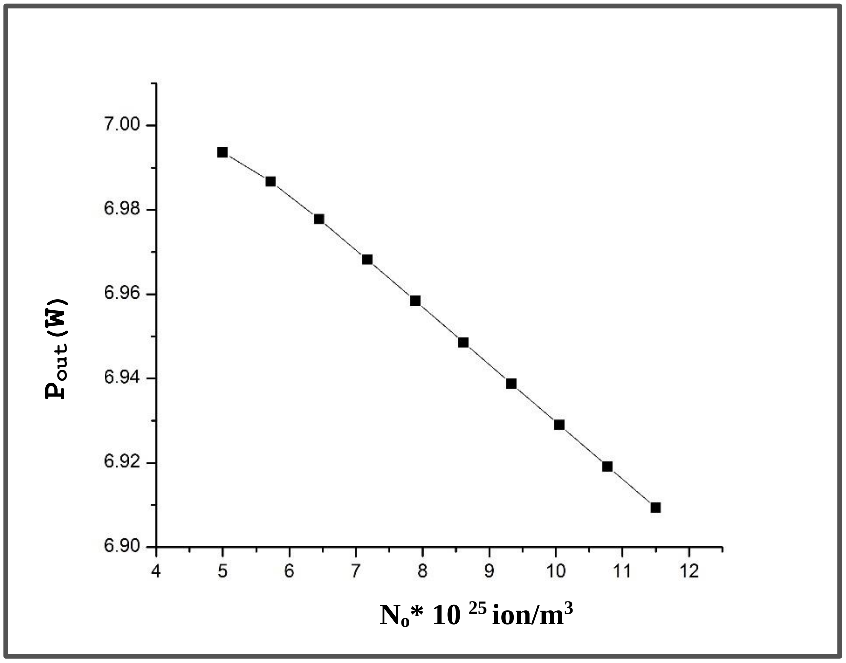

Figure (3.24). Lasing output power vs concentration.

We observe from the above that the value of the Lasing output power (P_{out}) decrease by increasing each value of (NA, a ,b, L, N_O) and the cause of that is because of each of efficiency (η_s) and absorbed pump power (P_{abs}) are decrease while the value of threshold lasing power(P_{th}) increase by this increasing and this is satisfy the equation(2-61)

(3.2.3.6) The effect of (R_2)

Table (3.34). shows all the coefficients that cannot be affected with the increase of the laser output mirror reflectivity (R_2), while table (3.35). shows how (G_{th}) reduces with this increase.

Table (3.34). The values of coefficients that are not effected by increasing (R_2).

Parameters	value	Unit
V	0.473578	-
M	0.090896	-
A_{eff}	9.360152×10^{-8}	m^2
Γ_p	0.160000	-
Γ_L	9.001193×10^{-6}	-
α_p	15.999999	m^{-1}
α_L	0.001125	m^{-1}
P_{abs}	9.993638	W

Table (3.35). The values of (G_{th}) vs (R_2)

R_2	G_{th} (m^{-1})
0.090	18.617332
0.180	17.863911
0.270	17.423188
0.360	17.110491
0.450	16.867943
0.540	16.669768
0.360	16.502213
0.720	16.357069
0.810	16.229045
0.900	16.114522

The Figure (3.25). shows that (P_{th}) reduces with (R_2) increases, while Figures (3.26) and (3.27). show how (η) and (P_{out}) increase with (R_2) increasing respectively.

The highest output power can be obtained at (R_2= **0.9**).

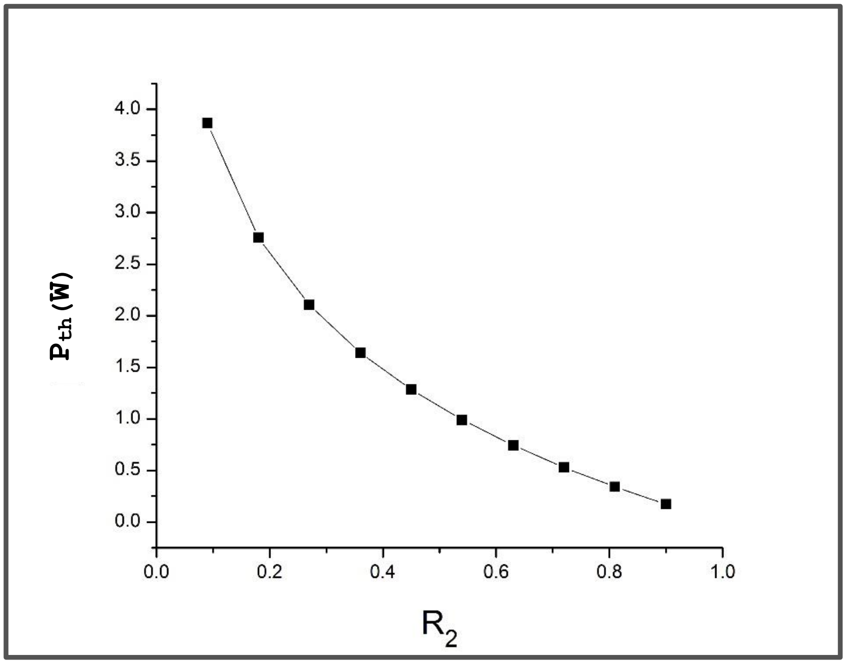

Figure (3.25). Lasing threshold power vs reflectivity of mirror (2).

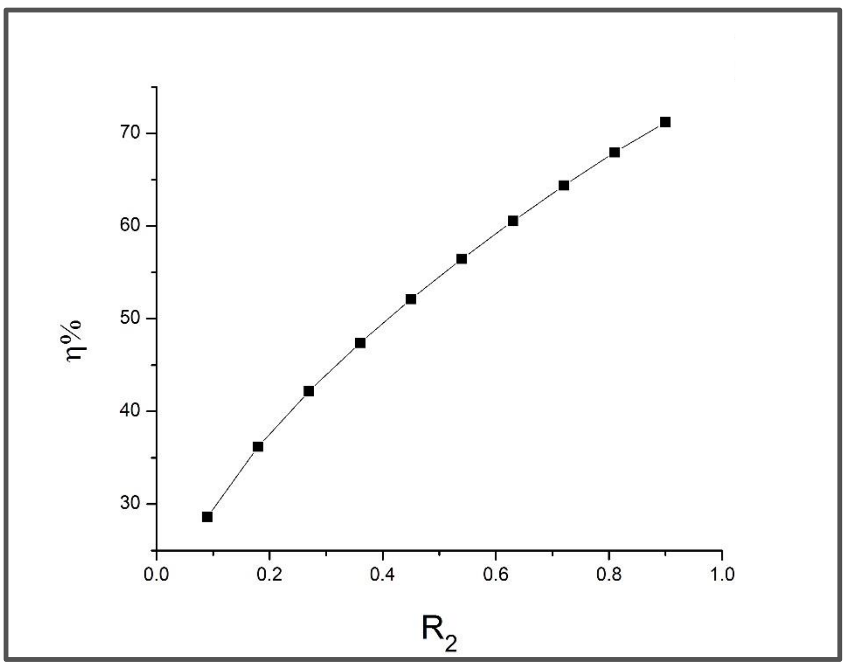

Figure (3.26).Efficiency vs reflectivity of mirror (2).

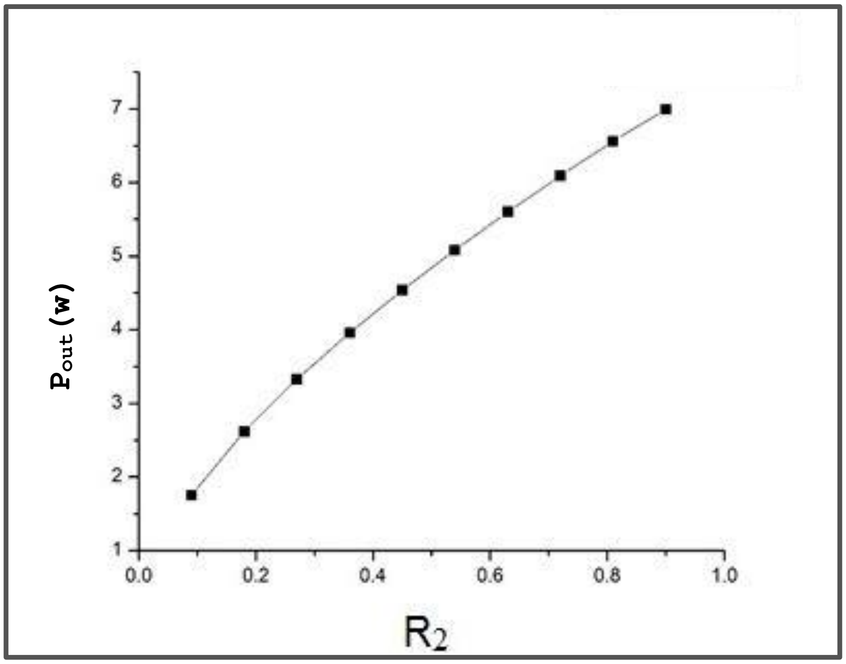

Figure (3.27). Lasing output power vs reflectivity of mirror (2).

(3.2.3.7) The effect of (T_2)

Table (3.36). shows all the coefficients that cannot be affected with increase of the higher laser level life time (T_2)

Figure (3.28). illustrated the slightly decrease when (T_2) increased while Figure (3.29). illustrated the slightly increase with this increase, the highest value of the laser output power can be obtained at (T_2=485 x10^{-6} s)

Table (3.36). The values of parameters are not effected by increasing (T_2).

Parameters	value	Unit
V	0.473578	-
M	0.090896	-
A_{eff}	9.860152×10^{-8}	m^2
Γ_p	0.160000	-
Γ_L	9.001193×10^{-6}	-
α_p	15.999999	m^{-1}
α_L	0.001125	m^{-1}
G_{th}	16.114522	m^{-1}
P_{abs}	9.993638	W
η%	71.198285	-

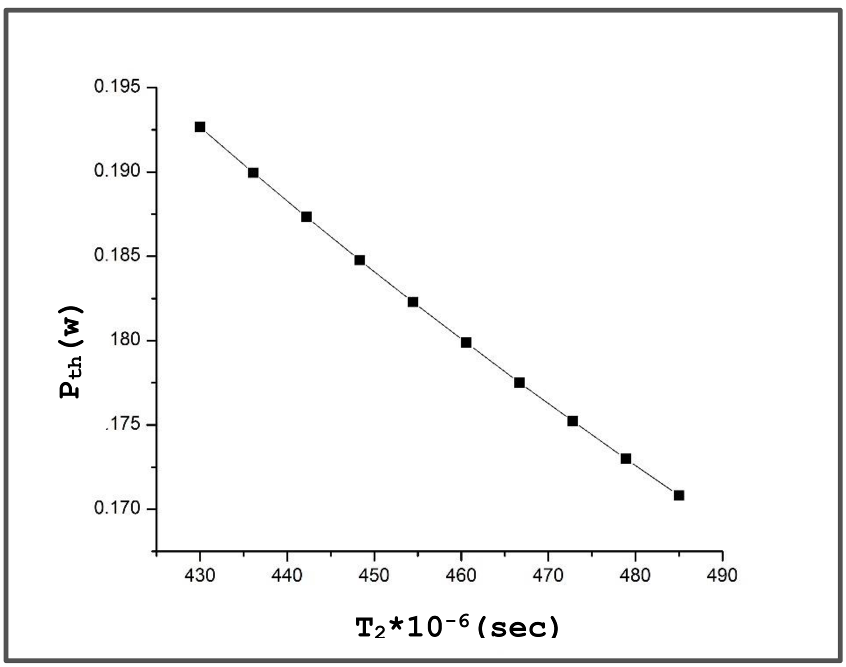

Figure (3.28). Lasing threshold power vs lifetime of upper laser level

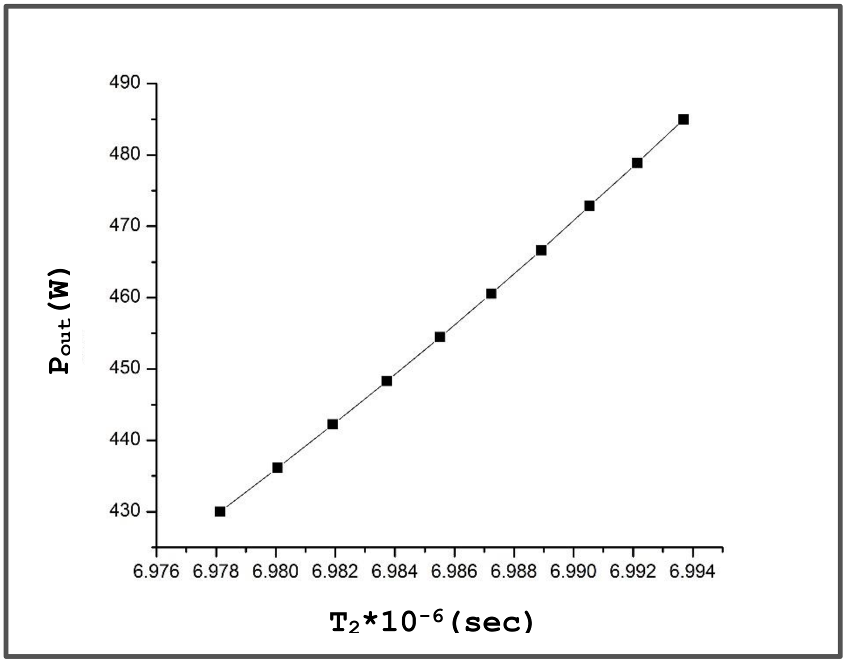

Figure (3.29). Lasing output power vs lifetime of lasing upper level.

(3.2.3.8) The effect of (P_o)

Table (3.37) all the coefficients that cannot be affected with the increase of pumping power (P_o)

Table (3.37) The values of parameters are not effected by increasing (P_o).

Parameters	value	Unit
V	0.473578	-
M	0.090896	-
A_{eff}	9.860152×10^{-8}	m^2
Γ_p	0.160000	-
Γ_L	9.001193×10^{-6}	-
α_p	15.999999	m^{-1}
α_L	0.001125	m^{-1}
G_{th}	16.114522	m^{-1}
P_{th}	0.170806	W
η%	71.198285	-

Figure (3.30) illustrated the increase of (P_{abs}) with (P_o) increase while figure (3.31) illustrated the increase of (P_{out}) with (P_o) increase, the highest value of output power can be obtained at (P_o= 10 W).

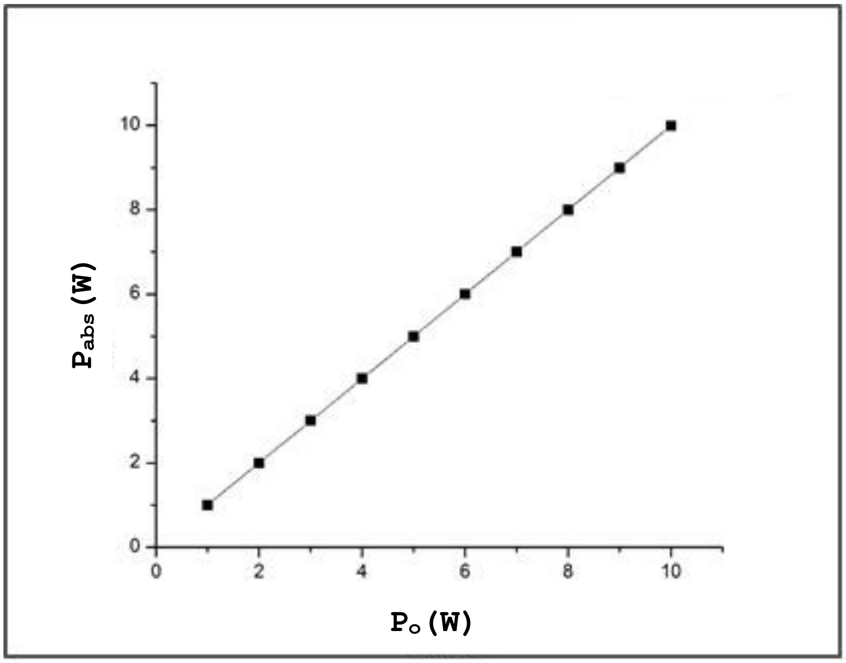

Figure (4.30) Absorbed power vs pump power.

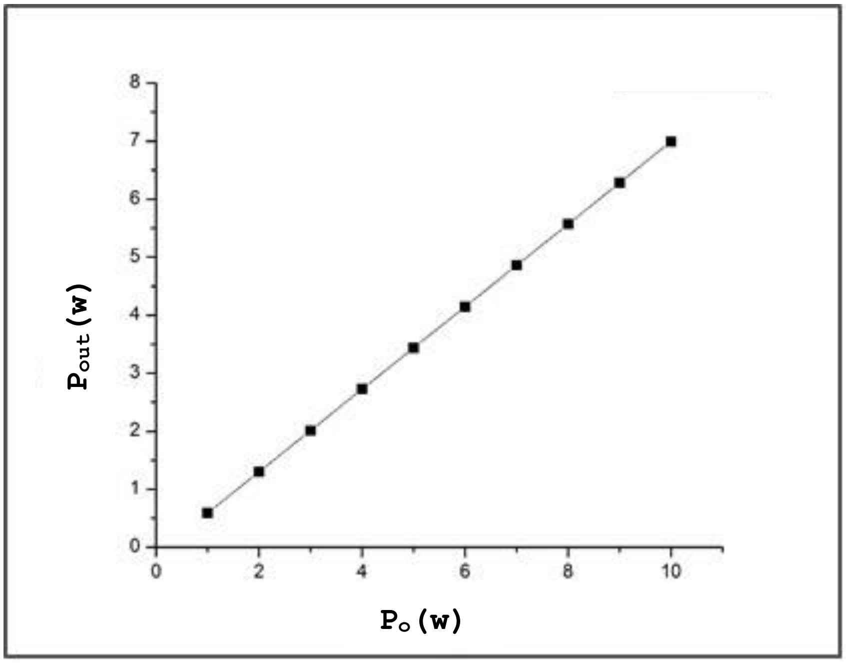

Figure (4.31). Lasing output power vs pump power

We observe from the above that the value of losing output power increase by increasing each value of(R_2, T_2 ,P_o) and the cause of that is each value of efficiency (η_s) and absorbed pump power (P_{abs}) are increase while the value of threshold power(P_{th}) is decrease by this increasing and this is satisfy the equation (2-61)

(3.2.3.9) Typical values

According to calculation of coefficients effect on laser output power (P_{out}), the optimal values of these coefficients in order to obtain the highest laser output power can be presented in table (3.38).

Table (3.38) The Typical values are used to obtain highest output laser and efficiency.

parameters	Value	Unit
NA	0.045	-
a	1.35×10^{-6}	m
b	3.375×10^{-6}	m
L	46×10^{-2}	m
R_1	1	-
R_2	0.9	-
N_o	5×10^{25}	ion/m^2
T_2	485×10^{-6}	sec
P_o	10	W

Chapter four

Conclusion and future work

Conclusions.

1-In case that the host type is (Silica), the highest value of (P_{out}) and (η) for the wavelength (Nd_1) can be obtained when the design (d_3) are used while in case of the host type is (ZBLAN), the highest value of (P_{out}) and (η) can be obtained when the wavelength (Nd_3) is used.

2-When using the host (Silica) of the design(d3) at the wavelength (Nd_1), the value of (P_{out}) will be decreased with the increase of the values of (NA, a, b, L and N_o), while it will be increased with the increase of the (R_2, T_2 and P_o) values.

3-The host type (Silica) with the design (Nd_1), the optimal values were determined for these coefficients, that is the highest value of (P_{out}) and (η) will be given.

Future work

1- A theoretical study of the output power for up-convertion Nd^{+3}-Doped ZBLAN glass fiber laser.

2- A theoretical study of the output power for a mode-locked Nd^{+3}-Doped ZBLAN glass fiber laser.

3- A theoretical study of the output power for Nd^{+3}-Doped Silica glass double – clad fiber laser.

4- A theoretical study of the effects of Nonlinearity and Dispersion on the output power of Nd^{+3}-Doped Phosphate glass fiber laser.

5- A theoretical study of the output power for Q-switched Nd^{+3}- Doped Silica glass double-clad fiber laser.

REFERENCES

[1]- R.Paschotta.″ Optical Fiber Technology ″

Book, FG 16 SPIE Field Guides Volume FG 16(USA) University of Arizona. PP. (1-32), (2010).

[2]- G.Keiser.″ Optical Fiber Communication ″

Book, Third Education,Singapore University of Micihigan, PP(25-86), (2000).

[3]- G.P.Agrawal.″ Nonlinear Fiber Optics ″

Book, Third Edition,Academic press(USA)University of Rachester, PP.(1-63), (2001).

[4]- M.Yamance and Y.Asahara.″ Glasses for Potonics ″

Book, University of Cambridge, PP.(1-18), (2004).

[5]- S.O.Kasap″ Optoelectrnics and Photonics: Principles and Practices ″

Book, Upper Saddle River Prentice-Hall, PP.(10-30) (2001).

[6]- H.Zellmer, A.Tünnermann, H.Welling and V.Reichel.″ Double-Clad Fiber Laser with (30)w Output Power ″Trends in Optics and Photonics (TOPS) Vol. 16, PP.(137-140), (1997).

[7]- I.N.Duling, R.P.Moeller, W.K.Burns, C.A.Villarruel, L.Goldberg, E.Snitzer and H.Po.″ Output Characteristics of Diode Pumped Fiber (ASE) Sources ″

IEEE J.Quntum Electron, Vol.27,PP.(995-1003), (1999).

[8]- L.Reckie, I.M.Jauncey, S.B.Poole and D.N.Poyne.″ Diode Laser Pumped Nd^{3+} - Doped Fiber Laser Operating at (938)nm ″

Electron Lett. Vol.(23), PP.(884-5), (1987).

[9]- L.Reekie, R.J.Mears, S.Pool and D.V.Payhe.″ Tunable Single-Mode Fiber Laser ″J.Lightwave Technol. Vol.(4), PP.(956-961), (1986).

[10]- S.G.Grubb. ″ Diode Pumped (1-36) µm Nd^{3+} - Doped Fiber Laser ″

Electron Latt. Vol.(26), PP.(121-2), (1990).

[11]- I.P.Alcock, A.I.Ferquson, D.C.Hanna and A.C.Tropper.″ Tunable Continuous-Wave Neodymium-Doped Mono-Mode Fiber Laser Operating at (900-945) nm and (1070-1135)nm ″

Opt –Lett Vol.(11), PP.(709-711), (1986).

[12]- J.Nillsson and D.Payne.″ High-Power Fiber Laser ″
Science 332 (6032), PP.(921-922), (2011).

[13]- J.E.Townsend.″ The development of Optical Fiber Doped with Rare-Earth Ions ″PhD. Thesis, University of Southampton, Foculty of Electronics and Computer Science, PP.(81-94), (1998).

[14]- W.Koechner and M.Bass″ Solid-State Laser: A Graduate Text ″
Book, Springer, (ch 1), (2003).

[15]- M.J.F.Digonnet.″ Rate-Earth-Doped Fiber Laser and Amplifiers ″
Book, 2a ed Newyork: Marcel Dekker, Inc, PP.(10-21), (2001).

[16]- P.C.Becker, N.A.Olsson and J.R.Simpson.″ Erbium-Doped Fiber Amplifiers: Fundamentals and Technology ″
Academic press, Inc, San Diego, Calif, USA, PP.(18-34), (1997).

[17]- J.H.Campbell and T.I.Suratwala.″ Nd^{3+} - Doped Phosphate Glasses for High-Energy ″J.Non Crystal-Solids. Vol.(54), PP.(318-34), (2000).

[18]- C.Bibean.″ Direct Measurements of The Therminal Laser Level Lifetime in Neodymium-Doped Crystals and Glassses ″J.Opt. Soc. Am. B(12), PP.(1981-1992), (1995).

[19]- C.Bibeau and S.Payne.″ The Therminal-Level Relaxation in Nd^{3+} - Doped Laser Materials ″.ICF. Quarterly Report, UCRLLR-105821-95-2, PP.(1-11), (1995).

[20]- D.C.Descamps, C.Gamach, D.Hueeon and A.Migus. ″ Excited State absorption at (1.06)µm as The Origin of Non-Unity Quantum Yield in Neodumium Doped Glasses ″Opt. Commum. Vol.(168), PP.(123-130), (1990).

[21]- K.Arai, H.Namikawa, K.Kumata, T.Honda X.Ishii.″ Aluminum or Phosphors Co-Doping Effects on The Fluorescence and Structural Properties of Neodymium Doped Silic Glass ″J.Appl. Phys. Vol.(59), PP.(3430-3436), (1987).

[22]- W.J.Miniscalco.″ Optical and Electronic Properties of Rate-Earth Ions inGlasses ″Ny, Basel, Hongkong: Mareel Dekker, PP.(30-100), (1993).

[23]- A.EL.Hassonni, K.Lebbon, C.Gontandier, G.Boulon, A.Yosikawa and T.F ukudawa and T.Fukda.″ Single-Crystal Fiber Grown by Micro.pulling down Tecnique ″ Optical Materials, Vol.(24), No.(1-2), PP.(419-424), (2003).

[24]- Y.Ji, S.Zhao, Y.Huo, H.Zhng, M.Li and C.Huang. ″ Growth of LithiumTriborate Single Crystal Fiber by The Laser-Heated Pedestal Growth Method ″Journal of Crystal Growth, Vol.(112), No.(11), PP.(283-286),(1991).

[25]- A.Schülzgen, L.Li, V.L.Temyanko, S.Suzuki, I.V.Moloney and N.Peyghambarian.″ Single-Frequency Fiber Oscillator with watt-Level Output Power Using Photonic Optics Express, Vol.(14), No.(16), PP.(7087-7092), (2006(.

[26]- J.S.Sanghera, I.D.Aggrawal and L.B.Shaw.″ Nonlinear Properties of Chalcogenide Glass Fibers ″Journal of Opteclelectronics and Advanced Material , Vol.(8), No.(6), PP.(2148-2155), (2006).

[27]- X.Zhn and R.Jain.″ (10)w-Level Diode-Pumped Compact (2.78)µm ZBLAN Fiber Laser ″Optics Latters, Vol.(32), No.(1), PP.(26-28), (2007).

[28]- S.Tokita, M.Murakami, S.Shimizu, M.Itashida and S.Sakab.″ Liquid-Cooled (24)W mid-Ifrored Er: ZBLAN Fiber Laser ″Optics Letters, Vol.(34), No.(20), PP.(3062-3064), (2009).

[29]- Y.Miyajma, T.Komukai, T.Sugawa and T.Yamamoto.″ Rare-Earth-Diode Fluorid Fiber Amplifiers and Fiber Lasers ″Optical Fiber Tecnology, Vol.(1), No.(1), PP.(35-47), (1994).

[30]- D.S.Funk and J.G.Eden.″ Glass-Fiber Laser in The Ultraviolet and Visible ″ IEEE Journal on Selected Topics in Quntum Electronics Vol.(1), No.(3), PP.(784-791), (1995).

[31]- S.wang.F.Lou, M.wang, c.yu, S.Feng, Q.Zhou, D.Chem and L.Hu. "Characteristics and Laser Performance of yb^{3+}-Doped Silica Large Mode Area Fibers prepared by Sol-Gel Method. "Open Access Fibers, Vol.(111),PP.(93-100),(2013).

[32]- Y.Zhu and N.Peyghambarian "High-Power ZBLAN Glass Fiber Laser: Review and Prospect" Advantage in Optoelectronics, ID 501956 ,PP .(1-23) , (2010).

[33]- M. K.Davis, M.J.F.Digonnet and A.H.Pontell. "Characterization of Clusters in Rare- Earth-Doped Fiber by Transmission Measurements" J.Lightwave Technol. Vol.(13) , PP.(120-6), (1995).

[34]- R.Paschatla, J.Nillsson , P.R.Barber J.E.Coplen ,A.C.Tropper and D.C. Hanna. "Lifetime Quenching in yb^{3+}-Doped Fibers" Opt. Commun , Vol. (136), PP.(375-78) , (1997).

[35]- M.Yamane and y.Asahara. "Glasses for Photonics" Book, University of Combridge, PP.(8-29), (2004).

[36]- R.Reisfeld and C.K.Jurgensen"Excited State Phenomena in Vitreous Materials"Handbook on the Physics and Chemistry of Rare-Earth, Vol.(9),ed.K.A, North Holland,Hmsterdam,PP. (19),(1987).

[37]- D.J.Richardson."High Power Fiber Laser :Current Status and Future Perspectives "J.Opt.Soc.Am.B(27) PP. B (63-92), (2010).

[38]- E. Stiles "New Developments in IPG Fiber Laser Technology" In Procecding of the (5^{th}) , In ternationa workshop on Fiber Lasers (2009).

[39]- M. J. F. Digonnet and C. J. Gaeta “Theoretical analysis of optical fiber laser amplifirers and oscillators” Applied optics , Vol. (24) , No. (3) ,PP. (333-341) , (1985).

[40]- I. P. Alcock , A. I. Farguson , D. C. Hanna and A. C. Tropper, “continuous-wave oscillation of a monomode nerodymium-doped fiber laser at(0.9) μm on the $^4F_{\frac{3}{2}} \rightarrow {}^4I_{\frac{9}{2}}$ transition“ optics communication,Vol.58,no.6,PP (405-408),(1986).

[41]- I.P .Alcock , A.C. Troppre ,A.I.Ferguson . " Q- switching,mode-locking and tunable operation around 0.9µm of a neodymium-deped monomode fiber laser ". IEE PROCEEDINGS,Vol.(134),Pt.j,No.(3),PP (183-186)JUNE (1987).

[42]-M.m.phillIps,h.gong,a.i.ferguson and d.c.hanna. " optical chaos and hystresis in alaser-diode pumped Nd doped fiber laser ".North-Holland physics Puplishing Division,Vol (61),No.(3),PP. (215- 218), (1987).

[43]- P.r. morkel, m.c. farries and s.b. poole ; " spectral variation of excited state absorption in neodymium doped fiber lasers " optical communications, Vol.(67) , No.(5), PP (349-352), (1988) .

[44]- G.geister and R .ulrich." neodymium-fiber laser with integrated-optic mode locker, North-Holland physics Puplishing Division,Vol.(68),No.(3) ,PP(187-189),(1988).

[45]-A.a.madeg,W.E.Berger,G.R.Hanes."Tunable,Frequency Narrowed Nd^{+3}-Doed Fiber Laser For Excitation Of the 5P $^2P_{1/2} - 4d$ $^2D_{3/2}$ Transition in S_r^+ ". Optical Communications, Vol.(73), No.(2), PP (147-152), (1989).

[46] J. Hunkemeier , R. Bohm , V. M. Toschek . "Spectral dynamics of multimode Nd^{3+}- and Yb^{3+}- doped fibre lasers with intracavity absorption" , Optics Communications , Vol.(176) , No.(2000), PP (417-428) (2000).

[47] Nam Seong Kim , Toshihiro Hamada , Mahendra Prabhu , Cheng Li , Jie Song , Ken-ichi Ueda , Anping Liu , Hong Jin Kong , "Numerical analysis and experimental results of output performance for Nd-doped double-clad fiber lasers",Optics Communications, Vol.(6707), No.(2000),PP(1-9), (2000).

[48] Hong-Seok Seo , Yong Gyu Choi , Kyung Hon Kim , Hoon Jeong, and Kyunghwan Oh, "Single Mode Laser Oscillation in an Nd-Doped Large Core Double Clad Fiber Cavity with Concatenated Adiabatic Tapers" ETRI Journal , Vol.(24), No.(3) PP (255-258),(2002).

[49] M.Rusu , S.karirinne , M.Guina , A.B. Grudinin, and O.G. Khotnikov "Femtosecond Nedymium –Doped Fiber Laser Operating in the 894-909-nm Spectral Range"Vol.(16), No.(4), PP(1029-1031), (2004).

[50] Thomas J. Kane, Gregory Keaton, Mark A. Arbore, David R. Balsley, John F. Black, Janet L. Brooks , Mark Byer , Loren A. Eyres, Manuel Leonardo, James J. Morehead, Charles Rich, Derek J. Richard, Laura A.

Smoliar and Yidong Zhou , "Watt blue source based on 914- nm Nd:YVO_4 passively-Q-switched laser amplified in cladding-pumped Nd:fiber", Vol.(650),PP (526-1224), (2004).

[51] Daniel B. S. Soh, Seongwoo Yoo, Johan Nilsson, Jayanta K. Sahu, yunghwan Oh, Seungin Baek, Yoonchan Jeong, Member, IEEE, Christophe odemard, Pascal Duprie Jaesun Kim, and Valery Philippv, "Neodymium Doped Cladding-Pumped Aluminosilicate Fiber laser Tunable In the 0.9-µm Wavelength Range", Vol.(40), No.(9), PP (1275-1282) ,(2004).

[52] L. B. Fu, M. Ibsen, D. J. Richardson, J. Nilsson. D. N. Payne, and A. B. Grudinin ,"Compact High-power Tunable Thtree-Level Operation of Double Cladding Nd-Doped fiber Laser",Vol.(17), No.(2), PP (306-308), (2005) .

[53] J. SWDerSke, A. ZAJAC, M. SKORCZAKOWSKI,and P. KOEICZNY,"Q- switched Nd-doped double-clad fiber laser" ,Vol.(13) , No.(3) , PP (187-191) , (2005).

[54] Mathias Moenster, Peter Glas, and Gunter Steinmeyer, "Femtosecond Neodymium-doped microstructure fiber laser", Vol.(13), No.(21), PP (8671-8677), (2005).

[55]-G.Sargsjan,U.Stamm,C.Unger,W.Zschocke and M.Ledi"Characteristics of a neodymium-doped fiber laser mode-loked with a linear external cavity", optics communication ,Vol.(86),No.(6), PP (480.486), (1991).

[56]- M.Le Flohic,Pierre-Luc Francois,M.Jean-Yves Allain,F.Sanchez,and Guy Michel Stephan ; "Dynamics of the Transient Buildup of Emission in Nd^{3+} - Doped Fiber Laser", IEEE Journal of Quantum Electronics,Vol.(27),No.(7)PP (1910-1021),(1991).

[57]-P.R.Morkel.k.p.Jedrzejewski.E.R.Taylor.and D.N.Payne ; ",Short-pulse,High-power Q-Switched Fiber Laser ",IEEE Photonics Technology Letters,Vol.(4),No.(6),PP (545-547),(1992).

[58]-M.D.Selker and J.L.Dallas ; "Modelocked self-frequency doubling neodymium doped fiber laser ",Journal De Physique No,(2),
PP (675-678),(1992).

[59]–P.R.Morkel,K.P.Jedrzejewski.andE.R.Taylor;"Q-Switched Neodymium-Doped phosphate Glass Fiber Laser" ,IEEE Journal Of quantum Electronics,Vol.(29),No.(7),(1993).

[60]-Uri Ghera,Nir Friedman,Moshe Tur ; "polarization related phenomena in Nd-doped fiber lasers",optical materials4,PP (74-80),(1994).

[61]-H,Ammann,W.Hodel,H.P.Weber; "Experimental and numerical investigation of short pulse propagation and amplification around 1.3 μm in a Nd^{3+}-doped fluoride fiber ",optics communication113,PP (39-45),(1994).

[62]-F.Sanchez,B.Meziane,T.Chartier.G.Stephan,and P.L.Francois ; "Output-coupling optimization of Nd-doped fiber lasers ",Applied optics,Vol.(34),No.(33),PP (7674-7679),(1995).

[63]-J.Wang [a,*] , L.Reekie [a],W.S.Brocklesby [b] Y.T.Chow [a,1], D.N. Payne [a] ; "Fabrication, spectroscopy and laser performance of Nd^{3+}-doped lead-silicate glass fibers", Journal of Non-Crystalline solids Vol (180),PP (208-216),(1995).

[64]-M.Wegmuller *,W.Hodel,H.P.Weber ; "Diode pumped mode-locked Nd^{3+}-doped fluoride fiber laser emitting at 1.05μm",optics communication127,PP (267-272),(1996).

[65]-T.Chartier,B.Meziane,F.Sanchez,G.Stephan,and P.L.Francois ;
"optical feedback effects in Nd-doped fiber laser with broad band spectra"
Applied optics ,Vol.(35),No.(12),(1996).

[66]-Y.C.HOOl,h.b.AHMAD; " Technical note self-mode-locking in a Q-switched Nd^{3+}:doped silica fibre laser", Optics and laser Technology,Vol.(28),No.(3),PP (223.227),(1996).

[67]-R.Hofer,M.Hofer,G.A.Reider [1], M.Cernusca,M.H.Ober; "Modelocking of a Nd-fiber laser at 920 nm ",Optics Communications140,
PP (242-244),(1997).

[68]-R.Böhm,V.M.Baev*P.E.Toschek; "Measurement of operation parameters and nonlinearity of a Nd^{3+}-doped fibre laser by relaxation oscillations",Optics Communications134,PP (537-546),(1997).

[69]-J.M .Lee [1] ,M..K.Chum,C.H.Nam ; "Diode-pumped femtosecond Nd:glass fiber laser started with a moving mirror ",Optics Communications137,PP (64-68),(1997).

[70]-K.Ueda and A.Liu ; "Future of High- Power Fiber Laser ",
Laser physics,vol.(8),No.(3),pp (774-781),(1998).

[71]- Eldad Yahel, Ortwin Hess, and Amos A.Hardy, Fellow, IEEE,Fellow,OSA ; " Modeling and optimization of High-power Nd^{3+} -Yb^{3+} codoped fiber lasers", journal of lightwave technology, Vol.(24), No.(3), (2006).

[72]- Richard A. Martin and Jonathan C. Knight ; "Silica-Clad Neodymium-Doped Lanthanum Phosphate Fibers and Fiber Lasers ",IEEE PHOTONICS TECHNOLOGY LETTERS. Vol. (18), No.(4), (2006).

[73]- A. E. Siegmana, Ying Chen, Vikas Sudesh, Martin C. Richardson, Michael Bass, Paul Foy, Wade Hawkins, and John Ballato ; "Confined propagation and near single-mode laser oscillation in a gain-guided, index antiguided optical fiber ",Applied physics letters, 89, 251101 ,(2006).

[74]- Hamit Kalayciogly, Huseyin Cankaya, Jonul Ozen, Lutfu Ovecoglu, Alphan Sennaroglu ; " lasing at 1065nm in bulk Nd^{3+} doped telluride-tungstate glass ", optics communication 281, PP (6065-6060) ,(2008).

[75]- J. Azkargorta I. Iparraguirre1, R. Baida , J. Fernandez ; " On the origin of bichromatic laser emission in Nd^{3+}-doped fluoride glasses", optics express, Vol.(16), No.(16), (2008).

[76]- A. Peled, A. Chiasera, M. Nathan, M. Ferrari, and S. Ruschin ; " Monolithic rare-earth doped sol-gel tapered rib waveguide laser ",
Applied physics letters 92, 221104 (2008).

[77]- Zhang Fan, Wang Chuncan, Ning Tigang ; “A global design of high power Nd^{3+}-Yb^{3+} co-doped fiber lasers “,Optics Communications 281, PP (4442-4448), (2008).

[78]- Paolo Dallocchio, Federico Pirzio, Giancarlo Reali ; “Compact sub-100-fs Nd; silicate laser “,Optics Communications 282 PP (2070-2073), (2009).

[79]- C. N. Santos, D. Mohr, W. F. Silva, A. S. S. de Camargo, H. Eckert, M. S. Li, M. V. D. Vermelho, A. C. Hemandes, A. Ibanez, Did C. Jacinto ; “Luminescent and thermo-optical properties of Nd3+-doped yttrium aluminoborate laser glasses “, Journal of applied physics 106, 023512, (2009).

[80]- Euan Ramsay, Robert R. Thomson Member IEEE, Nicholas D. Psaila Member IEEE, Ajoy K. Kar Member IEEE and Derryck T. Reid ; “ Laser Action from an Ultrafast Laser Inscribed Nd-Doped Silicate Glass Waveguide “,IEEE, (2010).

[81]- I.Ipanraguirre, J. Azkargorta, R. Baida, K Venkata Krishnaiah, C.K. Jayasankar, M. Al-Saleh, and spectroscopy of a Nd3+-doped phosphate glass under wavelength selective pumping “,Optics Communications, Vol.(19), No.(20), (2011).

[82]- Takenobu Suzuki, Hiroyuki Kawai, Hiroyuki Nasu, Mark Hughesa, Yasutake Ohishi, Shintaro Mizunob, Hiroshi Ito , Kazuo Hasegawa ; “Quantum efficiency of Nd^{3+}-doped glasses under sunlight excitation “, optical materials, No(33), PP(1952-1957), (2011).

[83]- M. Klimczak and R. Piramidowicz ; “UV-violet emission properties of 2F(2)s/2 energy level of Nd3+ ions in ZBLAN glass “,Appl Phys B 106:PP(1019-1025), (2012).

[84]- NoeKo Oliveira Dantas, Elias Oliveira Serqueira, Anielle Christine Almeida Silva, Acacio Aparecido Andrade, Sidney Alves Lourenço ; " High Quantum Efficiency of Nd^{3+} Ions in a Phosphate Glass System using the Judd-Ofelt Theory ", Brafj Phys \ 43:PP(230-238), (2013).

[85] A. Ryasnyanskiy, N. Vorobiev, V. Smirnov, J. Lumeau, L. Glebova, O. Mokhun, Ch. Spiegelberg, Michael Krainak, A. Glebov, and L. Glebov ; "DBR and DFB lasers in neodymium- and ytterbium-doped photothermorefractive glasses ",Optical letters, Vol.(39), No.(7), (2014).

[86]- M. Venkateswarlu, Sk. Mahamuda, K. Swapna, M.V.V.ICS. Prasad, A. Srinivasa Rao, A. Mohan Babu, Suman Shakyad, G. Vijaya Prakash : "Spectroscopic studies of Nd3+ doped lead tungsten tellurite glasses for the NIR emission at 1062 nm ", optical material,(2014).

[87]- Cong Tian, Xi Chen', Yu Shuibao ; " Concentration dependence of spectroscopic properties and energy transfer analysis in Nd^{3+} doped bismuth silicate glasses ",Solid State Sciences 48, PP (171-176), (2015).

[88]- IL Leconte, B. Cadier, H. Gilles, S. Girard, T. Robin and M. Laroche ; "High-power Nd-doped fiber lasers tunable from 872 to 936nm ",Frontiers in Optics/Laser Science OSA, (2015).

[89]- S.O.kasap " Optoelectronics and photonics:principles an practices" Upper saddle:prentice-hall PP(41) (2001).

[90]- O.Svelto. "Principles of laser " Book, fifth Edition, Springer. Ch(1),Ch(7),Ch(18),Ch(19),Ch(20),and Ch (23) (2010).

[91]- R.S.Quimby "Output Saturation in Fiber Laser" Applied Optics , Vol.(29),No.(9) PP.(1268-1276) , (1990).

[92]- J.Yang"Neodymium-Doped Waveguide Amplifiers and Laser For Integrated Optical Applications" PhD Thesis , university of Twente ,PP. (1-25) , (2010).

[93]- M.I.Ghazaani and P.Parvin."Impct of cavity loss on the performance of Single Mode yb:silica MOFPA array"Optics and laser Technology Vol.(65) PP.(94.105), (2015).

[94]- R.M.Martin "Reciprocity between Emission and Absorption for Rare-Earth Ion in Glass" PhD ,Thesis, Worcester polytechnic, Institute PP. (1-25), (2006).

[95]- N.II.P.Verlinden " The Excited State Absorption Cross-Section of Neodymium-Doped Silica Glass Fiber in the (1200-1500)nm wavelength Range" Mss Thesis , Worcester Polytechnic Institute, PP.(10-33), (2008).

[96]- N.G.Boetti "Nd^{3+}-Doped Phosphate Glass optical Fiber Laser"PhD Thesis, university of Politeenicodi Torino, PP.(40-70), (2014).

[97]- M.E.Rochat "High Power Optical Fiber Amplifiers for Coherent inter-Satellite Communication" PhD .thesis, university of De Neuchatel PP .(5-38) (2000).

Appindex (A)

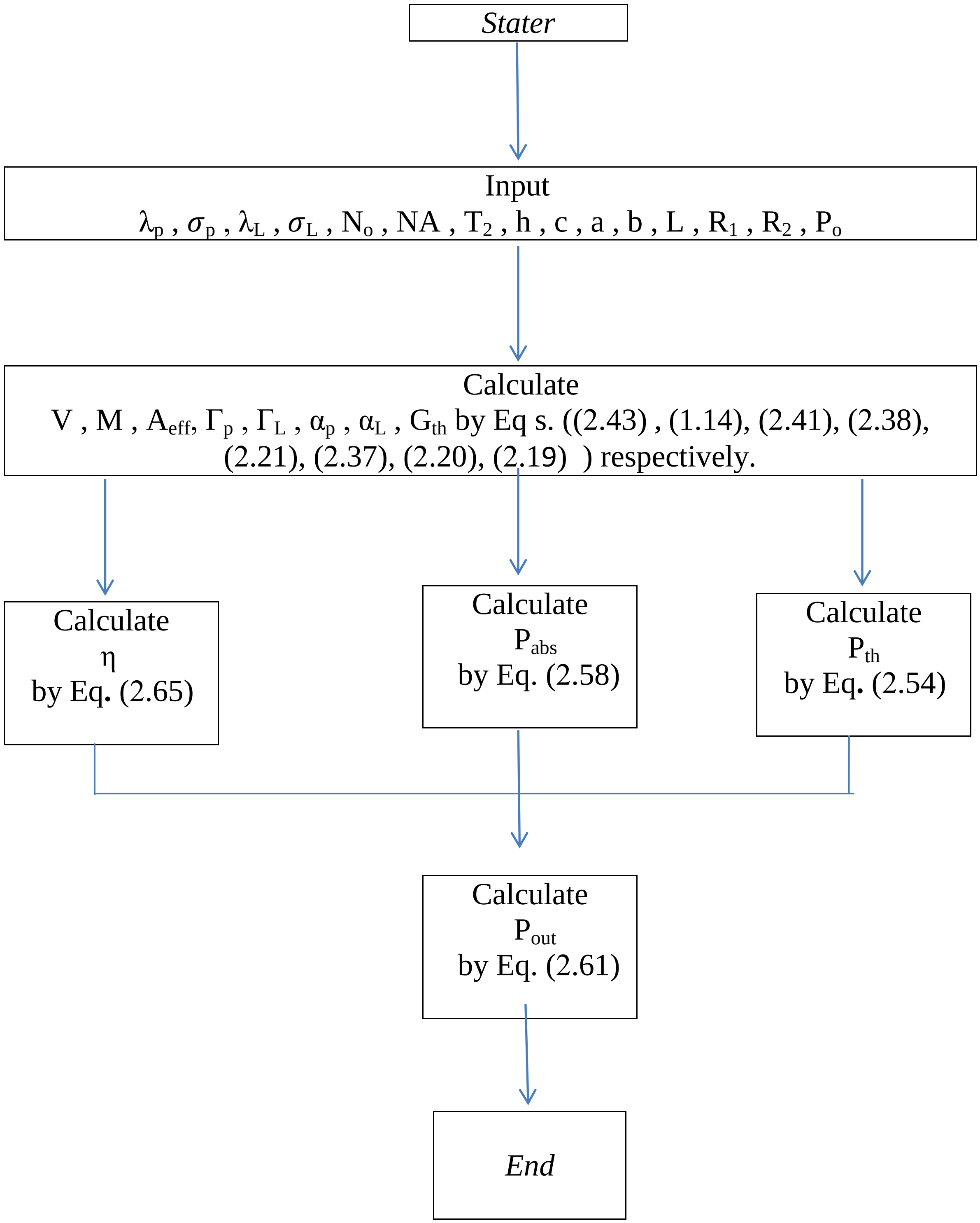

Stater
Input
λ_p , σ_p , λ_L , σ_L , N_o , NA , T_2 , h , c , a , b , L , R_1 , R_2 , P_o
Calculate
V , M , A_{eff}, Γ_p , Γ_L , α_p , α_L , G_{th} by Eq s. ((2.43) , (1.14), (2.41), (2.38), (2.21), (2.37), (2.20), (2.19)) respectively.
Calculate
η
by Eq. (2.65)
Calculate
P_{abs}
by Eq. (2.58)
Calculate
P_{th}
by Eq. (2.54)
Calculate
P_{out}
by Eq. (2.61)
End

الخلاصة (Abstract) :-

تضمنت الدارسة الحالية أولاً إستعمال الحل التحليلي لمعادلات المعدل و لليزرالليف البصري الذي يعمل وفقاً لخطة ضخ بنظام أربعة مستويات لأيجاد معادلة قدرة الخرج الليزري (P_{out}) ، وأستعمال الحل العددي ثانياً لحساب (P_{out}) لليزر الليف البصري المطعم بالنديميوم كمثال أنموذجي لليزر الليف البصري الذي يعمل وفقاً لهذا النظام ، حيث تمت برمجة المعادلات اللازمة لحساب (P_{out}) بأستعمال برنامج الماتلاب (أصدار 8.1) .

أستعملنا في هذه المحاكاة نوعين من المضيفات ، النوع الاول هو (Silica) وبتصاميم أربعة شائعة الأستعمال في هذا النوع من الليزر هم (IVA , York , Lycom (b) , Lycom(a)) ، وبأنبعاث ليزري عند الطوليين الموجيين (1064×10^{-9}m) ، (1331×10^{-9}m) ، أما النوع الثاني فهو (ZBLAN) بتصميم هو (Le Verre fluore) فقط وبأنبعاث ليزري عند الطوليين الموجيين (1048×10^{-9}m) (1317×10^{-9}m) .

الخطوة الأولى في هذه المحاكاة كانت تحديد قيمة (NA) لكل تصميم من هذه التصاميم الخاصة وعند الأطوال الموجية الخاصة بكل مضيف ، والتي يمكن عنده هذه القيمة لـ(NA) الحصول على أعلى قدرة خرج ليزري (P_{out}) وكفاءة (η) ،

أما الخطوة الثانية فكانت حساب (P_{out}) المناظرة لقدرة الضخ (P_o) لكل مضيف و للتصاميم والأطوال الموجية الخاصة بالمضيف حيث وجدنا في حالة المضيف نوع (Silica) أن (P_{out}) تكون أعلى عند أستعمال التصميم (York) لكلا الطوليين الموجيين الخاصة بهذا المضيف ، بينما في حالة كون المضيف نوع (ZBLAN) وجدنا ان (P_{out}) تكون أعلى عند إستعمال الطول الموجي (1048×10^{-9}m) للتصميم الخاص بهذا المضيف ، اضافة إلى ذلك وجدنا أنه من أجل الحصول على أعلى قيم لكل من (P_{out}) و (η) لهذا النوع من الليزر لابد من إستعمال المضيف من نوع (Silica) وعند الطول الموجي(1064×10^{-9}m) ،ووفقاً لذلك فأن الخطوة الثالثة كانت إستعمال هذا المضيف والطول الموجي لحساب تأثير كل من فتحة النفوذ العددية(NA) نصف قطر الليف البصري(a) ، نصف قطر الغلاف الواقي لليف البصري(b)،طول الليف البصري (L) ، انعكاسية مرآة الخرج الليزري(R_2)،تركيز النديميوم في لب الليف البصري(N_o) ، عمر مستوي الليزر العلوي(T_2)، وقدرة الضخ (P_o)، على قدرة الخرج الليزري(P_{out}) حيث أن تغير قيم هذه المعاملات كان محدداً بمداها الموجود في التصاميم الأربعة الخاصة بالمضيف (Silica) ، حيث وجدنا أن قيمة (P_{out}) تقل بزيادة قيم كل من ($NA\ a, b ,L ,N_o$) ، بينما تزداد بزيادة قيم كل من (R_2 ,T_2 , P_o) ، ومن خلال ذلك تم تحديد القيم المثلى لهذه المعاملات والتي لابد من إستعمالها من أجل الحصول على أعلى قيم لكل من (P_{out}) و (η) لهذا النوع من الليزر .

جمهورية العراق

وزارة التعليم العالي والبحث العلمي

جامعة بغداد

كلية التربية للعلوم الصرفة /ابن الهيثم

قسم الفيزياء

دراسة نظرية لليزر الليف البصري المطعم بالنديميوم

رسالة مقدمة الى

مجلس كلية التربية للعلوم الصرفة / ابن الهيثم – جامعة بغداد

وهي جزء من متطلبات نيل درجة ماجستير علوم في الفيزياء

من قبل

امجد عبدالحميد سلمان

بكالوريوس علوم فيزياء / 2013

بإشراف م. د. مظهر شهاب احمد

1437هـ　　　　2016 م